C 51.17/12:987/6 188-A-11
JUN - 3 1987
C 51.17/12:987/6

Tech Notes

JUNE 1987

PB87-925906

CONTENTS

PENNSYLVANIA STATE UNIVERSITY
JAN27 1988
DOCUMENTS COLLECTION

NTIS
U.S. DEPARTMENT OF COMMERCE
National Technical Information Service
Center for the Utilization of Federal Technology

U.S. DEPARTMENT OF COMMERCE
Malcolm Baldrige, Secretary of Commerce

National Technical Information Service
Joseph F. Caponio, Director

ISSN 0889-8464

COPYRIGHT WARNING
International Copyright © National Technical Information Service, 1987. All portions of this publication are protected against copying or other reproduction outside of the United States under the provisions of Article II of the Universal Copyright Convention. United States copyright is not asserted under the United States Copyright Law, Title 17, United States Code.

The Secretary of Commerce has determined that the publication of this periodical is necessary in the transaction of the public business required by law of this department. Use of funds for printing this periodical has been approved by the Director of the Office of Management and Budget through 1987.

Tech Notes

Highlighting Selected U.S. Government Technology & Resources

JUNE 1987

Contents

Agriculture & Food 518
Computers 524
Electrotechnology 530
Energy 541
Engineering 549
Environmental Science & Technology 556
Manufacturing, Machinery, & Tools 568
Materials 576
Medicine & Biology 592
Natural Resources Technology & Engineering 598
Physical Sciences 602
Transportation 616

Published monthly by the National Technical Information Service (NTIS), Tech Notes bring togeather individual one to two page fact sheets prepared by Federal agencies, their laboratories, or contractors. These fact sheets highlight current Federal technology determined to have commercial or practical application. Topics cover new processes, materials, techniques, software, instrumentation, and resources.

Some of the current sources are the Department of the Navy, Department of the Army, NASA, Department of Energy , Environmental Protection Agency, Department of the Interior, and the Department of Agriculture.

Special assistance is provided by the Federal Laboratory Consortium.

Change of address or questions concerning subscriptions should be sent to:
Subscriptions Department
National Technical Information Service
Springfield, VA 22161
(703) 487-4630

Suggestions, comments, or questions concerning Tech Notes should be directed to:
Tech Notes Editor
Room 11R
National Technical Information Service
Springfield, VA 22161
(703) 487-4838

How to Use Tech Notes

Every Tech Notes fact sheet lists a source for additional information. The source of this information may be a special support package from the originating agency, a personal contact, a licensing opportunity, or a backup report available from NTIS.

Each fact sheet also is perforated to allow for easy removal for those subscribers who may wish to keep a special fact sheet file or route to others in their organization

Sources of Further Backup Information

Below are two representative examples of how each Tech Note fact sheet provides you with a source of further information. In most cases, this information is provided directly by the agency or its laboratory.

However, there are cases where NTIS is the source for backup documentation. In these cases, use the order form at the end.

Examples:

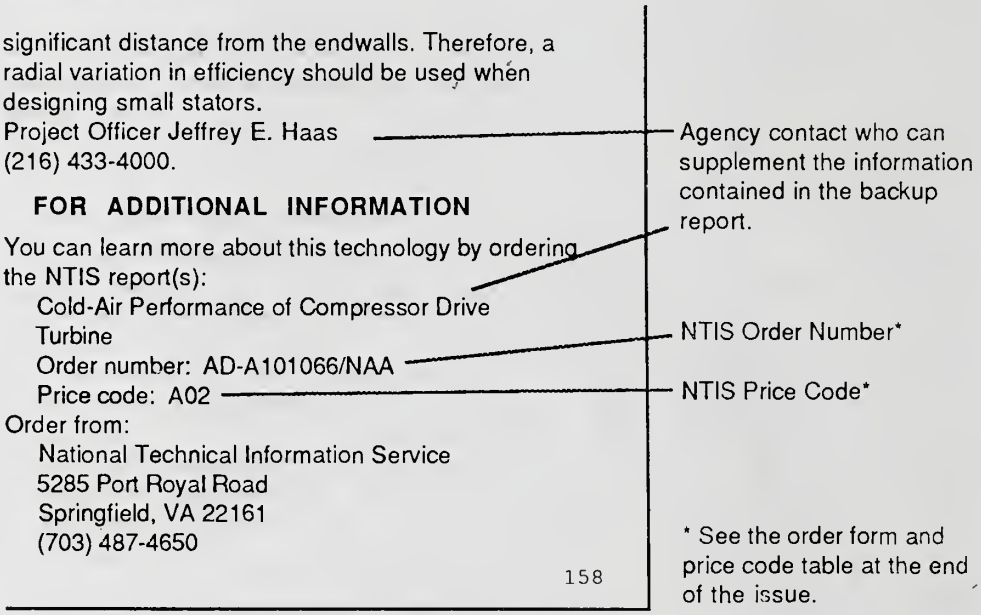
significant distance from the endwalls. Therefore, a radial variation in efficiency should be used when designing small stators.
Project Officer Jeffrey E. Haas
(216) 433-4000.
FOR ADDITIONAL INFORMATION
You can learn more about this technology by ordering the NTIS report(s):
Cold-Air Performance of Compressor Drive Turbine
Order number: AD-A101066/NAA
Price code: A02
Order from:
National Technical Information Service
5285 Port Royal Road
Springfield, VA 22161
(703) 487-4650
158
Agency contact who can supplement the information contained in the backup report.
NTIS Order Number*
NTIS Price Code*
* See the order form and price code table at the end of the issue.

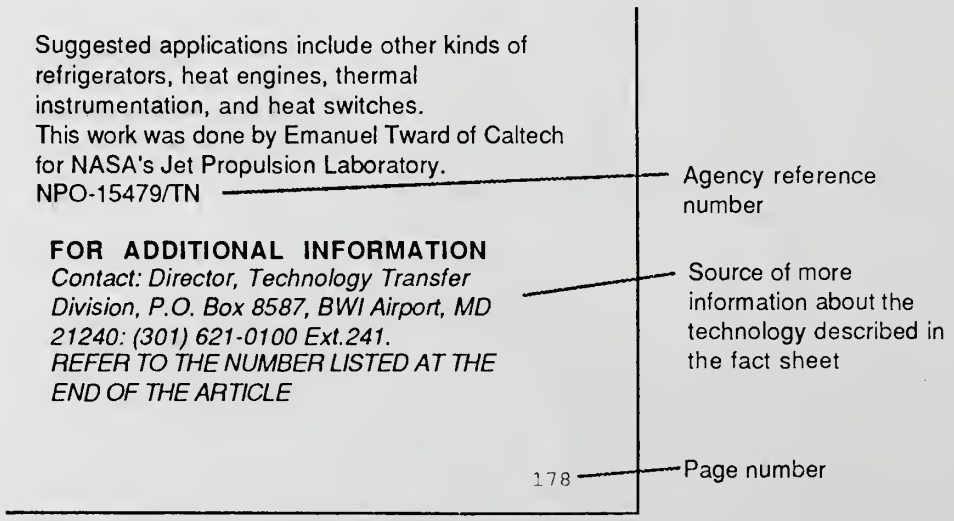
Suggested applications include other kinds of refrigerators, heat engines, thermal instrumentation, and heat switches.
This work was done by Emanuel Tward of Caltech for NASA's Jet Propulsion Laboratory.
NPO-15479/TN
FOR ADDITIONAL INFORMATION
Contact: Director, Technology Transfer Division, P.O. Box 8587, BWI Airport, MD 21240: (301) 621-0100 Ext.241.
REFER TO THE NUMBER LISTED AT THE END OF THE ARTICLE
178
Agency reference number
Source of more information about the technology described in the fact sheet
Page number

Tech Notes Title List for June 1987

Agriculture & Food

518 Research Assesses Ozone Damage to Crops
519 Carbon Dioxide Makes Heat Therapy Work for Virus Infected Plants
520 Gase Clues to Bruises
521 Economies of Short and Ultra-Short Rotation Forestry
522 Carbon Dioxide Enrichment Increases Crop Yield

Testing & Instrumentation

523 Inexpensive Meter for Total Solar Radiation— This instrument aids in deciding on the proper time to harvest crops.

Computers

524 Drawing Viewgraphs by Computer— A specially developed program prepares presentation-quality text for projection.
525 Ada and Its Effects: A Compendium— Conference proceedings cover problems and achievements associated with the computer language.
526 Emergency Personnel Notification System
527 Electronic Communications Between Wang Office Information Systems and IBM 5520 Office System

Software

528 Maximum-Likelihood Decoder on a Hypercube Multiprocessor— Efficient parallel processing is used to implement complex decoders. (Licensing Opportunity)
529 Listing Relationships Among Subroutines— Hierarchical charts of sub-programs are generated.

Other items of interest

593 Human Factors Guidelines and Methodology in the Design of a User-Computer Interface: A Case Study

Electrotechnology

530 Wrist Radio Receiver Allows Personnel to Assemble Even in Rough Terrain
531 Modular Optical Amplifier— A multipass device amplifies the output of a laser without being excessively long.
532 Interface States in MOS Capacitors— States build up in two stages.
533 Radiation-Hardened Microcontroller
534 High-Spatial-Resolution Digital Ultrasonic Imaging System— Video-rate real-time imaging is possible.
535 Designing dc Inductors With Airgaps— Optimal parameters are obtained by designing near the saturation point.
536 Theory of Periodic-Binary-Sequence Generators— Algorithms yield feedback shift registers with maximum regularity.
537 Effects of Radiation on Capacitor Dielectrics— Data have been gathered on key design parameters.
538 Reinforced Masks for Ion Plating of Solar Cells— Long fingers would be held more rigidly. (Licensing Opportunity)

Testing & Instrumentation

539 Microdiagnostics for Prototype Instrumentation
540 Step Generator Offers Improved Features

Energy

541 Miniature Thermal Battery— Component matches performance of larger units.
542 Advanced Research and Technology Development—Low-Rank Coal Physical Properties, Moisture, and Distribution of Inorganics
543 Recovering Heavy Oil by Carbon Dioxide Gas Immiscible Flooding
544 Energy from Biomass: Building on a Generic Technology Base
545 Small-Hydropower Development: The Process, Pitfalls, and Experience: Guide for Developers
546 Fuel-Cell Structure Prevents Membrane Drying— Embossed plates direct flows of reactants and coolant. (Licensing Opportunity)
547 Liquid-Hydrogen Polygeneration System— The system utilizes coal as an alternate chemical feedstock. (Licensing Opportunity)

Software

548 Evaluating Performances of Solar-Energy Systems— Efficiencies can be calculated and maximized.

Other items of interest

538 Reinforced Masks for Ion Plating of Solar Cells— Long fingers would be held more rigidly. (Licensing Opportunity)
550 Water Heater/Cooler for Vehicles— At the press of a button, thermoelectric unit changes from a heating device to a cooling device.
564 Modified Generator Puts Out More Power with Less Noise
585 Behavior of Pressurized Incoloy 800H Tubes in Environments Pertaining to Coal Gasification

Engineering

549 Simulating Damage in Wound-Filament Pressure Vessels— A model, founded in classical viscoelastic theory, produces results consistent with reported data.
550 Water Heater/Cooler for Vehicles— At the press of a button, thermoelectric unit changes from a heating device to a cooling device.
551 Technology Transfer Films Available on Loan
552 Cycle-Counting Methods for Fatigue Analysis
553 Scouring System Deepens Water in Ship Berthing Sites
554 Shape Determination for Large Static Structures— Parameter and shape estimates are updated from new measurements.
555 Balancing High-Speed Rotors at Low Speed— Flexible balancing reduces vibrations at operating speeds.

Engineering (Cont.)

556 Structural Error and Identifiability in Mathematical Models— Errors and previously implicit assumptions are treated explicitly.

557 Hose- and Tube-Cleaning Module— This device enables tubes and hoses to be cleaned easily, without other special equipment. (Licensing Opportunity)

558 Mobile Platform for Large Structures— A proposed platform would move forward and in reverse, turn left and right, and change planes. (Licensing Opportunity)

559 Blade-Tip-Clearence Forces in Turbines— A study reviews the field and proposes experiments.

560 Air-Powered Projectile Launcher— A small, high-pressure reservoir conserves compressed air.

Software

561 Urban Hydrology Software for Small Watersheds

Testing & Instrumentation

562 Use of Minaturized Tests to Predict Flow Properties and Estimate Fracture Toughness in Deformed Steel Plates

563 One-Piece Force-Transducer Body— A rugged unit is designed to operate in severe environment.

Other items of interest

567 An Interactive Computer Model for Calculating V-I Curves in ESPs Version 1.0

600 Software Package is an Integrated Finite Difference Program for Computing Two-Phase Nonisothermal Flow in Porous Media

Environmental Science & Technology

564 Modified Generator Puts Out More Power with Less Noise

565 An Evaluation of Densification Technologies for Solid Waste

566 Integrated Global Background Monitoring Network—Preliminary Results

Software

567 An Interactive Computer Model for Calculating V-I Curves in ESPs Version 1.0

Other items of interest

561 Urban Hydrology Software for Small Watersheds

611 A Virtual Impactor for Personal and Area Air Sampling

Manufacturing, Machinery, & Tools

568 Developing a Reliability-Centered Maintenance Plan— Effective preventive maintenance can be implemented with minimum expenditure of resources.

569 Manufacturing Fiber-Optic Bundles With Low-Loss Glass— It is feasible to make long bundles for highly sensitive imagescopes and similar optical instruments.

570 Draft Standard for Robots Issued

571 Turning Workstation Being Developed for Mare Island Naval Shipyard

572 Multifunction Vacuum Chamber for IC Metallization— One system performs several operations without transferring wafers between vacuum chambers. (Licensing Opportunity)

573 Laser Vacuum Furnace for Zone Refining— A laser beam is scanned to produce a moving melt zone. (Licensing Opportunity)

574 Producing Refractory Microballoons— Metals, ceramics, and glasses are just some of the possible raw materials. (Licensing Opportunity)

575 Redundant Pyrotechnic/Manual Release Mechanism— When all else fails, manual intervention is possible. (Licensing Opportunity)

Other items of interest

538 Reinforced Masks for Ion Plating of Solar Cells— Long fingers would be held more rigidly. (Licensing Opportunity)

578 Steels for High-Temperature Gears— Potential replacements for a standard steel are evaluated.

Materials

576 Compatibility of Greases With Seal Elastomers— Minimum swelling or shrinkage is not the sole criteria for choosing materials.

577 Yielding and Deformation of PWA 1480 Superalloy— Three distinct temperature regimes are found.

578 Steels for High-Temperature Gears— Potential replacements for a standard steel are evaluated.

580 Carburized Steels for High-Temperature Service— A 2.3-percent-nickel low-carbon steel is found to be both hard and tough; aircraft gears and bearings are likely applications.

581 Variability in Metal-Matrix Composites— Source of variability are analyzed, and metal matrices are compared with polymer matrices.

582 Deuterides of Rare-Earth/Transition-Metal Alloys— Neutron diffraction studies shed light on both crystal and magnetic structures.

583 Consolidation Methods for Rapidly Solidified Type 304 Stainless Steel

584 New Structural Materials Technologies— Opportunities for the Use of Advanced Ceramics and Composites

585 Behavior of Pressurized Incoloy 800H Tubes in Environments Pertaining to Coal Gasification

586 Fire-Resistant Belt Panel for Airplane Windows— The layered structure incorporates materials that generate little smoke. (Licensing Opportunity)

587 Two-Step Vapor/Liquid/Solid Purification— One process approaches the theoretical limit of multiple zone refining and distillation. (Licensing Opportunity)

588 Fire-Resistant Aircraft Ceilings— New materials retard flames but keep panel strong and light. (Licensing Opportunity)

589 Strong Adhesive Tape for Cold Environments— This strong tape remains sticky over a wide temperature range.

590 Fuel Manifold Resists Embrittlement by Hydrogen— A completely-cast hydrogen-compatible alloy is preferable to protective plating.

591 Neutron-Scattering Measurements of Tungsten Alloy— Neutron diffraction yields information about microstructure that x-ray diffraction cannot. (Licensing Opportunity)

Materials (Cont.)

Testing & Instrumentation

579 Thermal Analysis of Epoxy Mixtures— Differential scanning analysis is used to study the curing of resins.

Other items of interest

537 Effects of Radiation on Capacitor Dielectrics— Data have been gathered on key design parameters.

569 Manufacturing Fiber-Optic Bundles With Low-Loss Glass— It is feasible to make long bundles for highly sensitive imagescopes and similar optical instruments.

574 Producing Refractory Microballoons— Metals, ceramics, and glasses are just some of the possible raw materials. (Licensing Opportunity)

Medicine & Biology

592 Low-Molecular-Weight, Cobalt-Binding Proteins from Saccharomyces cerevisiae and Bacillus subtilis

593 Human Factors Guidelines and Methodology in the Design of a User-Computer Interface: A Case Study

594 Electron Microscopy Technique Improves Image Quality— Rapid sample freezing eliminates structural distortion.

595 Binding of Antiviral Agents to Cold Viruses

596 Information Available on Determining Radiopharmaceutical Dosages

597 Cutting Head for Ultrasonic Lithotripsy— Kidney stones are disintegrated safetly and efficiently. (Licensing Opportunity)

Natural Resources Technology & Engineering

598 Climate Assessment Information Service

599 Multichannel Seismic Reflection Data— Navarin Basin-Northern Bering Sea-Alaska

Software

600 Software Package is an Integrated Finite Difference Program for Computing Two-Phase Nonisothermal Flow in Porous Media

Testing & Instrumentation

601 Meteorological Sensor Package

Other items of interest

532 Interface States in MOS Capacitors— States build up in two stages.

613 Three-Frequency Water-Vapor Radiometer— Measurements increase the accuracies of delay predictions.

Physical Sciences

602 Detecting the Edges of Obstacles From Range Data— Edges of such terrain features as boulders or craters can be identified from geometrical relationships.

603 Measuring the Low-Energy Spectrum of Cobalt-60— Ionization chamber yields data for calculating dose-enhancement factor for a given specimen geometry.

606 Electromechanical Properties of Superconducting Magnets

607 JANAF Thermochemcial Tables

608 Attenuation Measurements on Deformed Optical Fibers

Testing & Instrumentation

604 Two-Beam Gamma Densitometer

605 Soft X-Ray Laser at Princeton University

609 Hydrogen CARS Spectrometer for Combustion Diagnostics— Coherent anti-Stokes Raman scattering produces data on chemical and physical events and flow.

610 Fast-Responding Thermal Fluence Gauge— With its small mass, a gauge can measure the effects of pulses as brief as 1 millisecond.

611 A Virtual Impactor for Personal and Area Air Sampling

612 X-Ray Microprobe Achieves 10 Micron Resolution

613 Three-Frequency Water-Vapor Radiometer— Measurements increase the accuracies of delay predictions.

614 Laser-Pulse/Fiber-Optic Liquid-Leak Detector— Several potential leak sites can be monitored using a single sensing fiber. (Licensing Opportunity)

615 Improved Spectrometer for Field Use— Instrument would give answers in the field without waits for lab processing. (Licensing Opportunity)

Other items of interest

579 Thermal Analysis of Epoxy Mixtures— Differential scanning analysis is used to study the curing of resins.

582 Deuterides of Rare-Earth/Transition-Metal Alloys— Neutron difffraction studies shed light on both crystal and magnetic structures.

587 Two-Step Vapor/Liquid/Solid Purification— One process approaches the theoretical limit of multiple zone refining and distillation. (Licensing Opportunity)

Transportation

616 Cost and Weight of Helicopter Landing Gear— Three types of landing gear are compared.

617 Stress Analysis of a Scale-Model Helicopter Rotor Hub— Margins of safety are positive in the components checked.

618 More Durable Tracks for Heavy Vehicles— Tie bars instead of threaded fasteners make track throwing less likely.

Other items of interest

550 Water Heater/Cooler for Vehicles— At the press of a button, thermoelectric unit changes from a heating device to a cooling device.

586 Fire-Resistant Belt Panel for Airplane Windows— The layered structure incorporates materials that generate little smoke. (Licensing Opportunity)

588 Fire-Resistant Aircraft Ceilings— New materials retard flames but keep panel strong and light (Licensing Opportunity)

Agriculture & Food

518 Research Assesses Ozone Damage to Crops

519 Carbon Dioxide Makes Heat Therapy Work for Virus Infected Plants

520 Gase Clues to Bruises

521 Economies of Short and Ultra-Short Rotation Forestry

522 Carbon Dioxide Enrichment Increases Crop Yield

Testing & Instrumentation

523 Inexpensive Meter for Total Solar Radiation— This instrument aids in deciding on the proper time to harvest crops.

Digitized by the Internet Archive
in 2013

http://archive.org/details/technxxxxxxx00cent

United States
Department of
Agriculture

Research Technology
Agricultural Research Service

Research Assesses Ozone Damage to Crops

Ozone and other air pollutants are costing farmers at least $1 billion in agricultural crop losses each year, according to Agricultural Research Service scientists studying the damage.

"Farmers don't see ozone damage happening to their field crops, but it is," says Walter W. Heck, a plant physiologist who heads the agency's air pollution research at Raleigh, NC, in cooperation with the Environmental Protection Agency (EPA).

Damaging ozone is caused by a photochemical reaction of sunlight with automobile and industrial exhausts containing nitrogen oxides and hydrocarbons. It is different from the ozone layer in the Earth's stratosphere that filters out ultraviolet sunlight but does not harm crops.

"Ozone is carried by prevailing winds, often for hundreds or thousands of miles," Heck says. "That's why rural areas, despite having fewer automobiles and industrial plants, often equal the ozone pollution levels for urban areas."

As a result, he says, crops far away from pollution sources are not necessarily safe from ozone.

"We see in field-test chambers and in greenhouses that ozone is causing leaves of soybean, wheat, cotton, peanut, and other agricultural crops to die prematurely, reducing yields and costing the farmer money," he says. "And the $1 billion figure doesn't include damage to horticultural crops and to forests."

Yield losses are based on crop studies done at sites across the country from 1980 to 1982. Findings from 1983 to 1985 are being analyzed, Heck says, and final results are expected in 1987.

Heck's laboratory has been studying the problem since 1980 as part of the National Crop Loss Assessment Network (NCLAN), set up by EPA to get estimates of agricultural crop losses from ozone and other air pollutants.

A typical long-term concentration, or level, of surface ozone is 0.05 ppm, Heck says. In test areas, ozone levels ranged from about 0.04 to 0.06 ppm during a 7-hour day, from 9 a.m. to 4 p.m.

Indoor chambers control environment of snap bean plants to test response to ozone under various conditions. Plant physiologist Walter Heck and botanist John Dunning review records.

"Ozone is carried by prevailing winds, often for hundreds or thousands of miles. That's why rural areas often equal the ozone pollution levels for urban areas."

—Plant Physiologist Walter W. Heck

That level can significantly damage crops when plants absorb it over an entire growing season. Among the yield losses assessed to date in the NCLAN studies:

- Soybean yields decreased 12 percent when exposed to 0.05 ppm of ozone in 1980-82 field tests at Argonne, IL, Beltsville, MD [see *Agricultural Research*, November 1981, pp. 4-6], Ithaca, NY, and Raleigh.
- Peanut yields also decreased about 12 percent during 1980 tests at Raleigh. Peanut and soybean losses

were among the highest for crops tested.

- Cotton yields at Shafter, CA, showed a 7-percent reduction, while 1982 tests at Raleigh showed that yields of a common type of cotton grown in the South decreased by 10 percent.
- Winter wheat yields at Argonne were reduced 7 percent.
- The lowest reduction at 0.05 ppm was 1.5 percent in corn tests at Argonne in 1981 and for sorghum there in 1982.
- As ozone increased, yields declined for all the crops tested. At 0.06 ppm, for example, soybean yields were cut by 17 percent, and at 0.09 ppm, the loss was 31 percent.

The results for soybeans, cotton, winter wheat, and corn were calculated on what Heck calls a "common ozone response" of several varieties for each crop. The peanut and sorghum results were based on data from a single variety for each crop.

Heck and agency plant pathologists Richard A. Reinert and Allen S. Heagle at Raleigh are studying ozone and other air pollutants in several ways. Heagle conducts outdoor field studies in specially designed test chambers; Reinert conducts indoor studies in exposure chambers placed in greenhouses and in a building called a phytotron, where environmentally controlled rooms and compartments allow scientists to study the problem under a variety of conditions.

"We study plants at different stages of development and expose them to different factors to see what ozone does to them," says Reinert. "In the greenhouses and phytotron, we can see how temperature, light, fertilizers, moisture and other variables affect a plant's response to ozone and other air pollutants. We can also determine how other factors such as plant diseases are influenced by air pollutants."

The outdoor studies are in cylindrical, open-top chambers specially designed to gauge the effects of air pollutants on different crops.

The chambers are 10 feet in diameter and 8 feet tall, with aluminum frames surrounded by plastic. They are placed on the ground, and crops are planted inside of them. Air is pumped into them, either through charcoal filters to remove ozone, or without filters to let ozone in.

Ozone in the different chambers can be regulated so that scientists can compare plant responses at various concentrations or when ozone is filtered out.

"We've only scratched the surface at this point," Heagle says, "but we're at the point where the trends we've seen are pretty clear. Now we want to continue studying how moisture affects a plant's response to ozone. We've only done that for the past 3 years."

Moisture plays a key role, according to Heck. When a plant lacks water, its stomates, the openings in its leaves, close to retain water in the plant. This, he says, reduces the amount of ozone a plant absorbs through the stomates from the air.

"This may explain, in part, why ozone appears to affect plants more in the East, where there is more rain," Heck says. "They probably absorb more ozone, whereas in the West, drier conditions may help plants cut down on the amount of ozone they absorb—unless they are irrigated."

Ozone enters a plant as its leaves absorb carbon dioxide necessary for photosynthesis, in which plants use sunlight to form carbohydrates. When damaged by ozone, a plant's leaves age prematurely and discolor, leaf cells die, and photosynthesis and growth decrease.

"It is frustrating for growers that we don't have anything really simple to tell them that they can do about ozone pollution," Heck says.

One research option is to breed plants that have genetic resistance to ozone, he says. "Such resistance apparently exists in all crop species that have been examined."

Meanwhile, the national crop network is completing a series of field studies and will hold an international conference in Raleigh in late 1987 to discuss results and ways to deal with air pollution problems.—By **Sean Adams,** ARS.

Walter W. Heck is in USDA-ARS Air Quality Plant Growth and Development Research, Raleigh, NC 27695. (919) 739-3311

United States Department of Agriculture

Research Technology
Agricultural Research Service

Carbon Dioxide Makes Heat Therapy Work for Virus Infected Plants

Scientists can now propagate healthy blueberry and raspberry plants from virus-infected stock by treating it with heat and carbon dioxide.

"We grow plants at 100°F Fahrenheit, which makes them develop faster than the virus can spread," says ARS plant pathologist Richard H. Converse. "Then, we take cuttings of the new growth—less than an inch long—and raise them into full-sized, virus-free plants."

But in this race to outdistance the virus, some plant species are not able to take the heat. Some even die.

"Chemical reactions double for every 14°F rise in temperature," Converse says. "So, if you try to grow a plant at 100°F that was originally growing at 86°F, it will double its respiration rate. The danger is that the plant growing at the higher temperature could soon exhaust its stored food reserves much like a runner who runs too hard and tires."

Adding carbon dioxide increases the rate of photosynthesis in plants, which increases the plant's food reserves.

Converse's findings on blueberries and raspberries are based on earlier research Australian scientists did on grapes.

The Australians had discovered that they could successfully grow plants in growth chambers at continuously high temperatures if the slight amount of carbon dioxide normally present in the air (about 350 ppm) was increased to 1,200 ppm.

"What carbon dioxide does," says Converse, "is to make the heat treatment safe. It allows some plants to grow at temperatures they would otherwise not survive and allows other plants to grow for longer periods at 100°F."

One problem with the process, says Converse, is that the longer plants are exposed to heat the greater the mutation rate. So, resulting clones should be closely examined for trueness to horticultural type.—By **Howard Sherman,** ARS.

Richard H. Converse is at the USDA-ARS Horticultural Crops Research Laboratory, 3420 Southwest Orchard St., Corvallis, OR 97330.

[A technical paper covering this subject, by R.H. Converse and R.A. George, will appear in early 1987 in volume 71 of the journal Plant Disease.] (503) 757-4544

United States
Department of
Agriculture

Research Technology
Agricultural Research Service

Gas Clues to Bruises

Excess carbon dioxide given off by bruised fruits and vegetables provides a telltale clue to rough treatment during picking and handling.

As a result, scientists can use carbon dioxide readings that are above normal respiration levels (for dark storage conditions) to quickly and reliably measure damage, says Clyde L. Burton, a plant pathologist with the USDA Agricultural Research Service in East Lansing, MI.

Carbon dioxide is a byproduct of the breakdown of malic acid spilled from damaged cells near the site of a bruise.

To relate carbon dioxide release to the degree of damage, Burton and technician Nancy L. Schulte-Pason dropped freshly harvested cherries and blueberries one to five times from a height of 3 feet. The impacts simulated those that might occur during harvesting and handling.

They immediately placed the dropped fruit in sealed plastic food containers. One hour later, after carbon dioxide accumulated in the containers, needles attached to the intake and exhaust lines of an infrared gas analyzer were inserted into the containers. "The gas analyzer is so sensitive to carbon dioxide that we must be careful in breathing or talking around the machine," Burton says.

The higher the amount of carbon dioxide in a sample, the greater the damage and the higher the amount of eventual decay. The test takes 2 hours compared with a wait of several days for visual observation of decay.

Burton says that information gained from testing fruit can be used to improve mechanical harvesters and the handling equipment in packing houses.

In Michigan, it is estimated that 40 to 50 percent of mechanically harvested cherries and blueberries suffer damage.—By **Linda Cooke-Stinson**, ARS.

Clyde L. Burton is in USDA-ARS Fruit and Vegetable Harvesting Research, Room 138, Plant Biology Lab., Michigan State University, East Lansing, MI 48824

energygram

Economies of Short and Ultra-Short Rotation Forestry

DOE/TIC/EG-86/149
OFFICE OF SCIENTIFIC AND TECHNICAL INFORMATION

This technical note was based on research conducted by Argonne National Laboratory for the U.S. Department of Energy.

Argonne National Laboratory

A model for determining a long-run optimal stationary harvesting cycle for short rotation forestry for the production of biomass has been developed.

The model uses a linear complementary approach and is adapted from recent work in the area of economic growth theory. Use of the model in analysis of the effect of tree spacing on production cost and woody biomass production patterns allows the identification of least-cost production systems and research and development needs. Two types of short rotation plantations, one with relatively large spacings within and between rows and the other involving very dense plantings, are analyzed.

The approach of planting cuttings at very high density results in trees growing in a manner similar to tall grasses and thus is called the "wood-grass" approach. The wood-grass system, which would be the least-cost method when the cost of planting stock is reduced through mechanical production and new high productivity planting equipment is developed, shows promise of acceptance as an annual crop by farmers. This approach is viable chiefly with species that lend themselves to the coppicing method of regeneration.

Revenues from the production of wood-grass would be realized annually, and because the coppicing stumps would be small, land use for the production of wood-grass could be readily converted to the production of other crops and thus offer a high degree of crop flexibility.

FOR ADDITIONAL INFORMATION

Reference(s):
S. Y. Shen, A. D. Vyas, and P. C. Jones. Economic Analysis of Short and Ultra-Short Rotation Forestry. Resour. Conserv., *10: 255-270 (1984).*

For program-related information, contact
Sinyan Shen
Argonne National Laboratory
9700 South Cass Avenue
Argonne, IL 60439
Telephone No.: (312) 972-6276

energygram

Carbon Dioxide Enrichment Increases Crop Yield

DOE/TIC/EG-86/134
OFFICE OF SCIENTIFIC AND TECHNICAL INFORMATION

This technical note summarizes a project achievement selected from the U.S. Department of Energy 1985 Basic Energy Sciences Program.

Lawrence Livermore National Laboratory

Crop yield is increased by higher levels of carbon dioxide in the atmosphere. Field data from 10 outdoor experiments involving food, forage, and fiber crops provide convincing evidence that carbon dioxide enrichment enhances growth and productivity. When grown at levels twice today's atmospheric concentration, five of six crops examined yielded 31 to 82% more harvestable product. The species showing gains were black-eyed peas, soybean, sweet potato, cotton, and sorghum. One crop, corn, failed to increase productivity when enriched with carbon dioxide.

Through photosynthesis, plants produce food and fiber from light and carbon assimilated as carbon dioxide. Rising atmospheric carbon dioxide is thus an important factor in the food-producing process, and effects of carbon dioxide enrichment have far reaching implications for agricultural and ecological productivity.

Much of the theory and historical data that support the idea of carbon dioxide enhancement of plant growth come from laboratory experiments where light, nutrients, carbon dioxide levels, water, and other environmental factors are controlled artificially. Although short-term experiments inside such chambers are useful for studying physiological mechanisms and environmental interactions, they have produced very few reliable data on full-season growth and yield at natural light and for variable outdoor conditions.

Field studies have been emphasized in this project on the direct effects of carbon dioxide on plants: most of the research has been done with open-top or flow-through chambers positioned in fields planted and maintained according to normal farming practice. Test plants are exposed to natural light, soil, and other conditions, whereas precise control is maintained of the desired carbon dioxide enrichment for an entire growth cycle.

Corn exhibited no direct yield response to carbon dioxide enrichment, although other experimental results showed a significant carbon dioxide effect on water use. Doubling carbon dioxide concentration reduced by one-third the water required to produce a normal yield of corn, and this effect is expected to enhance productivity indirectly. (Tuskegee Institute, P. K. Biswas; U.S. Department of Agriculture/Agricultural Research Service, L. H. Allen, B. A. Kimball; Lawrence Livermore National Laboratory, J. Shinn; Kansas State University, E. Kenemasu)

FOR ADDITIONAL INFORMATION

For additional information, contact:
J. Shinn
Lawrence Livermore National Laboratory
P.O. Box 808
Livermore, CA 94550

NASA Tech Brief
National Aeronautics and Space Administration
NASA's Jet Propulsion Laboratory, Pasadena, California

Inexpensive Meter for Total Solar Radiation

This instrument aids in deciding on the proper time to harvest crops.

A pyranometer containing solar cells measures the combined intensity of direct light from the Sun and diffuse light from the sky. The instrument includes a polyethylene dome that diffuses entering light so that the output of the light detectors does not vary significantly with the changing angle of the Sun during the day. The instrument therefore does not have to be calibrated for the response of each detector to the Sun angle, and the sensor outputs do not have to be corrected separately before they are summed and integrated.

The pyranometer was developed as a simple, rugged, and inexpensive unit for agricultural use. In particular, it can help in deciding when to harvest such crops as sugarcane and grapes, the ripenesses of which are closely tied to total solar exposure.

Five silicon solar cells are placed with one on each of the sides and one on the top of a truncated pyramid (see figure). The cells are connected in parallel, and their outputs feed to a current meter or recorder. The current could also be fed to an integrator that indicates the cumulative solar radiation in terms of the solar-cell energy output, perhaps in convenient units of milliwatt-hours. A leveling screw adjusts the tilt of the cell assembly to suit the local latitude. No further adjustments are needed to allow for seasonal changes in the solar declination.

This work was done by Eric G. Laue of Caltech for **NASA's Jet Propulsion Laboratory.** *NPO-16741 /TN*

FOR ADDITIONAL INFORMATION: *Contact: Director, Technology Transfer Division, P.O. Box 8757, BWI Airport, MD. 21240; (301) 621-0100 Ext. 241*
REFER TO THE NUMBER LISTED AT THE END OF THE ARTICLE

Computers

524 Drawing Viewgraphs by Computer— A specially developed program prepares presentation-quality text for projection.

525 Ada and Its Effects: A Compendium— Conference proceedings cover problems and achievements associated with the computer language.

526 Emergency Personnel Notification System

527 Electronic Communications Between Wang Office Information Systems and IBM 5520 Office System

Software

528 Maximum-Likelihood Decoder on a Hypercube Multiprocessor— Efficient parallel processing is used to implement complex decoders. (Licensing Opportunity)

529 Listing Relationships Among Subroutines— Hierarchical charts of subprograms are generated.

Other items of interest

593 Human Factors Guidelines and Methodology in the Design of a User-Computer Interface: A Case Study

MANUFACTURING TECHNOLOGY NOTE

U.S. ARMY MATERIEL COMMAND

Deputy Chief of Staff for Manufacturing Technology, Alexandria, VA

Project Number: NONE

Filing Code: 62B113

Drawing Viewgraphs by Computer

A specially developed program prepares presentation-quality text for projection.

A report describes PCVUGRAF, a user-friendly charting utility program for an IBM PC or an equivalent microcomputer. Developed by the U.S. Army Missile Command, the program generates presentation-quality viewgraphs and charts of various forms.

In addition to a microcomputer with a 128 K random-access memory, the program requires Microcompatibles, Plotmatics, and Graphmatics (or equivalents) as library routines; a text editor or word processor program capable of handling up to 160 characters per line; a monochrome or graphics monitor; and a pen plotter.

PCVUGRAF assumes that the final chart will have a format consisting of a title section and a body section, optionally contained within a frame (see figure). The title section usually contains one to three lines of text and is automatically centered, horizontally and vertically by the program. The code adjusts the letter size to ensure that the information can be contained in the allotted space.

The body section may contain up to 110 lines of text. The code does not automatically center the text horizontally, but allows the user complete control over the layout. The program determines the total number of lines in this section and the number of letters in the longest line. From this information, it adjusts the letter size so that all the text will fit within the bounds of the length and height of the body section.

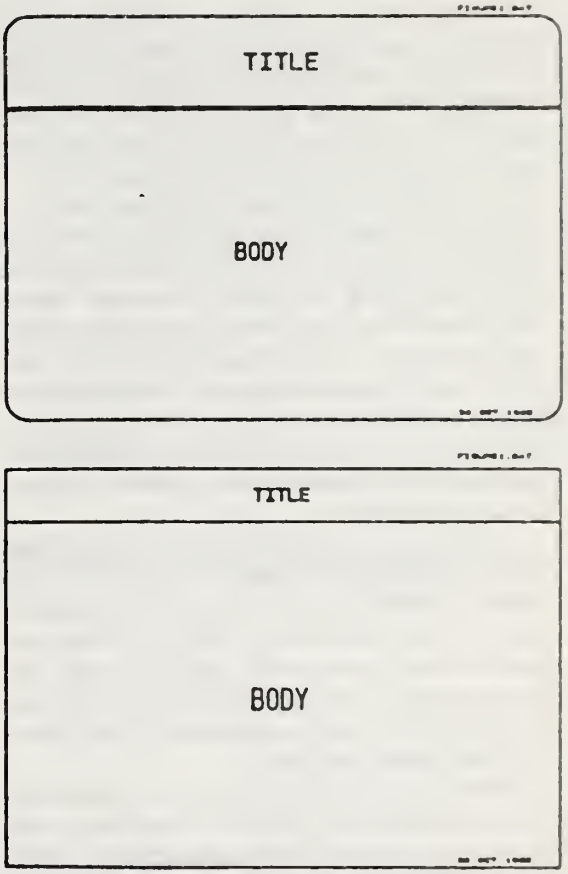

A **PCVUGRAF Chart** contains two sections, title, and body. Either the rounded-edge or sharp-edge option may be selected. The program automatically writes the figure number at the upper right and the data at the lower right.

FOR ADDITIONAL INFORMATION:

You can learn more details about this technology by ordering the NTIS report(s).
PCVUGRAF PC Based Code for Text Charts and Visual Aids.
Order number: AD-A169812/NAA
Price code: A03
Order from:
National Technical Information Service
5285 Port Royal Road
Springfield, VA 22161

This document was prepared under the sponsorship of the U.S. Government. Neither the United States Government nor any person acting on behalf of the United States Government assumes any liability resulting from the use of the information contained in this document, or warrants that such use will be free from privately owned rights.

MANUFACTURING TECHNOLOGY NOTE

U.S. ARMY MATERIEL COMMAND

Deputy Chief of Staff for Manufacturing Technology, Alexandria, VA

Project Number: NONE

Filing Code: 62D006

Ada® and Its Effects: A Compendium

Conference proceedings cover problems and achievements associated with the computer language.

A report contains 25 papers presented at the Fourth National Conference on Ada Technology. The papers cover applications, research and methodology, impact on secure operating systems, education and training, program support, and development tools. The report was compiled the U.S. Army Communications-Electronics Command.

One of the papers describes a spiral model of Ada software development and enhancement. The model (see figure) describes a risk-driven rather than specification- or prototype-driven approach. The introduction of Ada has established a risk-laden transitional era, especially in the development of system support software. The spiral model provides a way to view the successful approaches and may, as it matures, provide effective guidance for future projects.

Another paper, representative of the versatility of the Ada language, discusses an experimental use of Ada in real-time interactive avionic communication. All coding was done in Ada, and the subject device drivers were written entirely in Ada. The code execution times warranted utilization of Ada in an embedded real-time application in the case of the crew aircraft interface.

Yet another paper considers the implementation of a graphics package in Ada. The authors note that they are drawn to Ada by its expressive power and standardization. They feel, however, that some effort is still needed to set up an Ada system that is convenient for students to use.

Ada® is a registered trademark of the U.S. Government, Ada Joint Program Office (AJPO).

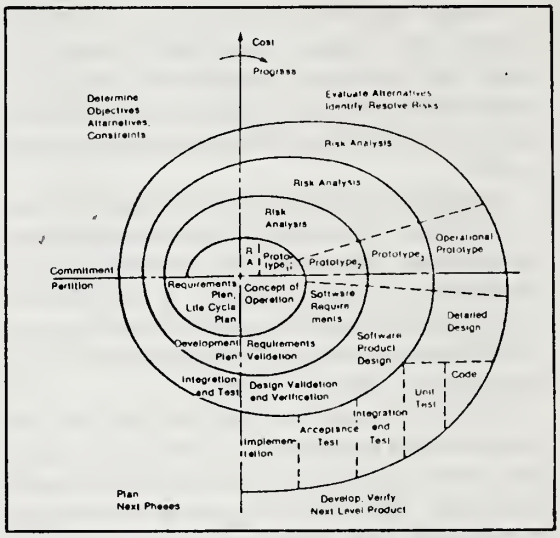

In the spiral model of **Ada Software Development**, the radial dimension indicates the cumulative cost incurred. The angular dimension indicates the progress in completing the development. The trajectory of the spiral indicates the efficiency of the software development project.

FOR ADDITIONAL INFORMATION:

You can learn more details about this technology by ordering the NTIS report(s):
Proceedings of the 4th Annual National Conference on Ada® Technology.
Order number: AD-A167802/NAA
Price code: A09

Order from:
National Technical Information Service
5285 Port Royal Road
Springfield, VA 22161

This document was prepared under the sponsorship of the U.S. Government. Neither the United States Government nor any person acting on behalf of the United States Government assumes any liability resulting from the use of the information contained in this document, or warrants that such use will be free from privately owned rights.

energygram®

Emergency Personnel Notification System

DOE/TIC/EG-86/128
OFFICE OF SCIENTIFIC AND TECHNICAL INFORMATION

This technical note was based on research conducted by Idaho National Engineering Laboratory for the U.S. Department of Energy.

Idaho National Engineering Laboratory

A system has been developed to replace manual dialing of key personnel at the time of an emergency. The system can call over 200 people in 30 minutes and notifies personnel of the exact message, not a voice synthesized message.

The system was developed to dynamically select and notify key personnel, deliver a message, log, and acknowledge response over phone lines in response to any emergency situation. The roster is not static but is a function of the emergency type and location. The number of personnel (or alternates) called is limited only by the storage capability of the main computer. The message to be transmitted is generated at the instant of the emergency and is not "canned."

The software will direct the dialing of the primary names on the specific emergency list. It will replay the message to the person, if voice patterns match, and recognize "yes" or "no" responses, busy tones, disconnected numbers and trunk transfers. If the primary person is not available, the phone is busy or disconnected, there is no answer, or the person declines, the system will automatically dial the alternate number. This assures that at least one person with expertise in the type of emergency is able to respond.

The system uses the VOTAN software and consists of a MASSCOMP microcomputer linked via an RS232 interface to three VOTAN VTR 6050 series II voice systems.

The system, called the ENS, has potential applications to disaster or emergency response for any civil or private organization that must plan for emergencies, such as chemical/nuclear accidents, terrorist activities, and acts of nature.

FOR ADDITIONAL INFORMATION

For additional information, contact:
W. J. Swenson
EG&G Idaho, Inc.
P.O. Box 1625
Idaho Falls, ID 83415
Telephone No.: (208) 526-9468

or

Jane M. Welch
EG&G Idaho, Inc.
P.O. Box 1625
Idaho Falls, ID 83415
Telephone No.: (208) 526-8318

0526

energygram®

Electronic Communications Between Wang Office Information Systems and IBM 5520 Office System

DOE/TIC/EG-86/130
OFFICE OF SCIENTIFIC AND TECHNICAL INFORMATION

This technical note was based on research conducted by Idaho National Engineering Laboratory for the U.S. Department of Energy.

INEL
Idaho National Engineering Laboratory

A direct bridge between the previously incompatible Wang Office Information Systems and the IBM 5520 Information System has been designed to establish information transfer. This was done by using a Wang character translation table and a set of machine instructions developed at EG&G Idaho.

To accomplish the translation, information in the form of word processing documents is keyed into the Wang equipment, sent to the IBM Displaywriter, and sent, in turn, to the IBM 5520 Information System. The bridge was designed to eliminate the need for personnel operating the IBM Displaywriter equipment as in the communications link between the Wang equipment and the 5520. The new automated method of text transfer from one system to another is more cost effective as well as more convenient.

This technology has application to all sectors of industry using the Wang and/or IBM 5520 equipment. Duplication of effort in rekeying documents would be eliminated because the information can be transferred between the two pieces of equipment.

FOR ADDITIONAL INFORMATION

For additional information, contact:
Barbara Morris
EG&G Idaho, Inc.
P.O. Box 1625, TSA
Idaho Falls, ID 83415
Telephone No.: (208) 526-9285

or

Jane M. Welch
EG&G Idaho, Inc.
P.O. Box 1625
Idaho Falls, ID 83415
Telephone No.: (208) 526-8318

NASA Tech Brief

National Aeronautics and Space Administration

Licensing Opportunity

NASA's Jet Propulsion Laboratory, Pasadena, California

Maximum-Likelihood Decoder on a Hypercube Multiprocessor

Efficient parallel processing is used to implement complex decoders.

A hypercube multiprocessor connection scheme makes it practical to decode long convolutional codes with efficient use of hardware. The hypercube design reduces both the communication time among processors and the space needed for their interconnection. This decoding concept is applicable to concurrent processing of digital signals using convolutional codes for error correction.

A convolutional code produces encoded symbol sequences based on the input information bits and on the state of a finite-state machine with m memory cells. The task of the decoding algorithm (Viterbi algorithm) is to search among all possible received symbol sequences, which are corrupted by errors, and select the most likely transmitted sequence. Such a machine is called a maximum-likelihood decoder.

The complexity of the decoder increases exponentially with m, because it is necessary to compare the likelihoods of all possible 2^m sequences. For long codes (m >10), a single microprocessor is inadequate as a maximum-likelihood decoder.

A multiple-microprocessor system can be used to decode long codes. In a concurrent formulation, it is necessary to divide the algorithm into equal parts, to share equally the resources available in each processor, and to minimize the communication among the processors so that only nearest neighbors need to exchange messages. The hypercube configuration arises from topological considerations concerning the equivalence of networks: it turns out that a maximum-likelihood decoder can be constructed by connecting the processors to their nearest neighbors as though each processor was located at a vertex of an m-dimensional cube.

Each processor, at a given stage k, receives the surviving sequence and the accumulated metric (the measure of the likelihood of the surviving sequence) from its neighbor along dimension k of the hypercube. In practice, about 5m stages are required to obtain performance close to optimum. This corresponds to using the m dimensions of the hypercube five times. To minimize internode communications, the number of stages is increased slightly, enabling the input/output operations to be simplified and the decoded bits to be read out at node zero (the origin of the cube coordinate system).

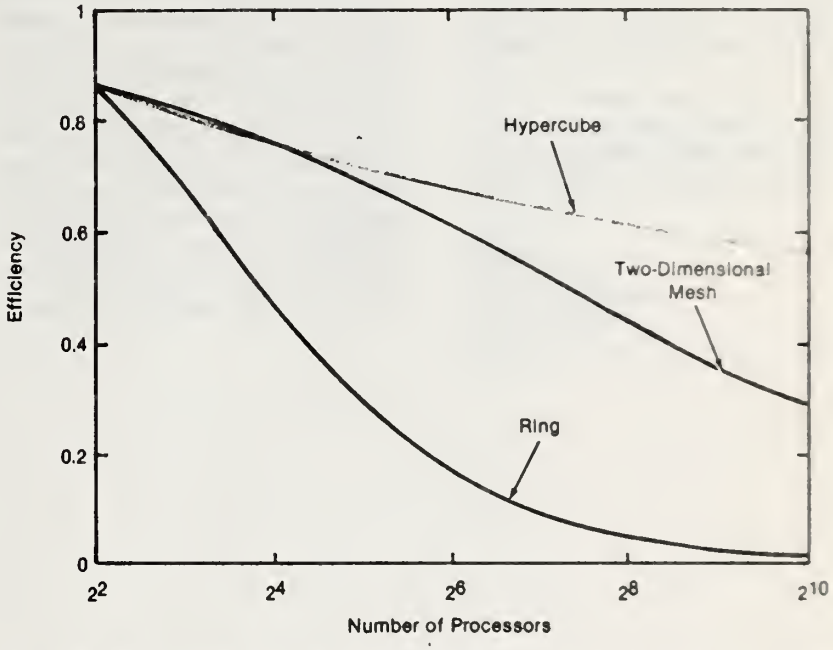

The Efficiencies of Different Decoder Configurations are shown as functions of the number of processors. The hypercube configuration gives the greatest speedup for maximum-likelihood decoding of long convolutional codes.

The decoding operation requires that blocks of data be loaded into every processor. In the hypercube network, data from the host processor are inserted only through node zero. These data are then broadcast throughout the hypercube by transmission between neighboring nodes.

In general, when the number of available processors 2^n is less than the number of states in the decoder 2^m, 2^{m-n} states can be assigned to each processor.

The efficiency, η, of a parallel architecture is related to the speedup factor, s, and to the number of processors, N, by $s = \eta N$. The figure compares the efficiencies of 2^{13}-state decoders having different interconnection configurations; each decoder has a communication time equal to the time for one operation. The hypercube configuration exhibits the greatest efficien-

cy for large decoders. Decoders for m up to 14 have been tested successfully on a 64-node hypercube multiprocessor.

This work was done by Fabrizio Pollara of Caltech for **NASA's Jet Propulsion Laboratory**.

This is the invention of a NASA employee, and a patent application has been filed. Inquiries concerning license for its commercial development may be addressed to the inventor, Mr. Edward Ansell (CIT Waiver), Director of Patents and Licensing, California Institute of Technology, Pasadena, CA 91125. Refer to NPO-16724./TN

Jet Propulsion Laboratory
Technology Utilization Manager:
Norman L. Chalfin
Mail Stop 201-110
4800 Oak Grove Drive
Pasadena, CA 91109
(818) 354-2240

FOR ADDITIONAL INFORMATION: *Contact: Director, Technology Transfer Division, P.O. Box 8757, BWI Airport, MD. 21240; (301) 621-0100 Ext. 241*

REFER TO THE NUMBER LISTED AT THE END OF THE ARTICLE

NASA Tech Brief
National Aeronautics and Space Administration

Listing Relationships Among Subroutines

Hierarchical charts of subprograms are generated.

The HIERARCHY program is a tool that assists users in obtaining information about the relationships among subroutines in a computer program. HIERARCHY uses the FORTRAN source code and load maps generated by the Cray FORTRAN compiler to generate tables of attributes for each module, including input and output operations, entry points, arguments, and NAMELIST's. These tables also describe the relationships of modules to modules and of modules to COMMON's.

The COMMON's, both labeled and unlabeled, are checked for consistent length. HIERARCHY will note the frequency distribution of calls to other modules and library or service routines. The program generates an optional hierarchical chart of subprograms to show how they relate to the main program. HIERARCHY can accommodate programs of up to 50 calls deep.

HIERARCHY is written in FORTRAN 77 for batch execution and has been implemented on a Cray X-MP computer operating under COS with a central-memory requirement of approximately 133K (octal) words. This program was developed in 1984.

This program was written by Clayton Guest of Informatics General Corp. for **Ames Research Center**. *ARC-11609 [illegible]*

FOR ADDITIONAL INFORMATION

CONTACT
COSMIC®
112 Barrow Hall
University of Georgia
Athens, GA 30602
(404) 542-3265

Electrotechnology

530 Wrist Radio Receiver Allows Personnel to Assemble Even in Rough Terrain

531 Modular Optical Amplifier—A multipass device amplifies the output of a laser without being excessively long.

532 Interface States in MOS Capacitors— States build up in two stages.

533 Radiation-Hardened Microcontroller

534 High-Spatial-Resolution Digital Ultrasonic Imaging System— Video-rate real-time imaging is possible.

535 Designing dc Inductors With Airgaps— Optimal parameters are obtained by designing near the saturation point.

536 Theory of Periodic-Binary-Sequence Generators— Algorithms yield feedback shift registers with maximum regularity.

537 Effects of Radiation on Capacitor Dielectrics— Data have been gathered on key design parameters.

538 Reinforced Masks for Ion Plating of Solar Cells— Long fingers would be held more rigidly. (Licensing Opportunity)

Testing & Instrumentation

539 Microdiagnostics for Prototype Instrumentation

540 Step Generator Offers Improved Features

U.S. Army Research

Natick RD&E Center, Natick, MA 01760

Wrist Radio Receiver Allows Personnel to Assemble Even in Rough Terrain

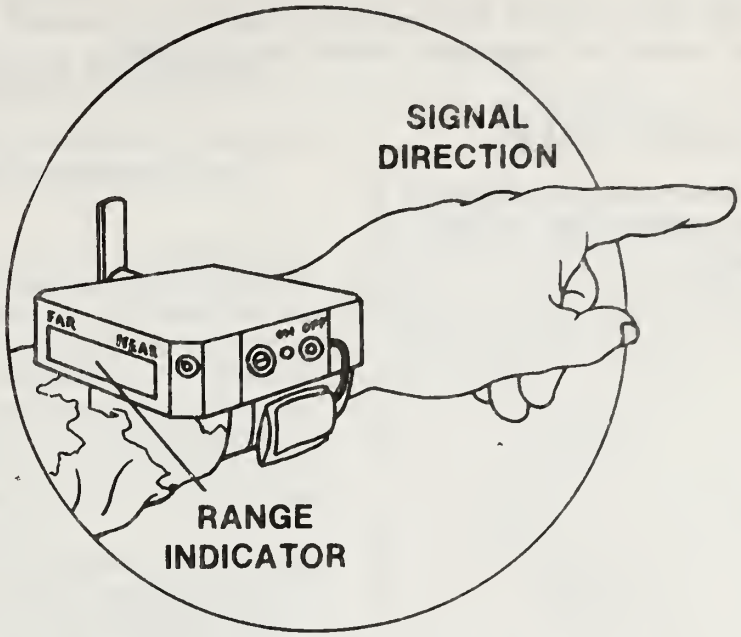

DROP ZONE ASSEMBLY AID SYSTEM (DZAAS)

For paratroopers just landing on a drop zone in the middle of unfamiliar territory, in rough terrain, at night to assemble as a unit as quickly as possible is quite a feat considering the confusion and dispersion that may occur. Natick Research, Development & Engineering Center's Aero-Mechanical Engineering Directorate, working on a USA Infantry School requirement, is developing a Drop Zone Assembly Aid system (DZAAS) to solve a problem which has existed for four decades.

DZAAS is the assembly aid system that has been likened to the Dick Tracy wrist radio. It is comprised of a rugged, two-component system--a transmitter and a receiver.

The transmitter is carried by an airborne group leader to the assembly point or is placed on a selected airdrop load and is set to turn on automatically.

The receivers are wrist-mounted with antennas that pick up the distinct signal from the transmitter. A LED light will turn on only when the receiver is pointed in the direction of the transmitter.

According to Project Officer, George Laliberte, engineering tests at the Electronic Proving Ground, FT Huachuca, AZ and Yuma Proving Ground, AZ confirmed that the system can "expeditiously locate the transmitter, even in rough terrain.

At FT Benning, GA and FT Bragg, NC, where the operational tests took place, test reports concluded that the "system appears to have high potential for improving

paratrooper assembly and recovery of airdropped equipment loads on the drop zone in the required 1500 meter range."

Among the test subjects were senior officers of the 82nd Airborne Division. Soldiers rated the DZAAS as "very easy to use in locating loads at night and simple to rig, operate and maintain." They preferred the DZAAS over assembly aids such as colored panels, helmet markings and strobe and chemical lights because the DZAAS eliminates visibility requirements.

While it used to take up to two to four hours to assemble an assault force, it now takes only 30 minutes on unfamiliar drop zones during day or night.

FOR ADDITIONAL INFORMATION:

U.S. Army Natick Research, Development &
Engineering Center, Natick, MA 01760
(617) 651-4300/5340.
Refer to No. 46-86/TN.

MANUFACTURING TECHNOLOGY NOTE

U.S. ARMY MATERIEL COMMAND

Deputy Chief of Staff for Manufacturing Technology, Alexandria, VA

Project Number: 1L161101A91A

Filing Code: 46C085

Modular Optical Amplifier

A multipass device amplifies the output of a laser without being excessively long.

An investigation by the U.S. Army Night Vision and Electro-Optics Center has demonstrated the feasibility of constructing multipass optical amplifier modules that can be easily attached to existing low-power oscillators such as those in rangefinders. The attachment of such a module would turn a rangefinder into a crosswind sensor or a designator transmitter, for example. The module would also allow the shape of pulses from the oscillator to be modified.

The new device is not just a simple extension of the resonator optical cavity. Clearly, a device 10 times as long as the present rangefinder transmitter would be unacceptable. Instead, the device is not part of a resonant cavity. It is, therefore, relatively insensitive to alignment — much less so than the laser-rangefinder oscillator itself.

Both a single-pass and triple-pass oscillator-amplifier module (see figure) were constructed in the investigation. The modules were transversely-excited atmospheric (TEA) lasers operating at a 10.6-μm wavelength.

Various preionization schemes were considered; of them, a series-connected sliding-arc arrangement proved to be the most satisfactory. Measurements were made of the voltage and current waveforms as well as of power, energy, and gain. Significant increases of peak power — by a factor greater than 2.5 — and a 10-percent pulse narrowing were observed. The feasibility of the modular device was thus established.

There is evidence that operation above atmospheric pressure would enhance the shortening of the pulses and boost power further. It might even be possible to select a specific laser spectral line for amplification by incorporating a grating within the amplifier.

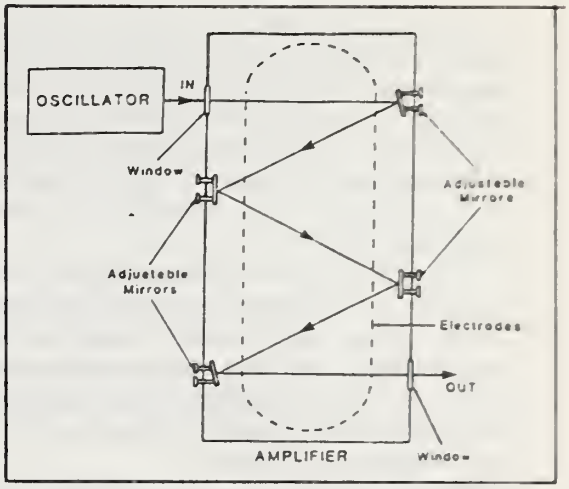

A **Triple-Pass Amplifier** consists of a transversely excited atmospheric laser. The electrodes, in the form of a series-connected sliding-arc arrangement, preionize the gas in the laser.

Project officer Jay Fox
(703) 664-6041 or AV 354-6041.

FOR ADDITIONAL INFORMATION

You can learn more details about this technology by ordering the NTIS report(s):
A Modular Amplifier for Mini-TEA Lasers.
Order number: AD-A166971/NAA
Price code: A02

Order from
National Technical Information Service
5285 Port Royal Road
Springfield, VA 22161

This document was prepared under the sponsorship of the U.S. Government. Neither the United States Government nor any person acting on behalf of the United States Government assumes any liability resulting from the use of the information contained in this document, or warrants that such use will be free from privately owned rights.

MANUFACTURING TECHNOLOGY NOTE

U.S. ARMY MATERIEL COMMAND

Deputy Chief of Staff for Manufacturing Technology, Alexandria, VA

Project Number: 1L161102AH44 Filing Code: 49B075

Interface States in MOS Capacitors

States build up in two stages.

A study has examined the buildup of interface states in Al/SiO_2/Si metal-oxide-semiconductor capacitors after exposure to pulsed electron-beam irradiation. The study by Harry Diamond Laboratories varied the polarity and magnitude of the field across the oxide during the two stages of the buildup — the early (10^{-6} to 1 s) and late (1 to 10^4 s) stages (see figure).

An empirical model of radiation-induced interface states at the SiO_2/Si interface was developed. The formulation, which explicitly addresses the time-dependent two-stage nature of the buildup process, gives the mathematical dependencies of the experimentally observed buildup with time, field, temperature, and dose.

The study found that many experimental observations of interface states generated by such stresses as holes from ionizing radiation, injected electrons, and high electric fields can be explained by a two-stage process. The first stage is the bulk release of a mobile species by the action of the stressing agent (holes, electrons, and high fields). The second, long-term, buildup stage is associated with the drift of the released mobile species to the interface, where a subsequent reaction results in the observable interface states. It seems likely that the mobile species is a water-related ion or defect — perhaps H^+ in the case of ionizing radiation.

Project officer F. Barry McLean
(202) 394-3070 or AV 290-3070.

FOR ADDITIONAL INFORMATION:

You can learn more details about this technology by ordering the NTIS report(s):
Physical Processes Associated With Radiation-Induced Interface States.
Order number: AD-A167280/NAA
Price code: A03

Order from
National Technical Information Service
5285 Port Royal Road
Springfield, VA 22161

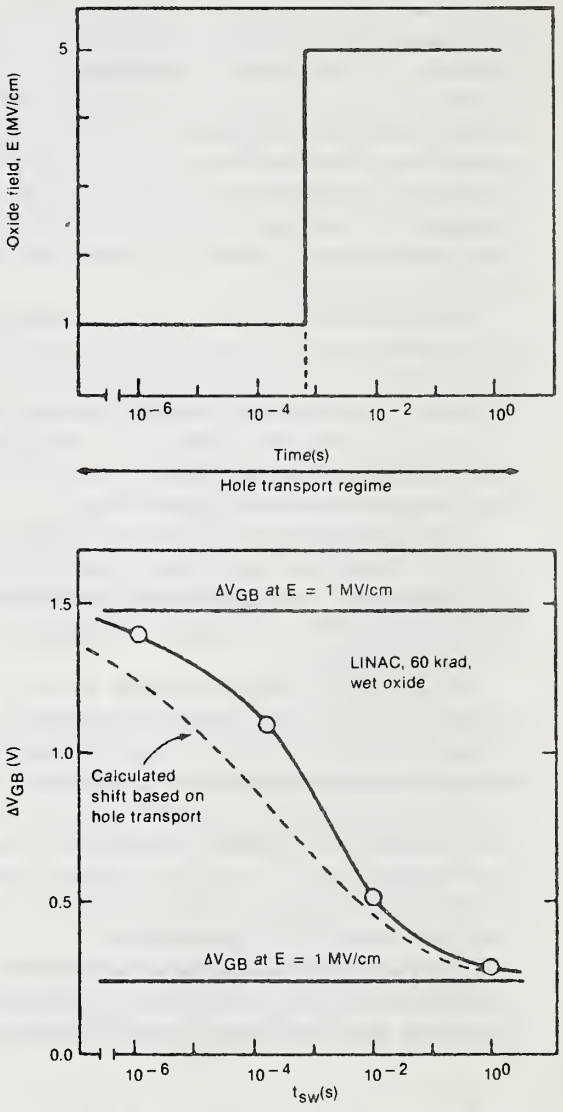

At a Predetermined Time, t_{SW}, the oxide field is switched from 1 to 5 MV/cm (top). The resulting increase in Gray-Brown shift V_{GB} is represented by the solid line (bottom). The dashed line is a calculation of the expected increase in V_{GB} based on details of hole transport.

This document was prepared under the sponsorship of the U.S. Government. Neither the United States Government nor any person acting on behalf of the United States Government assumes any liability resulting from the use of the information contained in this document, or warrants that such use will be free from privately owned rights.

Radiation-Hardened Microcontroller

Sandia National Laboratories and Intel Corporation have entered into an agreement that calls for the Labs' Center for Radiation-Hardened Microelectronics (CRM) to develop a radiation-tolerant version of Intel's 80C51 microcontroller.

The quarter-inch-square CMOS (complementary metal oxide semiconductor) circuit, with 2-micron feature sizes, will be able to withstand a total dose exposure of 1 million rads of ionizing radiation, 10 times more than the commercially available circuit. A rad is a unit of radiation energy absorption. A whole body dose of about 1,000 rads is typically fatal to humans.

The new very large scale integrated (VLSI) circuit will be suitable for use in a wider variety of Department of Defense and Department of Energy applications than is the current device. In addition, Sandia researchers believe that the radiation-hardened 80C51, which will have about 80,000 to 100,000 transistors, could have a variety of weapon control and space applications and that it also could be adapted for use in nuclear power plant safety systems.

Could activate safety operations

"For example, sensors could provide the microcontroller with information about pressure vessel conditions in a nuclear reactor," says Wilson Barnard, supervisor of Sandia's Special Processors Division. "The microcontroller then could activate appropriate safety operations, if conditions warrant."

Microcontrollers incorporate a central processing unit, random access memory, and a read-only memory on a single VLSI circuit. Designers tailor operations for real-time processing of incoming information and immediate activation of control functions based on that information. Microcontrollers have a more sophisticated logic decision-making capability than typical microprocessors. This makes them more appropriate for real-time data processing. Additionally, microprocessors usually require several separate chips to make a system. That increases costs and can reduce reliability.

The agreement calls for Intel to provide Sandia with its logic schematic and other design and definition details.

Prototype ready in a year

With that information, CRM researchers will then design the new version and produce an engineering prototype before the end of 1987. Plans then call for the first production circuits to be ready a year later. Fabrication

will be either at the fabrication plant of a commercial microelectronics firm or at the CRM.

In return, Sandia will supply Intel with all design and fabrication details necessary for it to manufacture the new circuit.

Radiation hardening, a process pioneered about 15 years ago at Sandia, involves fabricating circuits in extremely clean surroundings and tailoring the chemical and physical processes so that the degrading effects of radiation on the circuits are reduced.

Other keys to radiation-tolerant processing include the use of low-temperature processing during fabrication and careful circuit design techniques.

Uses static logic circuits

For example, Barnard says, conversion of the 80C51 to a radiation-hardened device will involve substituting static logic circuits for the original dynamic circuits, and circuit design charges that will permit the new device to operate over a much wider transistor performance range than the current version.

Sandia's interest in radiation-hardening began when scientists noticed that communications satellites suffered performance degradations after long periods in space.

Researchers have since determined that ionizing radiation causes a buildup of unwanted positive and negative electrical charges at the boundary between a CMOS transistor's silicon substrate and its adjacent silicon dioxide layer. These charges reduce a transistor's operating speed, meaning that a microprocessor will not be able to execute instructions at the required speed.

Sandia's CRM was established in 1981 for researchers to develop technologies and design capabilities for production of large-scale and very large-scale ICs capable of operating in high-radiation environments, and to transfer those capabilities to private industry for commercial production.

FOR ADDITIONAL INFORMATION

Public Information Division,
Code 3161,
Dept. of Energy,
Sandia National Laboratories,
Albuquerque, NM 87185-5800
(505) 844-4207.

MANUFACTURING TECHNOLOGY NOTE

U.S. ARMY MATERIEL COMMAND

Deputy Chief of Staff for Manufacturing Technology, Alexandria, VA

Project Number: 1A52F51D1A1A Filing Code: 76A006

High-Spatial-Resolution Digital Ultrasonic Imaging System

Video-rate real-time imaging is possible.

The U.S. Army Armament Research and Development Center has designed and partially prototyped an architecture for a high-resolution 256-channel ultrasonic imaging system (see figure). This system was designed to explore the quality of the images produced by practical-trapped-energy-mode, hybrid-trapped-energy-mode, and other types of arrays.

The system implements a 256-channel parallel set of analog-to-digital and digital-to-analog converters for attachment to an arbitrary array. All 256 channels operate simultaneously at a maximum sampling frequency of 10 MHz. Hence, the total throughput of sample signals reaches 2.5 billion samples per second in a "burst mode".

The multiple-ported dynamic random-access memory (DRAM) has 1×10^6 bytes of local high-speed storage. Because all of the input and output signals are in digital form, a wide variety of image-processing techniques can be employed. For example, from a single pulse, it is possible to reconstruct the two-dimensional hologram of the ultrasonic imaging through the use of fast digital hardware. The images can also be prepared by pulse-echo techniques, using the same system.

Transmission from one portion of the array and monitoring the signal in another portion simultaneously to detect interelement coupling is possible. In this way, all of the key array parameters can be controlled and calibrated. Because of the digital-to-analog capability of the system, various signals can be transmitted from each array element, thereby permitting focusing and design of optimum probing signals.

Project officer G. Capsimalis
(518) 266-5641 or AV 974-5641.

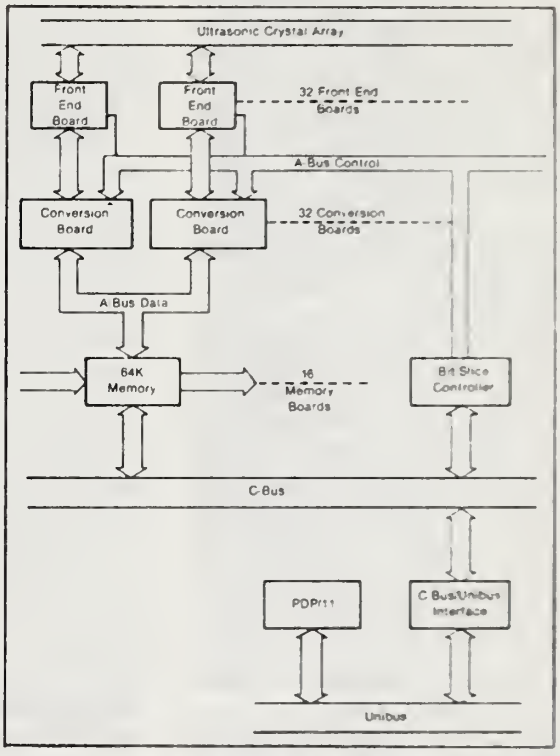

A 256-Channel Ultrasonic Imaging System, the overall architecture of which is shown, was designed to investigate the quality of the images resulting from energy trapping as a means of enhancing the spatial confinement of element radiation in the ultrasonic array.

FOR ADDITIONAL INFORMATION

You can learn more details about this technology by ordering the NTIS report:
A High Spatial Resolution Digital System for Ultrasonic Imaging
Order number: AD-A166741/NAA
Price code: A02

Order from:
National Technical Information Service
5285 Port Royal Road
Springfield, VA 22161

This document was prepared under the sponsorship of the U.S. Government. Neither the United States Government nor any person acting on behalf of the United States Government assumes any liability resulting from the use of the information contained in this document, or warrants that such use will be free from privately owned rights.

NASA Tech Brief
National Aeronautics and Space Administration
NASA's Jet Propulsion Laboratory, Pasadena, California

Designing dc Inductors With Airgaps

Optimal parameters are obtained by designing near the saturation point.

An iterative procedure aids the design of dc inductors with airgaps in the cores (see figure). For a given core area and length, the technique gives a design having the specified inductance and the peak flux density in the core, using the minimum required copper weight. The new technique is superior to the previous trial-and-error technique, which often resulted in cores larger than necessary or in less inductance than could be obtained from a core of given size. Typical applications include lightweight inductors for aircraft electronics.

The new approach is based on the full use of the core: The inductor is designed to operate at the saturation flux density of the core material (or at another maximum flux density related to the saturation value). Subject to this constraint, the airgap length, g, and the number of turns, N, are selected to give the required inductance, L. Because there is only one combination of g and N that will satisfy the inductance and saturation criteria for a given core, the procedure quickly leads to an optimal design.

The procedure depends on the fact that N/g is nearly constant, regardless of variations in L, for practical inductor dimensions and core materials. At first, the designer knows the maximum coil current, I; the cross-sectional core area, A; the incremental relative permeability, μ_s, of the core material at the operating point; the maximum flux density, B; the core length, m; and the dc relative permeability, U_s, at the operating point.

The first step is to select a trial airgap, g_1. (Typical gap sizes lie between 0.01 and 0.25 cm.) The designer calculates the initial value, F_1, of the fringing-flux factor, F: This factor depends on g_1 and the other core dimensions. The initial number of turns is then determined from

$$N = \frac{B(g_1 + m/U_s)}{(0.4\pi I)(F_1)}$$

Next, the designer calculates the initial inductance from

$$L_1 = \frac{0.4\pi(N_1)^2(AF_1)}{g_1 + m/\mu_s}$$

If L_1 differs from L by more than the tolerance, then a second airgap length is estimated from $g_2 = g_1 L/L_1$. The preceding sequence of calculations is then repeated to find F_2, N_2, and L_2. These iterations are continued until the computed inductance is sufficiently close to L. Most designs require one to three iterations to bring the inductance within 1 percent of L. The procedure can be executed rapidly on a programmable, hand-held calculator.

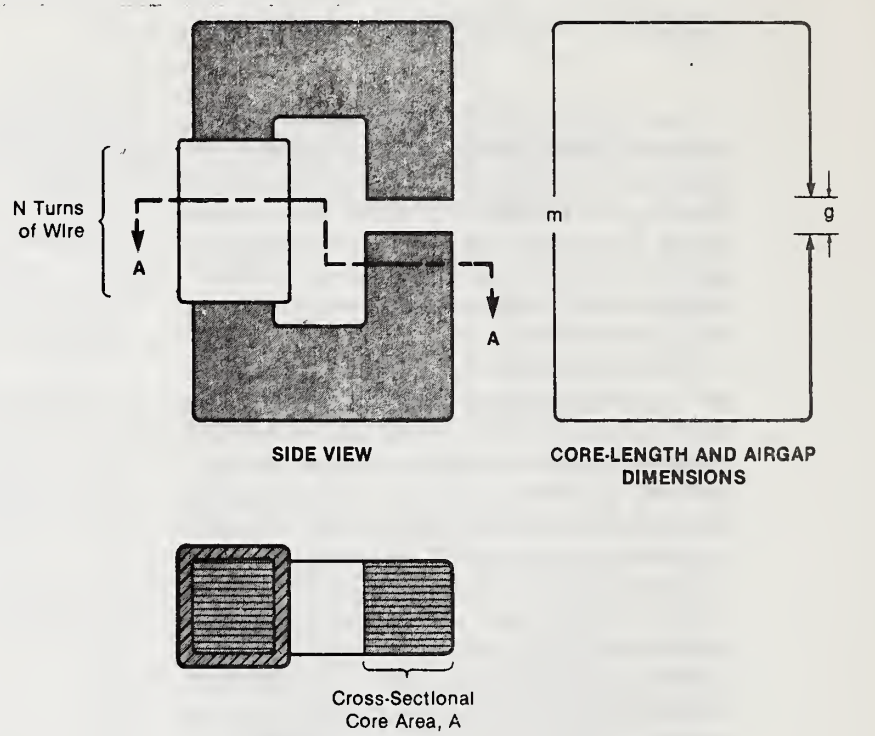

This **Inductor With a C-Shaped Core** is an example of the types that can be designed with the iterative procedure.

This work was done by Albert P. Wagner of Caltech for **NASA's Jet Propulsion Laboratory**.

NPO-16739 /TN

FOR ADDITIONAL INFORMATION: *Contact: Director, Technology Transfer Division, P.O. Box 8757, BWI Airport, MD. 21240; (301) 621-0100 Ext. 241*
REFER TO THE NUMBER LISTED AT THE END OF THE ARTICLE

NASA Tech Brief

National Aeronautics and Space Administration

Theory of Periodic-Binary-Sequence Generators

Algorithms yield feedback shift registers with maximum regularity.

A report provides an extensive mathematical treatment of new and previous results related to the generation of pseudo-noise binary sequences by feedback shift registers. The generator architectures are amenable to efficient implementation in very-large-scale integrated (VLSI) circuits. The report includes literature references to applications of such sequences in random-number generation, radar, VLSI testing, data encryption and decryption, algebraic error-detection and error-correction encoding and decoding, and feedback-shift-register synthesis of sequential machines.

Polynomials of degree r over a Galois field characteristic 2 [GF(2)] represent the behavior of shift registers with linear feedback. The object of the report is the algorithmic determination of the trinomial of lowest degree, when it exists, that contains a given irreducible polynomial over GF(2) as a factor. This corresponds to embedding the behavior of an r-stage shift register with linear-logic feedback into that of an n-stage shift register (n usually > r) with a single two-input exclusive OR gate in its feedback loop. The architecture of such feedback shift registers has maximum regularity (i.e., identical cells), with intercell communications serialized to a maximum degree.

Sections 1 and 2 of the report contain a thorough exposition of background material on Galois-field algebra, including cyclotomic theory. Section 3 develops logical-circuit theory of feedback shift registers. Two types of feedback shift registers are considered. The state behavior of shift registers with linear-logic feedback to a single stage is related to the mathematical properties of the characteristic polynomial of a linear recurrence relationship between the bit being fed back and the content of stages contributing to the feedback. The state behavior of shift registers with interstage linear-logic feedback is related to successive powers of the inverse of the root of the characteristic polynomial. A one-to-one correspondence between the successive states of two types of feedback shift registers associated with the same characteristic polynomial is derived.

The extensive collection of theorems and lemmas on the properties of classes of polynomials over GF(2), contained in Section 4, are the principal contributions of the report. The fruit of this work, presented in Appendixes B and C, is the compilation of polynomials (primitive and irreducible nonprimitive) and trinomials of lowest degree that, respectively, contain the foregoing polynomials as factors. The trinomials characterize feedback shift registers of maximum regularity and linear-logic feedback circuitry of minimum complexity for generating periodic binary sequences associated with the polynomial factors.

Number-theoretic functions including the Euler phi function and the Mobius function are briefly discussed in Appendix A because of their applicability to feedback shift-register theory. Appendix B exhaustively considers primitive polynomials over GF(2) through degree 12. It is proven in Section 4 that trinomials exist that contain any given primitive polynomial as a factor. Furthermore the trinomial of lowest degree is square free; i.e., its irreducible factors are distinct. Irreducible factors, determined by Berlekamp's factorization algorithm, of each (lowest degree) trinomial of degree less than 70 containing a given primitive polynomial as a factor are listed. Within the list are factors having degrees as high as 52. Also noted are the results of testing each additional factor to ascertain if the lowest-degree trinomial that contains a given primitive polynomial (of degree 12 or less) is also the lowest-degree trinomial that contains the factor in question. This leads to the extension of the table to a partial listing of primitive polynomials of degree 13 through 19 and of the respective trinomial that contains each as a factor. Appendix C deals with irreducible nonprimitive polynomials over GF(2) through degree 12. In contrast to primitive polynomials, there are many irreducible nonprimitive polynomials that are not a factor of existing trinomials.

In Section 4, a sufficient but nonnecessary condition is proved that guarantees the existence of one or more trinomials containing a given irreducible nonprimitive polynomial as a factor. Of these trinomials, those of lowest degree are square free. As in Appendix B, the irreducible factors of each (lowest degree) trinomial of degree less than 70 are listed. Among these are factors whose degrees are as high as 56. Also noted are the results of testing each additional factor to determine if the trinomial of lowest degree containing a given irreducible nonprimitive polynomial (of degree 12 or less) is also the lowest degree trinomial to contain the factor in question. The tables in Appendixes B and C enable one to design a feedback shift register with a single two-input exclusive OR gate in its feedback to generate periodic binary sequences. The structure and period of the sequence are governed by the mathematical properties of the characteristic polynomial selected from the tables.

This work was done by Marvin Perlman of Caltech for **NASA's Jet Propulsion Laboratory**. *Further information may be found in NASA-CR-175649 [N85-22886/NSP], "Periodic Binary Sequence Generators: Very Large Scale Integrated (VLSI) Circuits Considerations."*

Copies may be purchased from the National Technical Information Service, Springfield, Virginia 22161, [4/87] NPO-16628 /TN

FOR ADDITIONAL INFORMATION: *Contact: Director, Technology Transfer Division, P.O. Box 8757, BWI Airport, MD. 21240; (301) 621-0100 Ext. 241*

REFER TO THE NUMBER LISTED AT THE END OF THE ARTICLE

NASA Tech Brief
National Aeronautics and Space Administration

Effects of Radiation on Capacitor Dielectrics

Data have been gathered on key design parameters.

A report discusses a study of the electrical and mechanical properties of irradiated polymer dielectric materials. These data were compiled for use by designers of high-energy-density capacitors that operate in the presence of ionizing radiation.

The study focused on polycarbonates, polyetheretherketones, polymethylpentenes, polyimides (including polyetherimide), polyolefins, polysulfones (including polyethersulfone and polyphenylsulfone), and polyvinylidene fluorides. The properties considered were the dielectric loss factor or loss tangent, tensile strength, dissipation factor, volume resistivity, surface resistivity, dielectric constant, gas evolution (during irradiation), and mechanical-strength parameters. Recent test data, previously unpublished, were obtained from both foreign and domestic industry sources. Measurements of properties before, during, and after irradiation were sought. Radiation doses from zero to as much as 10^{10} rad were considered.

The data are presented in tables, graphs, and in text. The report also includes references to the published literature, diagrams of the molecular structures of the polymers studied, definitions of abbreviations, and a glossary.

On the basis of the compiled data, the study reached the following conclusions:

- The polyetheretherketones, polymethylpentenes, polyimides, and polysulfones retain their mechanical strengths at the highest radiation levels.
- The lowest dissipation factors were exhibited by polyetheretherketones, polymethylpentenes, and polyimides.
- Polyethylene and polypropylene should probably not be used, because they emit undesirable amounts of gases when irradiated.
- Of the materials studied, the polyimides and polyetheretherketones are the best materials for use in high energy-density capacitors.

This work was done by Frank L. Bouquet, Robert B. Somoano, and Peter O. Frickland of Caltech for **NASA's Jet Propulsion Laboratory**. *"Dielectric Materials for High Energy Density Capacitors," NPO-16761/TN*

FOR ADDITIONAL INFORMATION: *Contact: Director, Technology Transfer Division, P.O. Box 8757, BWI Airport, MD. 21240; (301) 621-0100 Ext. 241*
REFER TO THE NUMBER LISTED AT THE END OF THE ARTICLE

NASA Tech Brief
National Aeronautics and Space Administration
NASA's Jet Propulsion Laboratory, Pasadena, California

Licensing Opportunity

Reinforced Masks for Ion Plating of Solar Cells

Long fingers would be held more rigidly.

A proposed mask for the ion plating of surface electrodes on silicon solar cells would be reinforced to hold its shape better during handling. The need for reinforcement arises in a typical conventional mask (see Figure 1), because it includes long fingers that are unsupported at their ends.

The fabrication process for the improved mask would be similar to that of a conventional mask. However, additional cuts and bends would be made in the wide diametral strip (see Figure 2) to form bridges between pairs of mask fingers facing each other across this strip. The bridges would be high enough not to act as masks so that the entire strip area would still be plated.

This work was done by William R. Conley, E. Grant Swick, and Jack C. Volkers of Illinois Tool Works, Inc., for **NASA's Jet Propulsion Laboratory**.

This invention is owned by NASA, and a patent application has been filed. Inquiries concerning nonexclusive or exclusive license for its commercial development should be addressed to the Patent Counsel, NASA Resident Office-JPL. Refer to NPO-16417 /TN

Jet Propulsion Laboratory
Technology Utilization Manager:
Norman L. Chalfin
Mail Stop 201-110
4800 Oak Grove Drive
Pasadena, CA 91109
(818) 354-2240

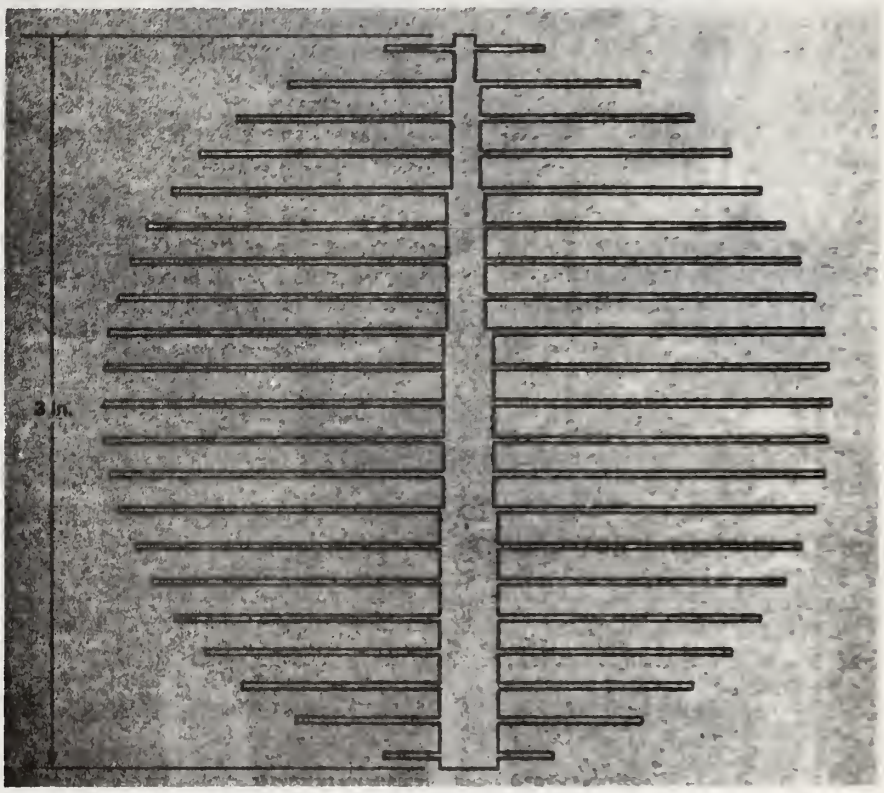

Figure 1. A **Typical Conventional Mask** is made from a thin sheet of steel by cutting out parallel narrow grooves and a wider perpendicular strip. The ends of the remaining metal strips at the edge of the wide cutout strip are unsupported.

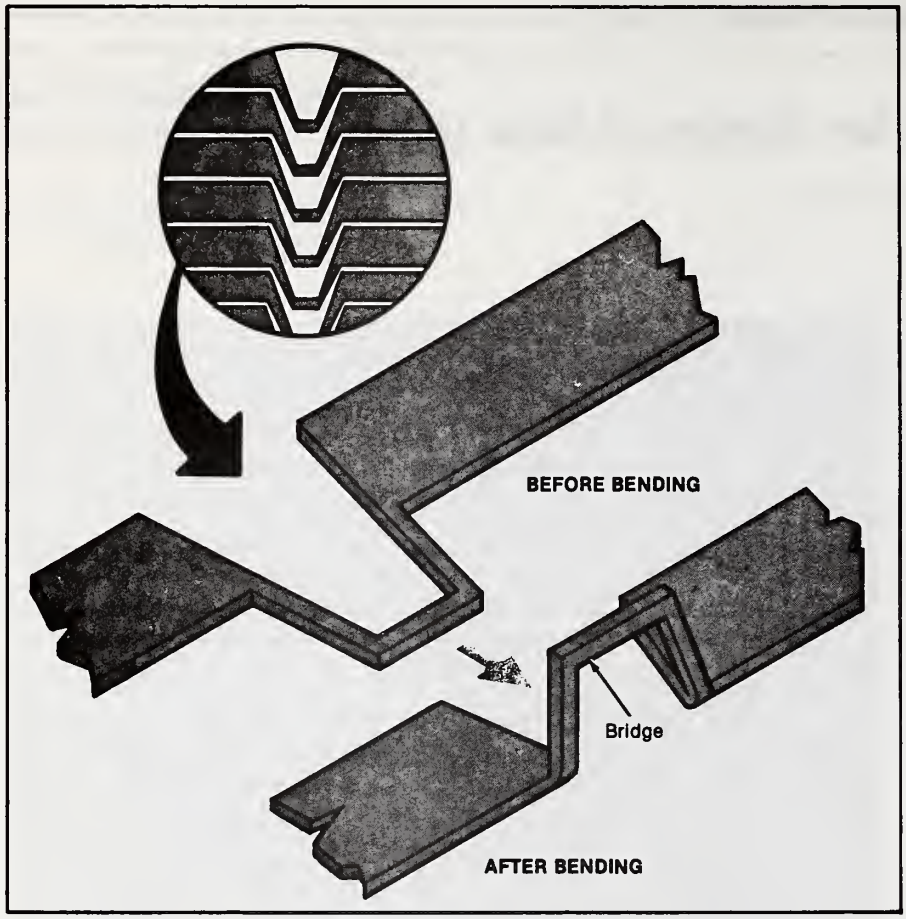

Figure 2. The **Reinforced Mask** is cut so that nesting bridges of metal are formed across the wide cutout strip, connecting the ends of the remaining metal strips. The bridges are then bent out of the mask plane.

FOR ADDITIONAL INFORMATION: *Contact: Director, Technology Transfer Division, P.O. Box 8757, BWI Airport, MD. 21240; (301) 621-0100 Ext. 241*

REFER TO THE NUMBER LISTED AT THE END OF THE ARTICLE

energygram

Microdiagnostics for Prototype Instrumentation

DOE/TIC/EG-86/111
OFFICE OF SCIENTIFIC AND TECHNICAL INFORMATION

This technical note was based on research conducted by Idaho National Engineering Laboratory for the U.S. Department of Energy.

INEL
Idaho National Engineering Laboratory

Research has resulted in a diagnostic technique called microdiagnostics, which enables a digital microprocessor-based electronic instrument to test all or part of itself with little user interaction and without the need of external test equipment.

Microdiagnostics is presented as a set of design rules and guidelines which assist the design engineer in implementing automatic fault diagnostics into his designs. Microdiagnostics allows the user of an electronic system to locate and repair hard system faults by stimulating the system under test, compressing the resulting test data, and presenting the test results to the user in simple, meaningful messages.

Microdiagnostics utilizes the resources of the existing central processing unit to make all test decisions. These decisions are based on a data compression technique known as signature analysis. Fault location consists of comparing good signatures obtained from a known good circuit with measured signatures of an identical system under test. If key signatures on the circuit under test match the good signatures, the circuit is assumed to be fault free. If any signatures do not match the ones produced by a known good circuit, the circuit under test has failed and a fault backtracking algorithm is automatically executed to isolate the fault. Microdiagnostics does not use an external signature analyzer but implements signature analysis as part of the system software.

A system that uses microdiagnostics becomes an "expert system" which automatically directs the user through the fault detection process until a fault is isolated. Microdiagnostics frees the troubleshooter from dependence on schematics, wire lists, and signature tables.

Microdiagnostics can be built into a system to improve reliability, availability, and maintainability; to reduce downtime, to extend operational lifetime; to lower maintenance costs; and to eliminate the need of an expert to accomplish repair. Empirical fault coverage data indicate that around 95% of the single stuck-at-faults can be detected by using microdiagnostics.

The technique is applicable to a wide variety of microprocessor-based instruments and controls.

FOR ADDITIONAL INFORMATION

DOE report(s):
Microdiagnostics for Prototype Instrumentation.
Report number: EGG-EA-7091/NAB
Order number: DE86005320/NAB
Price: $16.95

Order from:
National Technical Information Service
5285 Port Royal Road
Springfield, VA 22161

For additional information, contact:
J. M. Welch
EG&G Idaho, Inc.
P.O. Box 1625
Idaho Falls, ID 83415
Telephone No.: (208) 526-8318

or

Gary C. Bergeson
EG&G Idaho, Inc.
P.O. Box 1625
Idaho Falls, ID 83415
Telephone No.: (208) 526-8211

NBS technology update

National Bureau of Standards
U.S. Department of Commerce
Gaithersburg, MD 20899

Step Generator Offers Improved Features

Three NBS researchers have developed a calibration standard for transient waveform recorders that is an improvement over existing commercial instruments in either accuracy or variability of voltage levels. Transient waveform recorders are used to measure rapid voltage pulses in applications such as research into automotive engine performance or the testing of electric power equipment for its vulnerability to lightning. These instruments also play key roles in nuclear fusion research and weapons testing. The device generates precise, fully programmable voltage steps which exhibit fast transitions and exceptionally smooth settling to the final voltage value.

FOR ADDITIONAL INFORMATION: Technical details about the step generator's design are available from T. Michael Souders, B162 Metrology Building, National Bureau of Standards, Gaithersburg, MD 20899; (301) 975-2406.

Energy

541 Miniature Thermal Battery— Component matches performance of larger units.

542 Advanced Research and Technology Development—Low-Rank Coal Physical Properties, Moisture, and Distribution of Inorganics

543 Recovering Heavy Oil by Carbon Dioxide Gas Immiscible Flooding

544 Energy from Biomass: Building on a Generic Technology Base

545 Small-Hydropower Development: The Process, Pitfalls, and Experience: Guide for Developers

546 Fuel-Cell Structure Prevents Membrane Drying— Embossed plates direct flows of reactants and coolant. (Licensing Opportunity)

547 Liquid-Hydrogen Polygeneration System— The system utilizes coal as an alternate chemical feedstock. (Licensing Opportunity)

Software

548 Evaluating Performances of Solar-Energy Systems— Efficiencies can be calculated and maximized.

Other items of interest

538 Reinforced Masks for Ion Plating of Solar Cells— Long fingers would be held more rigidly. (Licensing Opportunity)

550 Water Heater/Cooler for Vehicles— At the press of a button, thermoelectric unit changes from a heating device to a cooling device.

564 Modified Generator Puts Out More Power with Less Noise

585 Behavior of Pressurized Incoloy 800H Tubes in Environments Pertaining to Coal Gasification

MANUFACTURING TECHNOLOGY NOTE

U.S. ARMY MATERIEL COMMAND

Deputy Chief of Staff for Manufacturing Technology, Alexandria, VA

Project Number: 65801A

Filing Code: 97D048

Miniature Thermal Battery

Component matches performance of larger units.

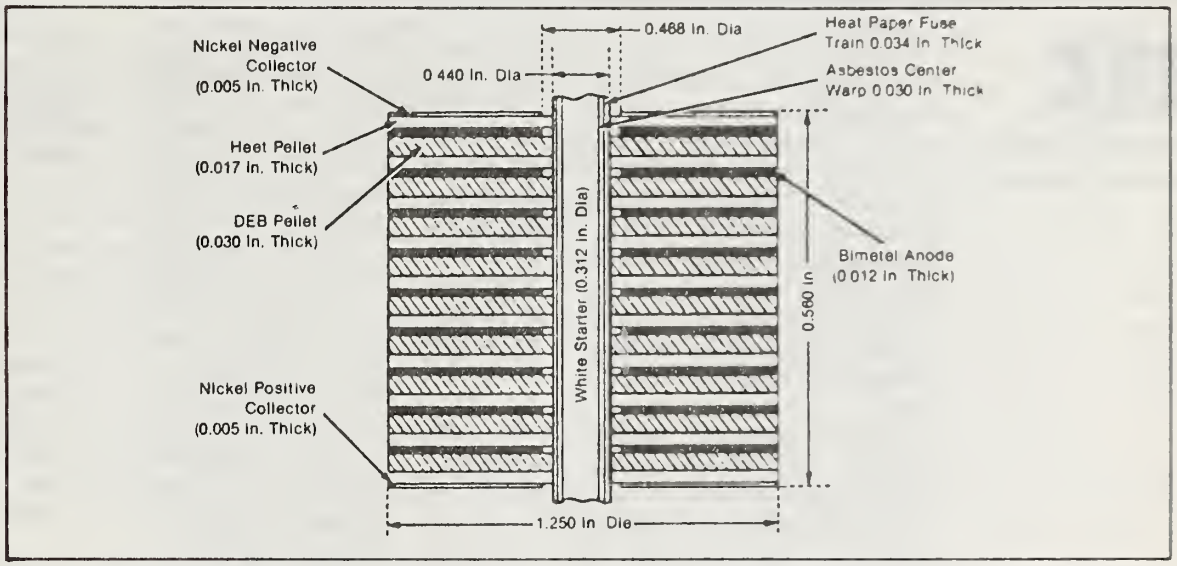
Nickel Negative Collector (0.005 In. Thick)
Heet Pellet (0.017 In. Thick)
DEB Pellet (0.030 In. Thick)
Nickel Positive Collector (0.005 In. Thick)
0.440 In. Dia
0.468 In. Dia
Heat Paper Fuse Train 0.034 In. Thick
Asbestos Center Warp 0.030 In. Thick
White Starter (0.312 in. Dia)
Bimetel Anode (0.012 In. Thick)
0.560 in
1.250 In. Dia

A **Pyrotechnic Starter** is at the center of a stack of cells. When the starter is fired, it heats the cells. The frozen electrolyte melts, and the cells can release their stored electrical energy.

The PS132 thermal battery is one of the smallest batteries of its kind capable of meeting its current, voltage, and lifetime requirements. The battery, developed at the U.S. Army Harry Diamond Laboratories, uses a Ca/LiCl-KCl eutectic-SiO_2/$CaCrO_4$ electrochemical system with pressed-pellet technology.

The electrolyte is frozen solid at all anticipated storage temperatures (−54 to +74 °C); therefore the cells remain chemically inert during storage. No significant chemical degradation occurs during extended storage — as long as 25 years. When a thermal battery is to be activated (see figure), a pyrotechnic heat source within each cell raises the cell temperature to 400 to 600 °C, the frozen electrolyte melts, and the battery operates like any other voltaic battery system until the cells cool.

Four hundred PS132 batteries have been built and tested. Each battery is required to deliver 18 to 26 V and to operate at a current of 15 mA for 120 seconds and deliver brief pulses of 1 to 2.5 A for millisecond periods. It is packaged as a right circular cylinder 1.625 in. (4.13 cm) in diameter and 1.5 in. (3.8 cm) tall. Its small size and relatively long life are made possible by using thin electrochemical cells, low current density, and a high maximum cell-operating temperature.

FOR ADDITIONAL INFORMATION

You can learn more details about this technology by ordering the NTIS publication:

Development and Operating Characteristics of the PS132 Thermal Battery
Order number: AD-A165149/NAA
Price code: A03

Order from:
National Technical Information Service
5285 Port Royal Road
Springfield, VA 22161

This document was prepared under the sponsorship of the U.S. Government. Neither the United States Government nor any person acting on behalf of the United States Government assumes any liability resulting from the use of the information contained in this document, or warrants that such use will be free from privately owned rights.

energygram®

Advanced Research and Technology Development—Low-Rank Coal Physical Properties, Moisture, and Distribution of Inorganics

DOE/TIC/EG-86/072
OFFICE OF SCIENTIFIC AND TECHNICAL INFORMATION

This technical note was based on an Application Assessment Record from the Morgantown Energy Technology Center, Office of Fossil Energy, for the U.S. Department of Energy.

METC
Morgantown Energy Technology Center

Technology Description. The program objectives are to provide information on the properties of low-rank coal applicable to its preparation, handling, and combustion. Information is being developed on mechanical properties, distribution of water before and after drying, the inorganic species that affect coal, combustion rates and temperatures of low-rank coal particles, adherence of low-rank coal fly ash to heat-exchange surfaces, and oxidation rates and explosive limits of low-rank coal dust.

Specific tasks will address bulk properties, particle hardness, structural order, chemical fractionation, geochemical relations between coal inorganics and the geological environment, moisture sorption rates, shrinking and swelling, pore size distribution, and evaluation of organic functional groups. Bulk properties to be investigated include shear strength of coal and coke, thermal and mechanical friability, and packed-bed permeability. Particle hardness, which affects erosion behavior, will be given a numerical ranking. Extended analytical procedures to chemically fractionate inorganic species will be developed. Moisture sorption rates will be evaluated microscopically and by low-angle X-ray scattering. Organic functional groups will be analyzed to determine their dependence on thermal history and their role in binding inorganics. This research will identify fundamental mineralogy and chemical compositions of particulate ash, temperature profiles, and factors affecting carbon burnout.

The composition and strength of fly ash deposits on flat plate alloys will be determined as a function of temperature and combustion atmosphere. Flame propagation rates and coal surface reactivity will be obtained for finely divided lignite and subbituminous coal. The electrical behavior of low-rank coal particles will be examined by studying their dielectric behavior, capacitance, and surface characteristics.

Why Is This Better Than Existing Technology? This data base provides the low-rank coal property data, currently not available, that are important to coal utilization.

Stage of Development. Basic science.

Potential Uses and Spinoffs. Possible applications are improved design of coal feed and combustion systems, selective coal mining, effective thermal dewatering of coal, and development of analytical methods.

FOR ADDITIONAL INFORMATION

DOE report(s):

C. Tye, R. M. Neumann, and H. H. Schobert, The Uses of Dielectric Spectra and Immersional Calorimetry in the Characterization of Low-Rank Coals. ACS Fuel Division Preprints.
Report number: DOE/FE/60181-114/NAB
Order number: DE85003165/NAB
Price: $9.95

Morgantown Energy Technology Center Proceedings of the 13th Biennial Lignite Symposium on Technology and Utilization of Low-Rank Coal, Vols. 1 and 2.
Report number: DOE/METC-86/6036-Vol. 1/NAB
Order number: DE86001076/NAB
Price: $28.95

Report number: DOE/METC-86/6036-Vol. 2/NAB
Order number: DE86001077/NAB
Price: $28.95

Order from:
National Technical Information Service
5285 Port Royal Road
Springfield, VA 22161

For additional information, contact:
H. F. Bauer
Grand Forks Project Office
Morgantown Energy Technology Center
P.O. Box 7206, University Station
Grand Forks, ND 58202
Telephone No.: (701) 795-8195

energygram®

Recovering Heavy Oil by Carbon Dioxide Gas Immiscible Flooding

DOE/TIC/EG-86/148
OFFICE OF SCIENTIFIC AND TECHNICAL INFORMATION

This technical note was based on research conducted by the National Institute for Petroleum and Energy Research for the U.S. Department of Energy.

National Institute for Petroleum and Energy Research

Gas displacement methods of enhanced oil recovery (EOR) include two types of processes: miscible and immiscible. In miscible recovery the injected gas (hydrocarbon, CO_2 and N_2) dissolves completely in the oil and thus creates a low-viscosity fluid that can be driven to producing wells. However, miscibility cannot be achieved if the crude contains a high percentage of heavy hydrocarbons or if the reservoir pressure is lower than the minimum miscibility pressure.

Immiscible gas displacement does not require that the injected gas and crude oil mix become a single phase. It requires only that the oil's viscosity be reduced enough to allow efficient mobilization through the reservoir to producing wells. That carbon dioxide has excellent viscosity reducing properties is known, but more information is needed about the effect on overall oil recovery. The scarcity of published work on immiscible displacement indicates a severe lack of knowledge about the immiscible gas displacement process.

NIPER Research. At the National Institute for Petroleum and Energy Research (NIPER), research scientists and engineers have extended research on the large deposits of extant heavy oil in U.S. reservoirs beyond the reach of current enhanced oil recovery (EOR) technology.

Through support from the Department of Energy and industry, NIPER began a 3-year research program on gas displacement methods in fiscal year 1985 to improve the recovery efficiency of the carbon dioxide immiscible gas displacement process by developing more effective injection strategies. During the first year the research was focused on the study of immiscible displacement mechanisms and methods of predicting oil viscosity reduction and carbon dioxide solubility.

During the second year (fiscal year 1986) work is being devoted to laboratory coreflood tests to investigate the recovery efficiency for various injection schemes—continuous carbon dioxide injection, carbon dioxide/water (WAG) or water alternating with gas injection, cyclic carbon dioxide injection, and carbon dioxide/hot-water alternate injection.

Coreflood tests are being continued while the research team develops improved screening criteria for carbon dioxide application based on computer modeling of the carbon dioxide flooding process in varied types of reservoirs. Special coreflood tests are being performed using nitrogen in combination with carbon dioxide to investigate the effect of nitrogen on the recovery efficiency of CO_2 immiscible displacement. In addition, experiments are being performed to determine the effects of temperature, pressure, and water saturation on recovery efficiency. All the carbon dioxide injection strategies in this research at NIPER are directed toward a single objective: efficient mobilization of heavy oil.

The Technology. Carbon dioxide immiscible flooding has been effective in producing heavy oil in large-scale field tests in California, Arkansas, Mississippi, and Texas. The crude oils from these fields are heavy—below 25 degrees American Petroleum Institute (API) gravity. Carbon dioxide was successfully used in these field tests because it triggers several mechanisms that result in crude oil displacement.

Viscosity reduction is the primary mechanism in the practical mobilization of heavy oil by carbon dioxide injection. Oil viscosity for nine heavy crudes (10 to 22 degrees API gravity) has been measured with and without CO_2 saturation. The results showed that a reduction of one to two orders of magnitude of original oil viscosity can be achieved when oil is saturated with carbon dioxide at pressures above 1000 psi. A correlation for predicting viscosity reduction for carbon dioxide flooding process design and for numerical modeling has been developed.

The solubility of carbon dioxide in crude oil is also an important mechanism in the carbon dioxide flooding process. NIPER investigators found that, by saturating the reservoir oil with carbon dioxide at high

pressure and then reducing the pressure, released gas would expand and push the oil out of the pores in the reservoir rock

Another characteristic of carbon dioxide is its ability to extract heavy hydrocarbons from crude oil. This mechanism allows oil trapped in dead-end pores to be recovered and reduces carbon dioxide mobility through the reservoir. Also, the carbon dioxide gas can be recovered from the produced field and reinjected into the reservoir.

Heavy Oil Resource. Estimates of original oil-in-place deposits of heavy oil in U.S. reservoirs range from 85 to 110 billion barrels. The largest deposits are in California and Alaska, but heavy oil exists in other parts of the country, including the Mid-Continent. Sizeable heavy oil accumulations are in the tri-state area of Oklahoma, Kansas, and Missouri.

Generally, heavy oil refers to a crude oil having an API gravity lower than 20 degrees. Consisting of a high percentage of asphaltenes, heavy oil is highly viscous, dark, and resists mobilization. For heavy oil to be made less viscous, and thus more mobile, its chemical or physical properties must be changed.

In the large oilfields of California's Kern County, which produces most of the heavy oil in the United States, heat is used as the viscosity reducing agent. Steamflooding and in situ combustion account for production of some 400,000 barrels of heavy oil per day, but both of these thermal recovery methods have disadvantages. Steamflooding is expensive, subject to stringent air pollution laws, and not currently amenable to deep reservoirs. In situ combustion and steamflooding can burn up profit margins by using as much as a third of the oil-in-place as fuel (or that equivalent) for the recovery process.

The vast disparity between the amount of heavy oil available and the amount produced indicates that alternate technologies are needed to fully exploit the resource. Carbon dioxide immiscible displacement, considered to be an effective and less expensive process for heavy oil recovery than thermal methods, may be the key to unlocking the door to economical heavy oil production.

FOR ADDITIONAL INFORMATION

DOE report(s)

T. H. Chung. Heavy Oil Recovery by Immiscible Displacement Method
Report number: NIPER-76, NAB
Order number: DE86000281, NAB
Price: $11.95

Order from

National Technical Information Service
5285 Port Royal Road
Springfield, VA 22161

For additional information, contact

Dr. T. H. Chung
National Institute for Petroleum and Energy Research
P.O. Box 2128
Bartlesville, OK 74005
Telephone No. (918) 336-2400

or

Dr. Thomas Burchfield
National Institute for Petroleum and Energy Research
P.O. Box 2128
Bartlesville, OK 74005
Telephone No. (918) 336-2400

energygram

Energy from Biomass: Building on a Generic Technology Base

DOE/TIC/EG-86/154
OFFICE OF SCIENTIFIC AND TECHNICAL INFORMATION

This technical note was based on research conducted by Argonne National Laboratory for the U.S. Department of Energy.

Argonne National Laboratory

The fourth in a series of technical review meetings was held in Phoenix, Arizona. The report contains technical papers presented to the participants.

The purpose of the series was to spur further expansion of the biomass energy industry by communicating results, capabilities, and needs to researchers, producers of biomass, and users of biomass energy. Significant developments have occurred in the biomass energy field in the past decade, and progress continues as a result of further projects. This meeting focused on the southwestern United States, including the seven Sunbelt States and Hawaii. The technical papers critically assessed the resource availability and constraints in the southwest, the selection of biomass species to be grown for energy and materials applications, and conversion technologies.

Major topics dealt with are:

(1) Potential of Biomass Energy in The Southwest

(2) Economics of Fuel Cycles and Supply

(3) Conversion Systems

(4) Case Studies

FOR ADDITIONAL INFORMATION

DOE report(s):

Energy from Biomass: Building on a Generic Technology Base, Proceedings of the Fourth Technical Review Meeting, Sept. 29-Oct. 1, 1985.
Report number: ANL/CNSV-TM-176/NAB
Order number: DE86012757/NAB
Price: $16.95

Order from:

National Technical Information Service
5285 Port Royal Road
Springfield, VA 22161

For program-related information, contact:

Sinyan Shen
Argonne National Laboratory
9700 South Cass Avenue
Argonne, IL 60439
Telephone No.: (312) 972-6276

0544

energygram®

Small-Hydropower Development: The Process, Pitfalls, and Experience: Guide for Developers

DOE/TIC/EG-86/156
OFFICE OF SCIENTIFIC AND TECHNICAL INFORMATION

This technical note was based on research sponsored by the U.S. Department of Energy, Idaho Operations Office, and the Electric Power Research Institute.

INEL
Idaho National Engineering Laboratory

Because of the sudden economic advantage of hydroelectric power after the rise in oil prices in the 1970's, many of those attempting to develop small-hydropower sites were unfamiliar with the government requirements and the developmental procedures necessary to take a project from conception to commercial operation. Small-Hydropower Development: The Process, Pitfalls, and Experience, Volume 4: Guide for Developers, provides guidelines for developers of such projects. Since the material is presented systematically, less-experienced technical personnel as well as nontechnical developers can use it easily. The general procedural outline of the volume will never lose its currency. However, because government regulations, tax law, the energy marketplace, and economic conditions change continually, some of the information and suggestions will become dated. They must always be viewed in the light of contemporary development climate.

The other three volumes summarize and analyze 240 feasibility studies (Volume 1), 41 license applications (Volume 2), and 17 completed constructions projects (Volume 3, forthcoming).

FOR ADDITIONAL INFORMATION

DOE report(s):

Small Hydropower Development: The Process, Pitfalls, and Experience, Volume 4: Guide for Developers.
Report number: DOE/ID/12254-1-Vol. 4/NAB
Order number: DE86008333/NAB
Price: $22.95

Small Hydropower Technology Transfer Project, Task A–Feasibility Studies.
Report number: DOE/ID/12254-1-Vol. 1/NAB
Order number: DE85004133/NAB
Price: Contact NTIS for price quote

Small-Hydropower Development: The Process, Pitfalls, and Experience, Volume II: Licensing Activities Summary and Analysis.
Report number: DOE/ID/12254-1-Vol. 2/NAB
Order number: DE85017035/NAB
Price: $22.95

Order from:
National Technical Information Service
5285 Port Royal Road
Springfield, VA 22161

For additional information, contact
Peggy A. M. Brookshier
USDOE Idaho Operations Office
785 DOE Place
Idaho Falls, ID 83401
Telephone No.: (208) 526-1403

NASA Tech Brief
National Aeronautics and Space Administration
Lyndon B. Johnson Space Center, Houston, Texas

Licensing Opportunity

Fuel-Cell Structure Prevents Membrane Drying

Embossed plates direct flows of reactants and coolant.

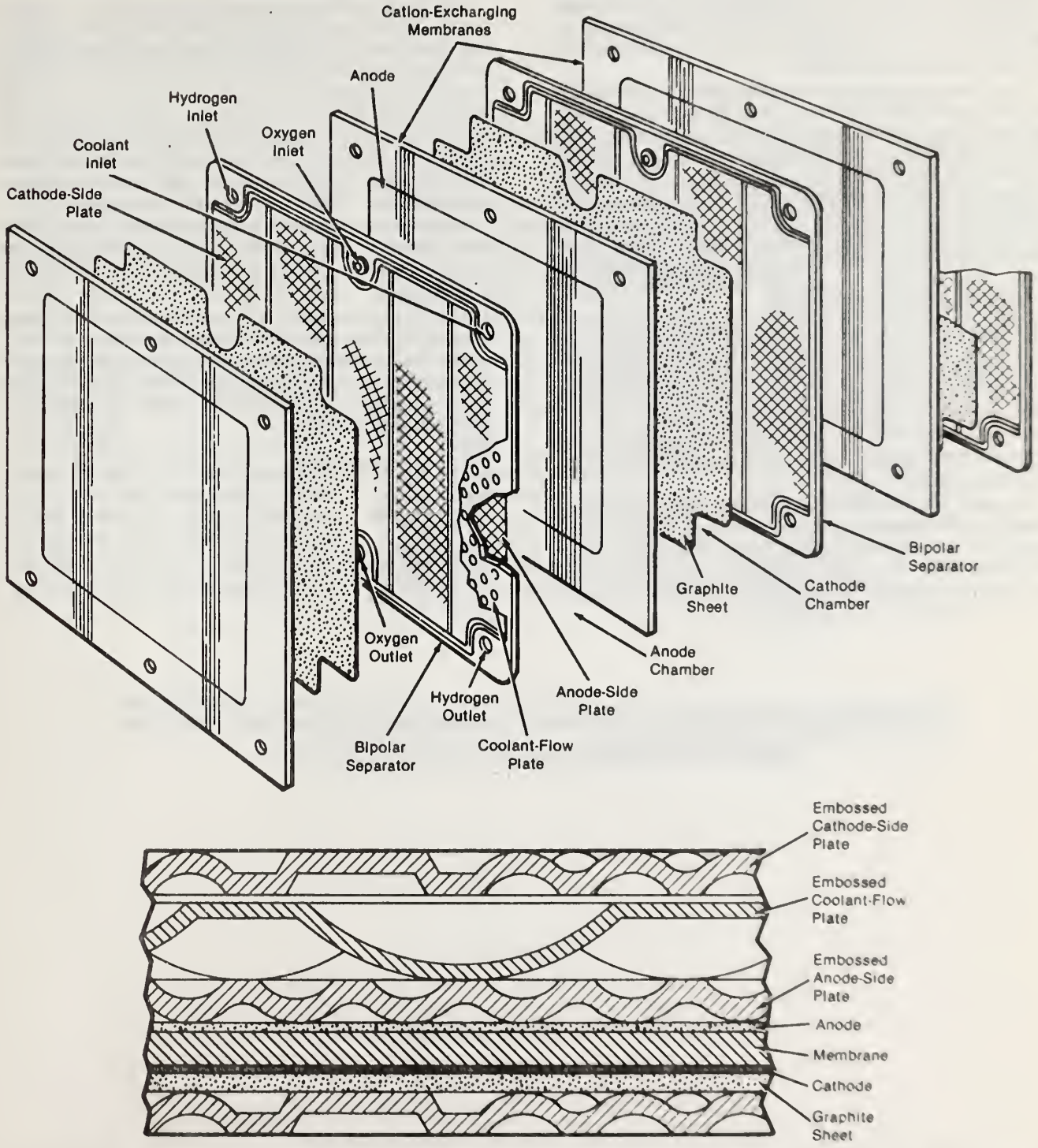

The Fuel-Cell Battery includes a series of membranes and separators. The anode graphite sheets, which support the cell membrane, do not appear in this view. The bottom part of the figure shows the internal structure of a separator in cross section.

A membrane-type fuel-cell battery has improved reactant flow and heat removal. The compact, lightweight battery can produce high current and power without drying of its membranes.

The battery consists of a series of fuel cells (see figure), each of which contains a cation-exchanging membrane between internally cooled bipolar separators. An anode is attached to one side of a membrane; the anode is an aggregate of liquid- and gas-pervious catalytic particles in a polymeric binder. A pervious cathode is bonded to the other side of a membrane; it too is composed of catalytic and binder particles.

The bipolar separators on opposite sides of a membrane form an anode chamber and a cathode chamber. Hydrogen gas is oxidized at the anode, releasing electrons to an external load circuit. The hydrogen ions thus created pass through the membrane to the cathode, where oxygen and electrons react with the hydrogen ions to form water. The water product collects at the bottom of the cell, where it drains away through the oxygen-outlet manifold. (Fuel/oxider combinations other than hydrogen/oxygen may be used. The reactants may be hydrogen/chlorine or hydrogen/bromine, for example.)

Oxygen enters the cathode chamber through an inlet at the top of the bipolar separator. Hydrogen enters the anode chamber through an inlet at a corner of the separator. In the new fuel-cell configuration, the separator contains embossed plates on its opposite faces to guide the flowing gases— hydrogen on the anode side and oxygen on the cathode side. The plates distribute the gases uniformly for efficient reaction.

A coolant plate between the anode-side and cathode-side plates forms two adjacent chambers through which coolant flows. The cathode-side plate is made of niobium, 5 mils (0.13 mm) thick. The anode-side plate is made of zirconium, which is resistant to embrittlement by the hydrogen flowing over it. The coolant plate is made of titanium. The three plates are held together by the frame of the separator. The concave bumps embossed in the coolant plate on the cathode side tend to collect coolant, so that flow there is slower and removes less heat than does the flow along the anode side. The anode side of the cell membrane is therefore maintained at a temperature lower than that of the cathode side.

The effect of this temperature differential is to prevent drying of the hydrogen side of the membrane. Without the differential, as hydrogen is oxidized the resulting hydrogen ions move through the membrane, carrying molecules of membrane water with them. Because each hydrogen ion can carry eight to ten water molecules with it, the water on the fuel side can quickly become depleted. This drying effect, which is aggravated as the battery power output—and hence the cell current density—increases, can limit the maximum power output.

With the temperature differential, however, water diffuses from the warmer cathode to the cooler anode. This reverse diffusion compensates for the loss of water on the fuel side.

This work was done by James McElroy of General Electric Co. for **Johnson Space Center**.

Inquiries concerning rights for the commercial use of this invention should be addressed to the Patent Counsel, Johnson Space Center Refer to MSC- 21031 /TN

Lyndon B. Johnson Space Center
Technology Utilization Officer:
Dean C. Glenn
Mail Code AL32
Houston, TX 77058
(713) 483-3809
Patent Counsel:
Marvin F. Matthews
Mail Code AL3
Houston, TX 77058
(713) 483-4871

FOR ADDITIONAL INFORMATION: *Contact: Director, Technology Transfer Division, P.O. Box 8757, BWI Airport, MD. 21240; (301) 621-0100 Ext. 241*
REFER TO THE NUMBER LISTED AT THE END OF THE ARTICLE

NASA Tech Brief
National Aeronautics and Space Administration

Licensing Opportunity

Liquid-Hydrogen Polygeneration System

The system utilizes coal as an alternate chemical feedstock.

A polygeneration system would use existing technology in an integrated process to produce liquid hydrogen space-vehicle propellant and such important secondary products as gaseous nitrogen, electrical energy, and thermal energy. The system can make the commercial launch services economically attractive against future competition. The system could lower the expected cost of liquid hydrogen by utilizing relatively cheap coal feedstocks and by reducing the electrical costs associated with producing liquid hydrogen.

The integrated process includes a coal-gasification and gas-cleanup system, a combined-cycle power-generation system, a hydrogen-production/liquefaction system, and an air-separation system. A clean, medium-BTU gas is produced by the coal-gasification system and is delivered to the power-generation system and the hydrogen-production/liquefaction system.

Steam, produced in the coal-gasification process, is delivered to a steam turbine combined with a gas turbine, to which the gas is delivered, to generate electrical and thermal power in a combined-cycle power-generation process. Steam from the coal-gasification process is also delivered to a shift-conversion unit in the hydrogen-production system to increase the hydrogen content of the gas before liquefication.

The air-separation system produces oxygen and gaseous nitrogen. The oxygen is used in the coal-gasification process, and the gaseous nitrogen is delivered for storage to the launch site, where it is used as an inert gas to purge critical environments. The gaseous nitrogen is also used in the hydrogen-production system, where the nitrogen is liquefied and used to refrigerate the hydrogen.

This work was done by P. A. Minderman, G. P. Gutkowski, L. Manfredi, J. V. King, and F. S. Howard of **Kennedy Space Center**.

This invention is owned by NASA, and a patent application has been filed. Inquiries concerning nonexclusive or exclusive license for its commercial development should be addressed to the Patent Counsel, Kennedy Space Center Refer to KSC-11304. / TN

John F. Kennedy Space Center
Acting Technology Utilization Officer: Thomas M. Hammond
Mail Stop PT-TPO-A
Kennedy Space Center, FL 32899
(305) 867-3017
Patent Counsel:
James O. Harrell
Mail Code PT-PAT
Kennedy Space Center, FL 32899
(305) 867-2544

FOR ADDITIONAL INFORMATION: *Contact: Director, Technology Transfer Division, P.O. Box 8757, BWI Airport, MD. 21240; (301) 621-0100 Ext. 241*
REFER TO THE NUMBER LISTED AT THE END OF THE ARTICLE

Evaluating Performances of Solar-Energy Systems

Efficiencies can be calculated and maximized.

The CONC11 computer program calculates the performances of dish-type solar thermal collectors and power systems. The solar thermal power system consists of one or more collectors, power-conversion subsystems, and power-processing subsystems. CONC11 is intended to aid the system designer in comparing the performance of various design alternatives.

The solar collectors may be flat or paraboloidal. Each is composed of a concentrator and a receiver to concentrate reflected or refracted sunlight and convert the energy to heat in a working fluid. The power-conversion subsystem converts this heat into mechanical or electrical energy. If the desired output is heat, this subsystem is omitted. The power-processing subsystem transfers the mechanical or electrical energy to the system output device.

Given the characteristics of the various subsystems, CONC11 calculates collector efficiency and overall power-system efficiency as functions of receiver temperature for a specified steady insolation. CONC11 has options to optimize the receiver aperture, receiver temperature, and intercept factor for providing the highest efficiency at a given insolation.

CONC11 is written in Athena FORTRAN and Assembler for interactive execution and has been implemented on a UNIVAC 1100-series computer with a central-memory requirement of approximately 16K of 16-bit (minimum) words. CONC11 was developed in 1984.

This program was written by Leonard D. Jaffe of Caltech for **NASA's Jet Propulsion Laboratory**. *NPO-16717 /TN*

FOR ADDITIONAL INFORMATION

CONTACT:
COSMIC®
112 Barrow Hall
University of Georgia
Athens, GA 30602
(404) 542-3265

Engineering

Engineering

549 Simulating Damage in Wound-Filament Pressure Vessels— A model, founded in classical viscoelastic theory, produces results consistent with reported data.

550 Water Heater/Cooler for Vehicles— At the press of a button, thermoelectric unit changes from a heating device to a cooling device.

551 Technology Transfer Films Available on Loan

552 Cycle-Counting Methods for Fatigue Analysis

553 Scouring System Deepens Water in Ship Berthing Sites

554 Shape Determination for Large Static Structures— Parameter and shape estimates are updated from new measurements.

555 Balancing High-Speed Rotors at Low Speed— Flexible balancing reduces vibrations at operating speeds.

556 Structural Error and Identifiability in Mathematical Models— Errors and previously implicit assumptions are treated explicitly.

557 Hose- and Tube-Cleaning Module— This device enables tubes and hoses to be cleaned easily, without other special equipment. (Licensing Opportunity)

558 Mobile Platform for Large Structures— A proposed platform would move forward and in reverse, turn left and right, and change planes. (Licensing Opportunity)

559 Blade-Tip-Clearance Forces in Turbines— A study reviews the field and proposes experiments.

560 Air-Powered Projectile Launcher— A small, high-pressure reservoir conserves compressed air.

Software

561 Urban Hydrology Software for Small Watersheds

Testing & Instrumentation

562 Use of Minaturized Tests to Predict Flow Properties and Estimate Fracture Toughness in Deformed Steel Plates

563 One-Piece Force-Transducer Body— A rugged unit is designed to operate in severe environment.

Other items of interest

567 An Interactive Computer Model for Calculating V-I Curves in ESPs Version 1.0

600 Software Package is an Integrated Finite Difference Program for Computing Two-Phase Nonisothermal Flow in Porous Media

MANUFACTURING TECHNOLOGY NOTE

U.S. ARMY MATERIEL COMMAND

Deputy Chief of Staff for Manufacturing Technology, Alexandria, VA

Project Number: NONE

Filing Code: 71F103

Simulating Damage in Wound-Filament Pressure Vessels

A model, founded in classical viscoelastic theory, produces results consistent with reported data.

A computer model predicts the viscoelastic-damage response of a wound-filament composite cylindrical pressure vessel to a proof-test load. The model, developed by the U.S. Army Missile Command, relates the circumferential strain to a damage index. The index in turn is related to the transverse modulus as a first approximation. A quadratic relationship between the transverse modulus and the circumferential strain results.

The matrix material of the composite system is assumed to be isotropic and linearly viscoelastic. The fiber is assumed to be isotropic and linearly elastic.

An iterative solution based on the damaged elastic response is employed to predict the time-dependent circumferential strain during the linearly increasing phase of the loading. Thereafter, an iterative solution based on the elastic/viscoelastic correspondence principle is used to predict the time-dependent circumferential strain, which is then used to determine the transverse modulus. A new expression for the time-dependent circumferential strain is then found from the previously calculated transverse modulus. This iterative procedure is continued until convergence is achieved.

A plot of the modeled response with and without damage (see figure) shows a very small negative residual strain for the response with damage, whereas the strain should be totally recovered because only elastic elements in the model are damaged and no plastic behavior is included. The discrepancy is believed to be a result of roundoff error and of a strong sensitivity to initial conditions.

Project officer Johnny L. Prater
(205) 876-2604 or AV 746-2604.

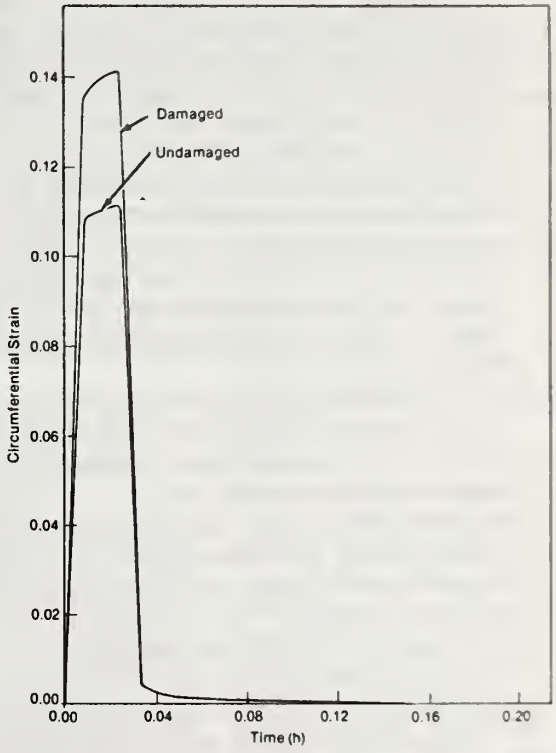

Comparison of Damaged and Undamaged Responses through recovery shows creep under constant load. The creep predicted for the damaged case is 2.54 times that predicted for the undamaged case.

FOR ADDITIONAL INFORMATION:

You can learn more details about this technology by ordering the NTIS report(s):

A Viscoelastic/Damage Simulation Model for Filament-Wound Pressure Vessels.
Order number: AD-A166389/NAA
Price code: A04

Order from:
National Technical Information Service
5285 Port Royal Road
Springfield, VA 22161

This document was prepared under the sponsorship of the U.S. Government. Neither the United States Government nor any person acting on behalf of the United States Government assumes any liability resulting from the use of the information contained in this document, or warrants that such use will be free from privately owned rights.

MANUFACTURING TECHNOLOGY NOTE

U.S. ARMY MATERIEL COMMAND

Deputy Chief of Staff for Manufacturing Technology, Alexandria, VA

Project Number: 1L162724 Filing Code: 79D028

Water Heater/Cooler for Vehicles

At the press of a button, thermoelectric unit changes from a heating device to a cooling device.

A simple, safe, and reliable thermoelectric device has been developed for heating or cooling drinking water in vehicles. The device can cool water to 60 °F (15.6 °C) in ambient temperatures up to 130 °F (54.4 °C) and heat water to 150 °F (65.5 °C) in ambient temperatures of 40 °F (2.5 °C). It protects against freezing, overheating, and undervoltage. It indicates whether it is heating or cooling and when the water is ready. It switches off automatically. A total of six units have been built, tested, and delivered to the sponsor, the U.S. Army Natick Research, Development and Engineering Center.

The principal mode of heat transfer within the water chamber is natural convection. Providing internal fins or mechanical or magnetic stirrers would augment the heat transfer in the device. Another useful addition would be coating the internal surface of the water chamber — now untreated stainless steel — with a thin layer of glass or other material. Such a coating may be necessary for commercial applications.

The unit consists of the water chamber, thermoelectric modules, heat-exchange fins, an electronic board, and a minifan (see figure). The unit is housed in a box measuring 9.47 by 7.43 by 6.5 in. (24.0 by 18.9 by 16.5 cm). One wall of the box is openable, giving access to the electronic board for adjustment or replacement of components.

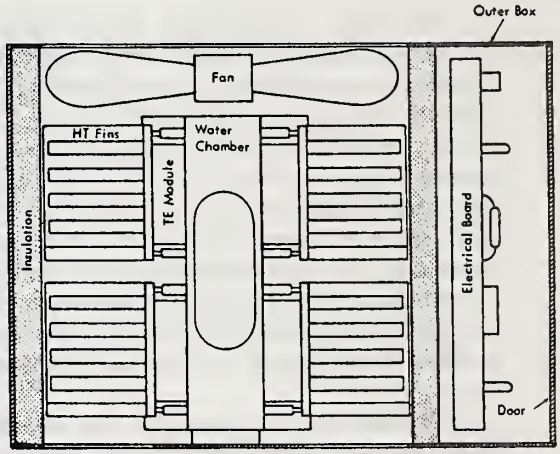

Thermoelectric Modules surround the water chamber, as viewed from the top. Water is poured into the chamber for heating or cooling through the oval opening.

The water chamber has a capacity of 12 ounces (354 cm^3). It can be filled from the top with an ordinary cup. It releases its cooled or heated contents through a faucet at its base.

FOR ADDITIONAL INFORMATION:

You can learn more details about this technology by ordering the NTIS report(s):
Development of Thermoelectric Water Heating/Cooling Devices.
Order number: AD-A166949/NAA
Price code: A03

Order from:
National Technical Information Service
5285 Port Royal Road
Springfield, VA 22161

This document was prepared under the sponsorship of the U.S. Government. Neither the United States Government nor any person acting on behalf of the United States Government assumes any liability resulting from the use of the information contained in this document, or warrants that such use will be free from privately owned rights.

Laboratory Technology
U.S. Department of the Interior

No. 264

Technology Transfer Films Available on Loan

Several short color films describing new technology developed through Bureau of Mines research are available on a loan basis. The films review results of Bureau research programs aimed at aiding the minerals industry by increasing mine productivity, ensuring worker health and safety, and enhancing minerals recovery, processing and recycling. Most of the films are available in a choice of formats: 16mm film, ½" VHS cassette tape, or ¾" U-matic tape. The films are loaned by the Bureau of Mines free of charge; borrowers are requested to pay only the return postage and for any damage to the films. All titles are also available for purchase in 16mm or videotape formats. Interested persons wishing to borrow or purchase a film should specify its title and the preferred and alternate showing dates. All requests should be addressed to:

Motion Picture Library
Bureau of Mines
Cochrans Mill Road
P.O. Box 18070
Pittsburgh, PA 15236

A short description of each film follows:

Safer Coal Mining Equipment

Traces the development of modified conventional and continuous mining equipment, beginning with an investigation of the problems encountered with mining equipment and continuing through long-term testing of the modified equipment in two mines. "Human engineered" coal mining machines are shown in operation. These machines include features such as adjustable cabs, easy access controls, improved illumination, and other safety improvements. (19 min)

Mine Shaft Smoke and Fire Protection Systems

Documents the development and testing of a system for sensing, isolating, and extinguishing fires in deep metal mines. The system features a novel ionization detector, multiplexed signal transmission, and back-up wiring networks for increased reliability. Detection and extinguishment of test fires by this system in a 3,000-ft.-deep metal mine are also shown. (9 min)

Fueling Area Fire Protection in Underground Metal and Non-metal Mines

The film covers the design and testing of a rugged, reliable system, adaptable to any mine layout, that detects and automatically extinguishes fires in underground fueling and fuel storage areas. (5 min)

Mine Face Ignition Quenching

The development and testing of an effective, non-toxic extinguishant for instantaneous quenching of coal mine face explosions is featured in this film. Various ignition quenching chemicals are compared, and the development of an optimum extinguishant is traced. A trial of the quenching system on a tunnel boring machine is also shown. (10 min, available in 16mm only)

Inductoslag Melting and Casting of Reactive Metals

Demonstrates a Bureau technique for melting refractory or reactive metals using induction heating. This technique offers important advantages over present welding and arc melting methods. A hopper-fed, cylindrical ingot furnace is shown in operation. The film also explains how inductoslag melting can be adapted (11 min, available in 16mm only)

Explosives Loading Through Expendable Tubing

Discusses a technique for leading explosives inside expendable, paper-based tubing which is dropped down the drillhole and through the kelly-bar. With the tube in place, the integrity of the hole is retained long after the kelly-bar is removed so that the explosives can be loaded safely and are drilled. (14 min, available in 16mm only)

Automatic Fire Protection Systems for Mobile Mining Equipment

Covers the development and testing of rugged and reliable systems which detect and extinguish fires automatically on large surface and underground mining equipment. Successful quenching of test fires on trucks, front-end loaders, downhole drills, and loading shovels are also demonstrated. (13 min)

A System for Re-Contouring Surface-Mine Spoil Banks

Shows how surface mined land can be recontoured both efficiently and economically with a specially designed, 48-foot reclamation blade mounted on two tandem tractors. Overhead shots reveal how the big blade can accomplish in one pass what conventional dozers would need many passes to do. Operator training for controlling the blade is also emphasized. (16 min)

Improved Visibility Aids on Large Haulage Vehicles

Shows how hazards posed by extensive blind areas around large haulage vehicles can be minimized with the use of low-cost, specially-designed mirrors and unique "flut lens" blind-area viewers developed by the Bureau of Mines. Scenes from the driver's point of view and graphics demonstrating the blind areas around the vehicles are also included. (14½ min)

A Retractable Diamond Bit System for Core Drilling

This film features the development of a unique diamond core drill bit which can be retracted and replaced when necessary without withdrawing the drill rods. This time-and-cost-saving equipment is shown in laboratory and field tests for drillability, ruggedness and reliability in hard rock. (16½ min)

Fire Protection Systems for Underground Metal and Nonmetal Mines

Documents the development and testing of a variety of fire detection, warning, and suppression devices which can be used singly or in integrated mine-wide fire protection systems underground. Tests of various smoke and flame detectors and automatic fire-suppression systems are highlighted in the film. (17½ min)

Soft-Soldering Aluminum

Features the development and testing of a unique and practical method that permits soldering aluminum and aluminum alloy products with conventional solders. The simple, four-step technique used is demonstrated and explained by Bureau researchers. (15 min)

Improved Stench Fire-Warning System for Underground Metal and Nonmetal Mines

This film demonstrates Bureau of Mines improvements made to a warning system which alerts underground mine workers to a fire by circulating odorant through ventilation and compressed air systems. Shortcomings of currently-used stench warning systems are explained, and the advantages of the Bureau's improved system are illustrated in actual field tests. (7 min)

Shield Supports for Longwall Coal Mining

Documents an actual Bureau in-mine test of shield-style, longwall mining roof supports. Shield supports are shown to offer important advantages over chock supports. The film shows how the shields operate and how they differ from other longwall supports. (19 min)

Discriminating Backup Warning Alarm Systems

A film is currently in production which will feature a description of the Bureau's discriminating backup warning alarm systems for mine haulage vehicles. Several types of systems will be discussed including ultrasonic, doppler-radar, and infrared detection systems.

NBS technology update

National Bureau of Standards
U.S. Department of Commerce
Gaithersburg, MD 20899

Cycle-Counting Methods for Fatigue Analysis

Structures such as bridges, aircraft, vehicles, pressure vessels, or offshore platforms are subjected to random cyclical loads that may result in structural failure. The designer or engineer needs information about the fatigue life of a structure in order to create a design that won't fail. Current approaches to random load fatigue analysis need the determination of stress cycles and associated stress ranges that are ambiguous in a random load history. NBS has devised Fortran IV programs that use the rainflow counting method and the mean crossing-range technique to determine the stress ranges and cycles of random load histories. These techniques reduce the complexity of the history so that results can be compared to non-random test results. Cycle-Counting Methods for Fatigue Analysis with Random Load Histories: A Fortran User's Guide (NBSIR 86-3055) presents the concepts and complete Fortran IV programs for these analysis methods.

FOR ADDITIONAL INFORMATION: A copy of the report is available form NTIS, Springfield, VA 22161; (703) 487-4600.

NTIS order number: PB87-104758/NAC
Price code: A04.

Scouring System Deepens Water in Ship Berthing Sites

Conventional dredging is no longer the most economical and practical method of providing adequate water depths for many Navy ship and submarine berthing sites.

To ensure adequate water depths in Navy berthing areas, the Naval Civil Engineering Laboratory (NCEL) is developing improved methods to maintain desired water depths.

NCEL's most advanced design is a prototype 13-jet scouring system, which will be installed this year at Mare Island Naval Shipyard (MINSY) for two years of operational testing and on-site evaluation.

The scouring actions of these water jets, submerged near the bottom of berthing sites, prevent buildup of sedimentation. The sediments are forcefully suspended in the water and then directed from the berthing area into the ebbing tidal flow and carried out to sea.

The test system will cover 250 feet of quay wall and will scour to distances of 75 feet from the point of installation. The test bed has been designed to explore systematically the effects of different jet flow rates, jet diameters, jet orientations, and jet duty cycle times.

The system features pneumatically-actuated butterfly valves, a vertical turbine pump, fiberglass pipe, and a microprocessor-based control system.

The jet array is powered by a 150-horsepower vertical turbine pump having a discharge flow rate of 4,500 gallons of seawater per minute. The pump is connected to a 12-inch diameter fiberglass manifold which distributes the water to the 13 jets. Each jet is connected to the manifold pipe via an 8-inch diameter flexible hose. The water flow to each jet is controlled by 8-inch diameter butterfly valves with pneumatic actuators.

An on-site portable computer, programmed with MINSY tidal cycles, controls valve operations. It automatically activates the water jets twice daily during ebb tides. The computer also collects pump and valve data.

Various sizes of jets and jet nozzle angles will be installed and tested. Varying jet heights above the mud line also will be tested for maximum scouring effects.

A jet's diameter and discharge velocity determine the distance of the scouring action. By increasing the diameter of the opening and the velocity of discharge, engineers can produce a greater scouring range. The maximum practical distance per jet is approximately 100 feet because of limits in pump design and systems economics. Beyond 100 feet, multiple jets are needed to achieve the desired scour distance.

The near-bottom water jets, activated at the onset of ebb tidal flow (duty cycle times for individual jets range between 5 and 10 minutes), resuspend any recently deposited sediment. The discharge creates a fan-shaped scour pattern in front of each jet. Once suspended, sediment is carried away from the berthing area by ebbing tidal currents.

For Additional Information:

Backup material on this effort is available from:

Navy Domestic Technology Fact Sheet Reader Reply Service
Code E211
Naval Surface Weapons Center
Dahlgren, VA 22448-5000
(703) 663-8921

Refer to 111102/TN

NASA Tech Brief
National Aeronautics and Space Administration
NASA's Jet Propulsion Laboratory, Pasadena, California

Shape Determination for Large Static Structures

Parameter and shape estimates are updated from new measurements.

A set of algorithms generates updated estimates of state vectors representing the static deflections or other responses of large structures and of physical parameters of structural components (for example, the elastic moduli of beams or ribs in a truss of many such elements). The algorithms result from a generalization of the Kalman statistical-filter technique. A degree of computational economy is achieved in that there are mathematical elements common to the estimates of the parameters and of the responses. This is an advance over prior filter methods, which have treated the estimation of the two types of quantities in different ways.

The mathematical model of a structure in this analysis is a set of elliptic partial differential equations that may be interconnected. The model includes the parameters, which, in principle, can be determined through measurements of the structural responses to applied loads. Because the model and the response and load measurements are contaminated by random errors, a statistical analysis is needed to find the best estimate of the parameters. The measurement and model errors are represented in the model equations as weighted white-noise components.

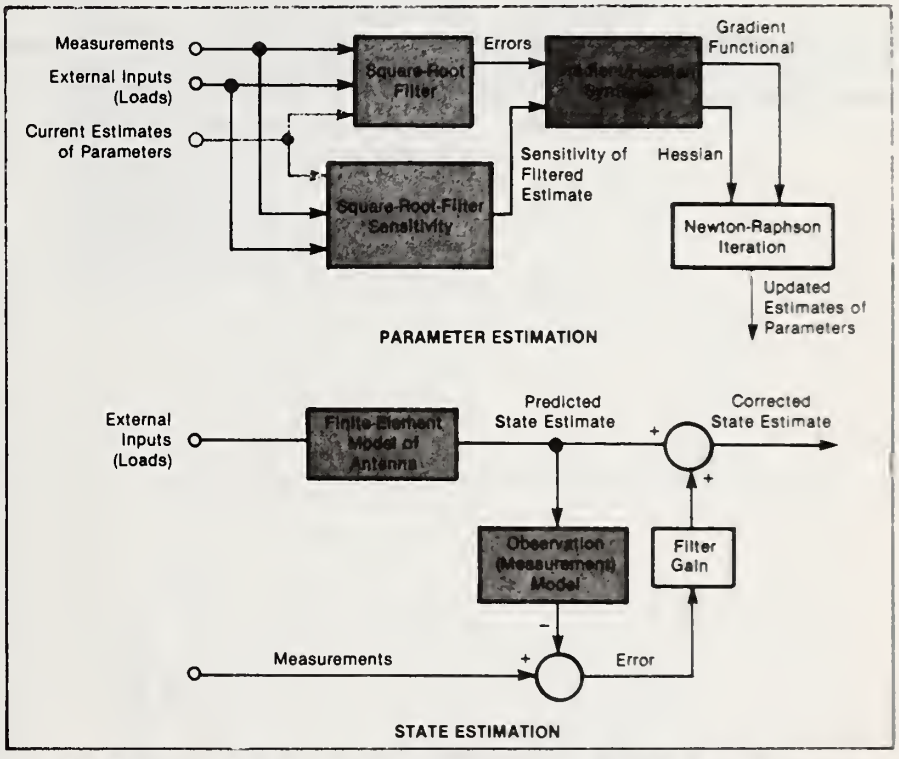

The Parameter and State Estimations involve statistical structural analysis, statistical electromagnetic-field analysis, filtering, measurement modeling, and iterative prediction/correction procedures. The estimating algorithms result from generalizations of Kalman statistical-filter theory.

The parameter estimation (see figure) involves a Newton-Raphson iteration process. The iteration begins with the current parameter estimate based on previous measurements and calculations. The square-root filter processes the external load inputs and measured deflections to obtain filtered measurements and filtered estimates of the deflections predicted theoretically from the load inputs and model. The square-root-filter output is the set of errors obtained by subtraction of the filtered predictions from the filtered measurements.

The gradient/Hessian synthesis block forms the function-space gradient of a likelihood functional and the approximate Hessian, which is the matrix of second derivatives of the likelihood functional. The likelihood functional takes an extreme value (usually a minimum) at the best estimate of the parameters. Using the gradient and the approximate Hessian, the Newton-Raphson iteration block calculates the updated parameter set, which is the next set that brings the

likelihood functional closer to the extremum.

The state-estimation algorithms were derived primarily for the determination of the shapes of large parabolic antenna reflectors. These algorithms are based on two sets of measurements; namely, the measured structural deflections of the first model plus measurements of the electromagnetic far field, which is affected by the deflections. The first model is thus expanded to include additional equations relating the field measurements, the deflection (state or response) estimate, and the additional noise that enters through the field measurements.

The problem is solved in two prediction/correction stages similar to that described above for the parameters. In the first stage, a predicted state estimate is generated by a finite-element model of the structure. This estimate is entered in the model of an electro-optical deflection sensor to predict the sensor output. The actual and predicted sensor data are then compared; the differences are processed through a three-dimensional spatially-distributed Kalman filter to obtain correction terms, which are used to further correct the deflection estimate. The second prediction/correction stage performs similar operations, using the field model and field measurements.

This work was done by Guillermo Rodriguez and Robert E. Scheid, Jr., of Caltech for **NASA's Jet Propulsion Laboratory**. *NPO-16781 /TN*

FOR ADDITIONAL INFORMATION: *Contact: Director, Technology Transfer Division, P.O. Box 8757, BWI Airport, MD. 21240; (301) 621-0100 Ext. 241*

REFER TO THE NUMBER LISTED AT THE END OF THE ARTICLE

NASA Tech Brief
National Aeronautics and Space Administration
Marshall Space Flight Center, Alabama

Balancing High-Speed Rotors at Low Speed

Flexible balancing reduces vibrations at operating speeds.

High-speed rotors in turbomachines can be dynamically balanced at a fraction of the operating rotor speed. The method results in a precisely balanced rotor at, say, 30,000 r/min even though the rotor weight distribution has been adjusted at a much lower speed — for example, 2,000 r/min.

Unlike other low-speed, rigid-body balancing, the new method takes into account that the rotor is flexible rather than rigid. The method is based on balancing "windows" — combinations of speed and support flexibility at which two conditions occur simultaneously. The system behaves flexibly (that is, distinct balance planes can be discerned along the shaft), and the system response to the addition of balance weights is large enough to measure reliably.

The method consists of the following four steps:

1. The balance planes are selected. They must be in axial planes where weight can be added or removed at any circumferential location. They must not be at vibrational nodes at the speeds of interest, and they must be active at the low speeds at which balancing will be performed.
2. The speeds are determined at which there is separation among the planes; that is, at which a weight in each plane would cause a different rotor response.
3. The speeds are determined at which the rotor response is measurable with sufficient accuracy.
4. Finally, the influence-coefficient balancing is performed at speeds where the rotor is both flexible and responsive.

The low-speed flexible balancing method was evaluated empirically with a rotor-dynamic test rig. The rig was assembled with supports that simulated those of an oxygen turbopump. For this arrangement, a low-speed balancing window was predicted at 8,000 r/min. The rig was balanced at this and other speeds. The balancing resulted in smooth operation of up to 24,000 r/min, and the two critical speeds below it were traversed without excessive vibration (see figure).

By way of comparison, a high-speed balance was done on the test rig. The quality of balance was approximately the same as it was for the low-speed, flexible balance. A low-speed, rigid-body balance was also done. This method produced little reduction in vibration amplitude, and the maximum speed was limited to 20,000 r/min.

This work was done by J. Giordano and E. Zorzi of Mechanical Technology, Inc., for **Marshall Space Flight Center**. *MFS-28130 /TN*

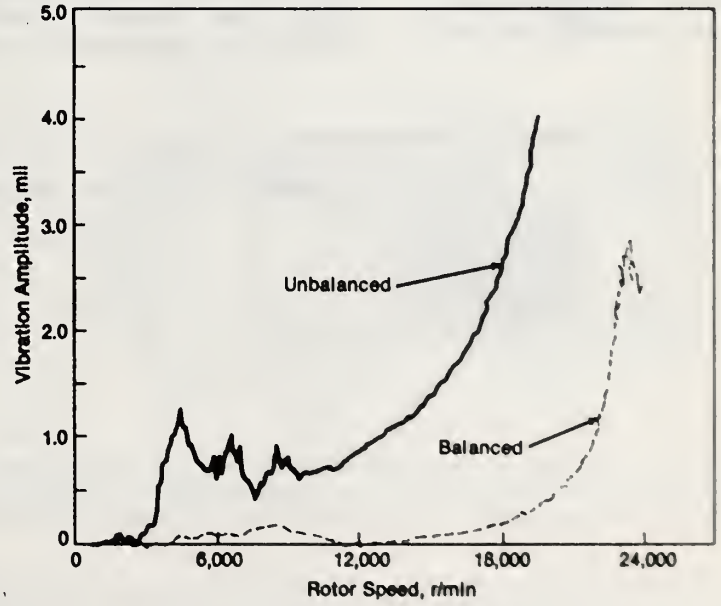

Before- and After-Balancing Curves show that flexible-body balancing at 8,000 r/min ensures smooth rotation up to at least 24,000 r/min. The vibration peaks at the critical speeds and the sharp rise of vibrations at intermediate speeds are eliminated.

FOR ADDITIONAL INFORMATION: *Contact: Director, Technology Transfer Division, P.O. Box 8757, BWI Airport, MD. 21240; (301) 621-0100 Ext. 241*
REFER TO THE NUMBER LISTED AT THE END OF THE ARTICLE

NASA Tech Brief
National Aeronautics and Space Administration

Structural Error and Identifiability in Mathematical Models

Errors and previously implicit assumptions are treated explicitly.

A paper discusses the errors in mathematical models of physical systems and the problem of identifying a model from the system input and output. This problem is approached by explicitly taking account of erroneous choices of model structure ("structural error"); for example, the neglect of nonlinearities or small effects, or the representation of a higher-order system by a lower-order model.

In this specialized context, "system identification" denotes the determination of a mathematical model that represents the physical system as closely as possible under the prescribed experimental conditions. In practice, system identification is often divided into the following three phases:

1. Selection of a model structure;
2. Testing of the structure to ensure that a unique solution for its parameters is possible (the identifiability test); and
3. Parameter estimation.

Structural error can affect both the identifiability of a model and the final values of the parameter estimates.

The paper is concerned specifically with linear or weakly nonlinear models. Two different sets of model equations represent the relationships among the system state, input, output, and model parameters; one of these sets describes the basic assumed (and somewhat erroneous) model while the other represents an ideal model that would completely and accurately describe the system. Included in the ideal model are an additive error term that specifies the structural error and a set of the "true" parameter values, which are generally not known.

The identifiability problem is then reformulated on the basis of equivalence and near equivalence between model and system. "Near equivalence" would be established if a rmodel-dependent criterion function is less than the acceptable maximum modeling error and if the absolute magnitude of the difference between model and true outputs is less than the maximum acceptable output error.

The practical identification problem then is to determine the parameters of a nearly equivalent model from observations of the inputs and outputs of the system and model. The paper derives a number of theorems concerning necessary and sufficient conditions for near equivalence and the identifiability of parameters.

This work was done by Fred Y. Hadaegh of **NASA's Jet Propulsion Laboratory** *and George A. Bekey of The University of Southern California.*
"Structural Error and Identifiability,"
NPO-16661 /TN

FOR ADDITIONAL INFORMATION: *Contact: Director, Technology Transfer Division, P.O. Box 8757, BWI Airport, MD. 21240; (301) 621-0100 Ext. 241*
REFER TO THE NUMBER LISTED AT THE END OF THE ARTICLE

NASA Tech Brief
National Aeronautics and Space Administration
Lyndon B. Johnson Space Center, Houston, Texas

Licensing Opportunity

Hose- and Tube-Cleaning Module

This device enables tubes and hoses to be cleaned easily, without other special equipment.

A self-contained, single-use module would enable a hose or tube to be cleaned thoroughly in the field, in one operation, using water of unknown or questionable quality. Previously, chemicals for flow cleaning had to be mixed, diluted, and pumped through tubes and hoses in many successive steps; moreover, deionizers, water-treatment facilities, and chemical storage were required. With the proposed device the cleaning can be performed safely, without special training. Ready to use, this device could be packaged as a cleaning kit with the tube to be cleaned.

Shown in the figure, the device includes a housing of polyethylene (or other polymer) with an adapter for a water tap at the inlet end and an adapter for the specific application at the outlet end. Beginning at the inlet end, the tube contains a mesh screen to prevent the entry of large particles. The screen also retains a layer of activated carbon particles, which remove organic contaminants in the water flowing into the device.

The activated carbon is followed by another screen and a layer of ion-exchange resin, which removes dissolved minerals. Following the resin is another retaining screen and a layer of water-soluble powdered cleaning compound. Next is a retaining screen followed by a stack of filters of decreasing size to remove particles from the waterflow.

The filtration zone has a cross section larger than that of the preceding zones to reduce the speed and the pressure drop of the water across the filters. This protects the filters from tearing or breaking and enables them to remove finely divided particles that might remain. The outlet cone of the filter stack contains an embedded litmus or pH chemical indicator to show when the detergent supply is exhausted. The indicator color change is viewed through a window in the filter holder. Alternatively, the housing could be made of transparent or translucent material through which the color change could be viewed.

The device inlet is attached to the water supply. The outlet is attached to the hose or tube to be cleaned. The detergent-laden flow cleans the hose or tube as long as detergent is dissolving in the cleaning device. The flow may be stopped at any time to permit a soaking period. The water is allowed to run until the detergent is depleted, as shown by the change of color in the indicator caused by the decrease of the pH. After this, the water is allowed to flow awhile longer so that the hose or tube is rinsed.

The selection of the materials for the four module zones and the sizes of the zones are based on the contamination expected in the water and on the projected

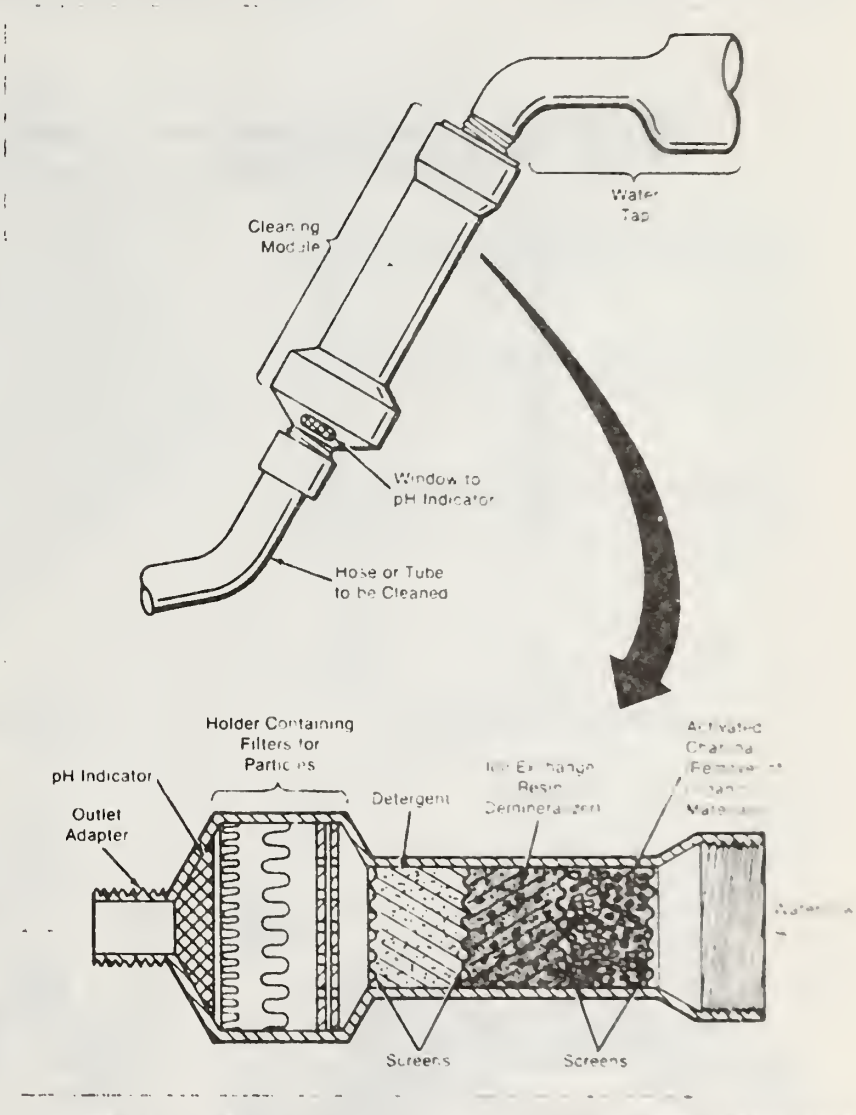

In this Cleaning Module, water entering through the inlet fitting is freed of organic matter by activated charcoal, then demineralized by ion-exchange resin, then laden with detergent, and finally filtered, before flowing to the hose, tube, or other system to be cleaned.

specific cleaning problem. The carbon absorber and the deionizer are made large enough to permit a rinse of sufficient duration or volume following detergent exhaustion. Additional units without detergent could be used for rinsing only, or for partial purification of water for drinking. After use, the module can be discarded; with simple modifications, a reusable device could be constructed.

This work was done by Fred P. Rollins and James S. Glass of Lockheed-EMSCO for **Johnson Space Center**. *For further information, Circle 93 on the TSP Request Card.*

This invention is owned by NASA, and a patent application has been filed. Inquiries concerning nonexclusive or exclusive license for its commercial development should be addressed to the Patent Counsel, Johnson Space Center Refer to MSC-20857 /TN

Lyndon B. Johnson Space Center
Technology Utilization Officer:
Dean C. Glenn
Mail Code AL32
Houston, TX 77058
(713) 483-3809
Patent Counsel:
Marvin F. Matthews
Mail Code AL3
Houston, TX 77058
(713) 483-4871

FOR ADDITIONAL INFORMATION: *Contact: Director, Technology Transfer Division, P.O. Box 8757, BWI Airport, MD 21240; (301) 621-0100 Ext. 241*
REFER TO THE NUMBER LISTED AT THE END OF THE ARTICLE

NASA Tech Brief
National Aeronautics and Space Administration
Lyndon B. Johnson Space Center, Houston, Texas

Licensing Opportunity

Mobile Platform for Large Structures

A proposed platform would move forward and in reverse, turn left and right, and change planes.

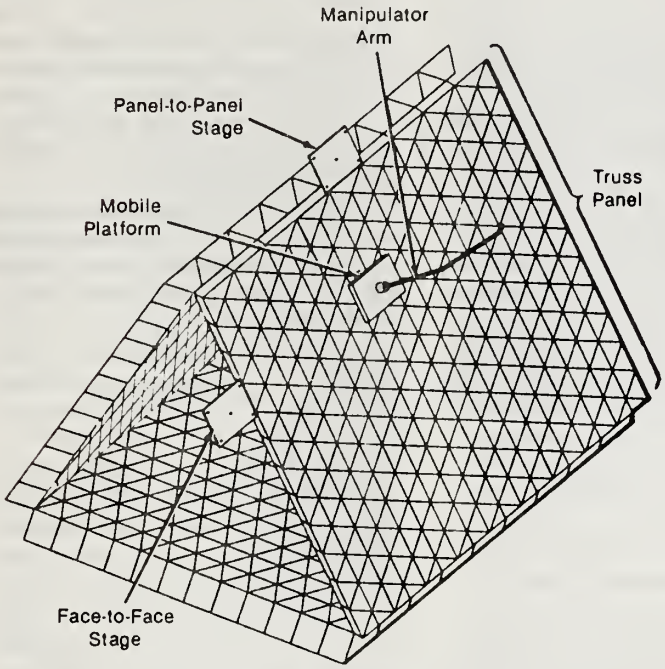

TRUSS STRUCTURE WITH PLATFORM

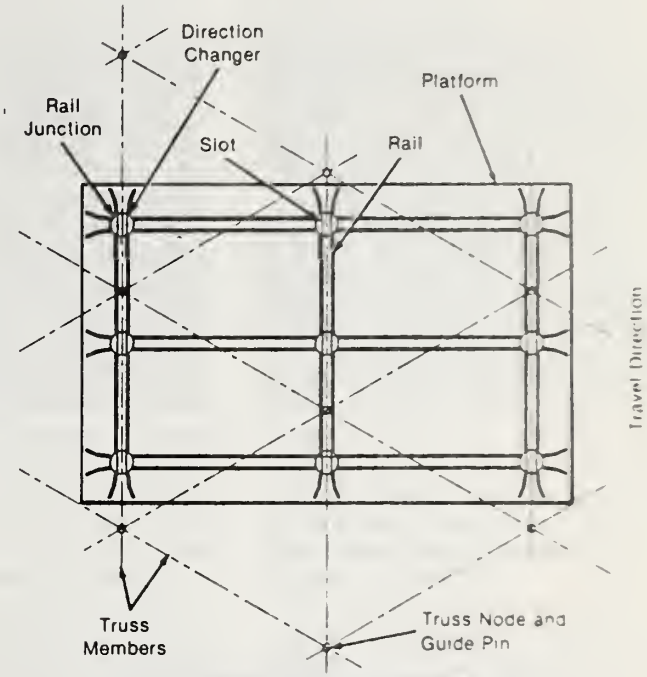

UNDERSIDE OF PLATFORM

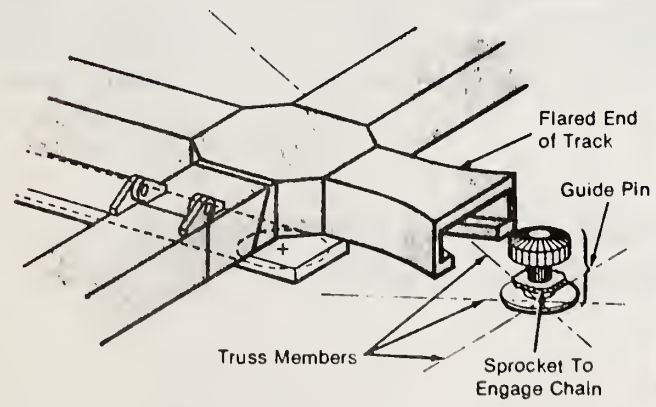

GUIDE PIN ABOUT TO ENGAGE END OF RAIL

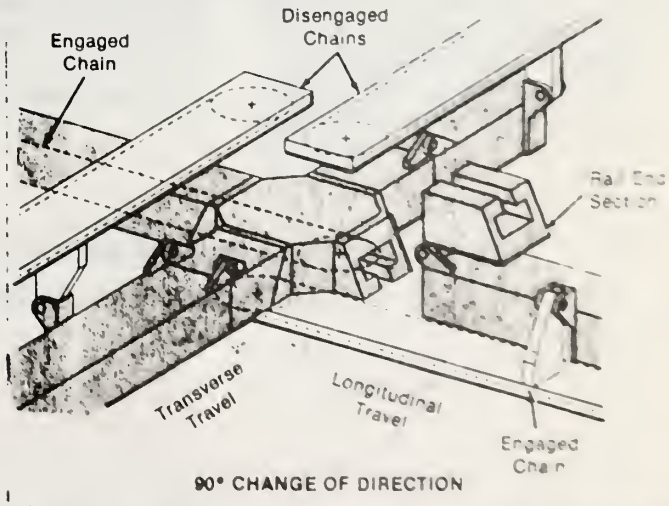

90° CHANGE OF DIRECTION

Tracks Slide on Pins on a truss panel. Although a truss member joins other members at angles of 0°, 120°, and 240°, the pin arrangement will allow the platform to travel at angles of 0° and 90° with a truss edge. The rails are flared at their outer ends so that the pins engage them smoothly. The drive chains under the platform engage sprockets on the guide pins. The drive chains are shown in position for longitudinal travel, with a rail end section opened for a change to transverse travel.

A mobile-platform concept is proposed to move remote manipulators, workers, or other loads over truss panels on large structures. Such a platform would move at a constant speed so that it does not cause a swinging motion in hanging loads and therefore overstress remote-manipulator arms. The platform could be transferred around corners to adjacent panels.

The platform would ride on sprocketed guide pins extending from the structure at truss joints (see figure). A set of orthogonal tracks under the platform slides on the pins, which have enlarged heads to interlock with the tracks. At least three tracks engage at least three pins at any position on the panel so that the platform is adequately and stably supported.

The platform can travel longitudinally and transversely on the panel, in both forward and reverse directions. To get from one point to another, the platform moves in a series of straight lines, making left and right turns as necessary.

Two sets of chain drives under the platform — one for longitudinal motion, the other for transverse motion — propel it by engaging the guide-pin sprockets. Electric motors turn the chain drives.

To change from longitudinal to transverse motion, the platform comes to a complete stop and goes through a brief series of events. First, direction changers — slotted disks at each rail junction — rotate 90°. The slots in the direction changers ensure that the platform does not slip sideways. When the disks have all turned 90° from the longitudinal direction, they permit transverse movement and prevent longitudinal slippage.

Next, the end sections of the rails pivot upward. This provides clearance for the previously-engaged drive chains (for longitudinal motion) to disengage and rotate upward into the platform base and for the previously disengaged drive chains (for transverse motion) to rotate downward into engagement with the guide-pin sprockets. After drive-chain rotation, the end sections resume their original positions. To change from transverse to longitudinal motion, the platform goes through a similar sequence.

The platform transfers to adjacent truss panels on flaplike stages at the panel edges. The platform drives onto a stage, the stage pivots first at the near edge and then at the far edge to align with the plane of the adjacent panel, and the platform drives off onto the new panel. To transfer to the opposite face of a panel, the platform uses a stage that pivots about an axis near its center; the stage does a complete flip-flop, thereby aligning the platform with the plane of the opposite panel face.

This work was done by Clarence J. Wesselski and William C. Schneider of **Johnson Space Center**.

Inquiries concerning rights for the commercial use of this invention should be addressed to the Patent Counsel, Johnson Space Center. Refer to MSC-20985 /TN

Lyndon B. Johnson Space Center
Technology Utilization Officer:
Dean C. Glenn
Mail Code EA4
Houston, TX 77058
(713) 483-3809
Patent Counsel:
Edward K. Fein
Mail Code AL3
Houston, TX 77058
(713) 483-4871

FOR ADDITIONAL INFORMATION: *Contact: Director, Technology Transfer Division, P.O. Box 8757, BWI Airport, MD 21240; (301) 621-0100 Ext. 241*
REFER TO THE NUMBER LISTED AT THE END OF THE ARTICLE

NASA Tech Brief
National Aeronautics and Space Administration

Blade-Tip-Clearance Forces In Turbines

A study reviews the field and proposes experiments.

A report summarizes the present knowledge and discusses plans for experiments on blade-tip-clearance excitation forces in turbines. Of particular interest are the Alford forces, named after a pioneering worker in this field. These are the cross forces due to uneven clearances, which are in turn caused by and also cause rotor vibrations. Because blade-tip clearances affect turbine efficiency and excitation forces affect rotor stability, the report should prove useful to researchers and designers of advanced turbomachinery.

The study was carried out in three phases documented in the report. The first phase was a literature search and evaluation. In addition to showing the state of the art, this phase exposed the need for theoretical and experimental efforts to provide design data and a rational basis for extrapolation to new configurations and operating conditions.

The authors found that a very small data base exists for excitation blade-tip forces in unshrouded turbines. A more extensive data base exists for shrouded blading under static effects. In both cases, however, a detailed fluid-mechanical understanding of the effect is lacking. Consequently, extrapolations to untested conditions remain dubious. Furthermore, there are no reliable data on forces proportional to the rate of change of the clearance.

In the second phase of the study, several of the assumptions contained in the usual theoretical analyses of the Alford force were removed. The problem was then posed in terms of a rigorous linearized flow analysis of the behavior of an eccentric rotor approximated by an actuator disk with two-dimensional flow. This theoretical study revealed an important contribution to the Alford force from the redistribution of flow around the turbine annulus. It also showed an important contribution from the annulus pressure, even in unshrouded turbines.

The third phase was a preliminary design study of a turbine-testing facility. The objective of this phase was to extend the data base by development of the capability to measure excitation forces and the associated (and causative) flow patterns over a realistic range of turbine-stage loadings, flow angles, flow speeds, and Reynolds numbers, among other parameters. This demands a variety of turbine configurations, especially in the blade-tip region, thereby necessitating frequent total or partial assembly and disassembly. Consequently, the facility was designed with modular parts.

The design also includes the instrumentation and numerous instrumentation ports in the turbine. Plans call for the measurement of mass-flow rates, temperatures, pressures, gas compositions, rotor speeds, braking torques, casing vibrations, rotor positions, bearing forces, and local flow velocities. The facility thus presents a problem in data reduction. There are 132 data channels, of which about 26 are likely to be used during a typical experiment. This will require some software development for correct data acquisition.

This work was by M. Martinez-Sanchez and Edward M. Greitzer of the Massachusetts Institute of Technology for **Marshall Space Flight Center**. *Further information may be found in NASA CR-171534 [N85-29963/NSP], "Turbine Blade-Tip Clearance Excitation Forces."*

Copies may be purchased from the National Technical Information Service, Springfield, Virginia 22161. [A05]
MFS-27122 /TN

FOR ADDITIONAL INFORMATION: *Contact: Director, Technology Transfer Division, P.O. Box 8757, BWI Airport, MD. 21240; (301) 621-0100 Ext. 241*
REFER TO THE NUMBER LISTED AT THE END OF THE ARTICLE

NASA Tech Brief

National Aeronautics and Space Administration

NASA's Jet Propulsion Laboratory, Pasadena California

Air-Powered Projectile Launcher

A small, high-pressure reservoir conserves compressed air.

An air-powered launcher fires plastic projectiles without using explosive propellants. It therefore does not generate high temperatures. The launcher was developed for combat training for the U.S. Army. It also has potential applications in seismic measurements, avalanche control, and testing impact resistance of windshields on vehicles.

In comparison with prior air launchers, the new launcher is lightweight and reliable. It is intended to consume a minimum amount of compressed air for each high-velocity launch and, therefore, was designed with a small-volume, high-pressure air reservoir. The reservoir surrounds the breech of the launcher so that the airflow path is short and flow losses small.

The valve that releases high-pressure air to the breech was built as a sleeve to keep the stroke short and enable the valve to open rapidly. The sleeve configuration also allows projectiles to be loaded in the conventional way, either manually or automatically.

When the reservoir is pressurized before a launch, the rear valve chamber is also pressurized. The valve is thus held in its closed (forward) position by differential pressure (see figure). Just before a launch, the pressure inlet is sealed. At the launch time, a pilot valve is energized and vents the rear valve chamber. The pressure in the reservoir then forces the sleeve to its open (rearward) position. As the sleeve opens, the high-pressure air in the reservoir discharges into the barrel and propels the projectile outward.

After the discharge, the valve is quickly closed again by differential air pressure, and the reservoir is recharged with compressed air. At the same time, the breech bolt is opened and a new projectile inserted into the barrel.

This work was done by Thomas Andrews, Roy A. Bjorklund, David G. Elliott, and Larry K. Jones of Caltech for **NASA's Jet Propulsion Laboratory**.

NPO-16763 /TN

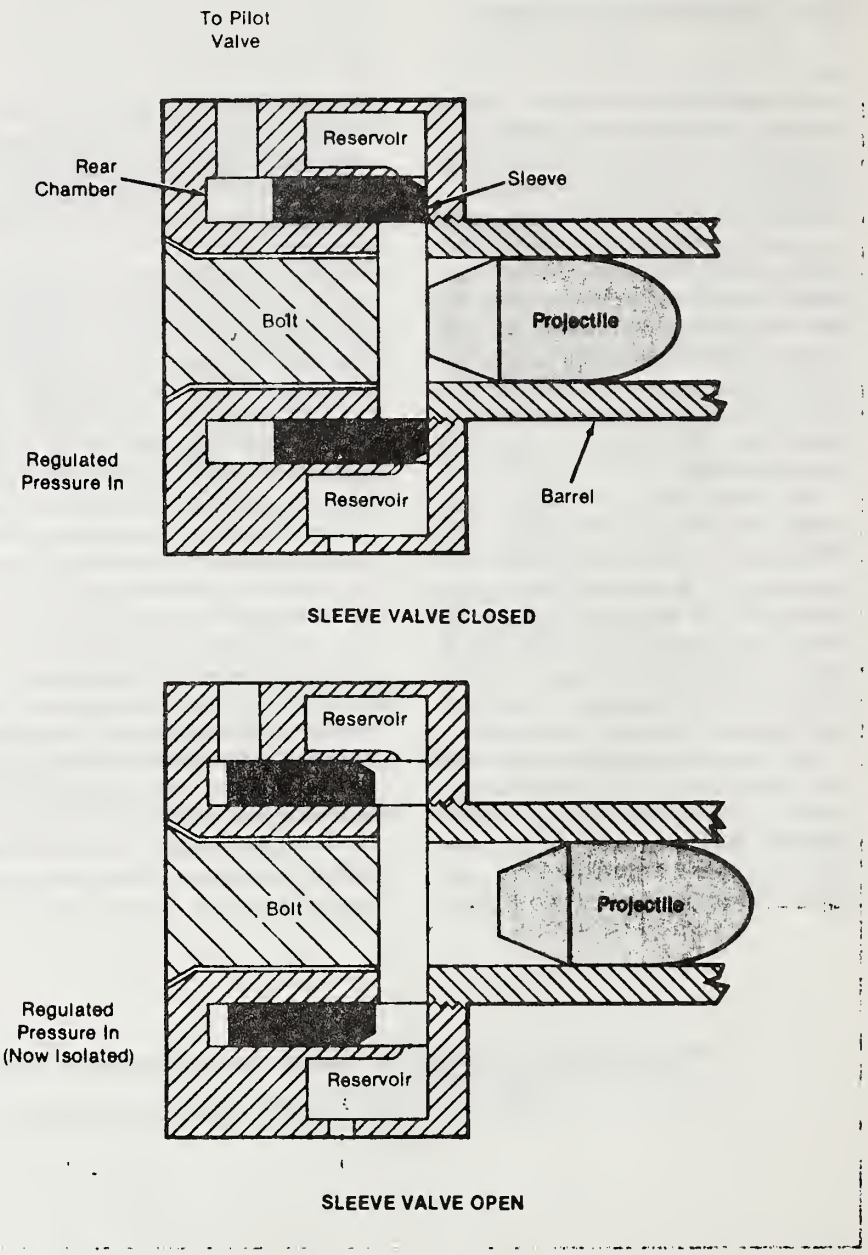

With Its Reservoir Pressurized, the air launcher is ready to fire (top). When the pilot valve is opened, the sleeve (the main valve) moves to the rear (bottom). The projectile is rapidly propelled through the barrel, pushed by air from the reservoir.

FOR ADDITIONAL INFORMATION: *Contact: Director, Technology Transfer Division, P.O. Box 8757, BWI Airport, MD. 21240; (301) 621-0100 Ext. 241*

REFER TO THE NUMBER LISTED AT THE END OF THE ARTICLE

Soil Conservation Service, Washington, DC. Engineering Div.

Urban Hydrology Software for Small Watersheds

The program provides simplified procedures to calculate storm runoff volume, peak rates of discharge, and storage volumes required for stormwater detention basins. These procedures are applicable in small watersheds, especially urbanizing watersheds. The program provides for hydrologic analysis of a watershed under various combinations of land uses using single-event storm rainfall frequency data.The program can accommodate division of the watershed into subareas and will estimate individual subareas as well as total area peak rates of runoff.

The software is contained on 5 1/4 -inch diskette, double sided, double density compatible with the Telex PC microcomputer. Diskettes are in the ASCII format. The SCS TR-55 program runs on IBM compatible microcomputers with MS-DOS (2.1) capabilities and 256 K storage.

FOR ADDITIONAL INFORMATION

Contact the NTIS Computer Products Center, NTIS Springfield, VA 22161; (703) 487-4763. Reference software number PB87-101598/NAC. Price includes documentation.

energygram®

Use of Miniaturized Tests to Predict Flow Properties and Estimate Fracture Toughness in Deformed Steel Plates

DOE/TIC/EG-86/115
OFFICE OF SCIENTIFIC AND TECHNICAL INFORMATION

This technical note was based on research conducted by Idaho National Engineering Laboratory for the U.S. Department of Energy.

INEL
Idaho National Engineering Laboratory

A miniaturized testing technique has been used to map the change in both flow and fracture toughness properties in a deformed area. The data obtained were then compared with tensile measurements on identical materials. The use of the data, coupled with micro-mechanical models of fracture, allows estimation of the deformed material's fracture toughness.

Prediction of instability in a structure requires knowledge of the mechanical properties of the materials involved. In the case of serious accident, prediction of instability in damaged components is difficult due to insufficient knowledge of: the deformed material fracture toughness, the cracks induced by the accident, and the stress state in the damaged region.

For the assessment of the structural integrity of damaged and deformed components, prior knowledge of the change in material fracture toughness, size and extent of induced defects, and subsequent stress distributions during reloading is required.

The paper cited here evaluates the change in fracture toughness and flow properties for a railroad tank car steel plate (A515 Grade 70) after deformation. It further describes a testing technique to measure changes in material flow properties. The data are then used with a critical fracture strain model to estimate relative changes in material fracture toughness.

The miniaturized test technique uses measurement with a miniaturized shear punch to estimate the relative change in fracture toughness of the material. Results using the shear punch technique are directly compared with measured fracture toughness and tensile data for the same strained material.

The information contained in this report will be of interest to such organizations as materials testing laboratories, industrial research organizations, and universities.

FOR ADDITIONAL INFORMATION

DOE report(s):
The Use of Miniaturized Tests to Predict Flow Properties and Estimate Fracture Toughness in Deformed Steel Plates.
Report number: EGG-M-05285/NAB
Order number: DE86007644/NAB
Price: $9.95

Order from:
National Technical Information Service
5285 Port Royal Road
Springfield, VA 22161

For additional information, contact:
J. M. Welch
EG&G Idaho, Inc.
P.O. Box 1625
Idaho Falls, ID 83415
Telephone No.: (208) 526-8318

or

F. M. Haggag
EG&G Idaho, Inc.
P.O. Box 1625
Idaho Falls, ID 83415
Telephone No.: (208) 526-9588

NASA Tech Brief

National Aeronautics and Space Administration

Marshall Space Flight Center, Alabama

One-Piece Force-Transducer Body

A rugged unit is designed to operate in severe environment.

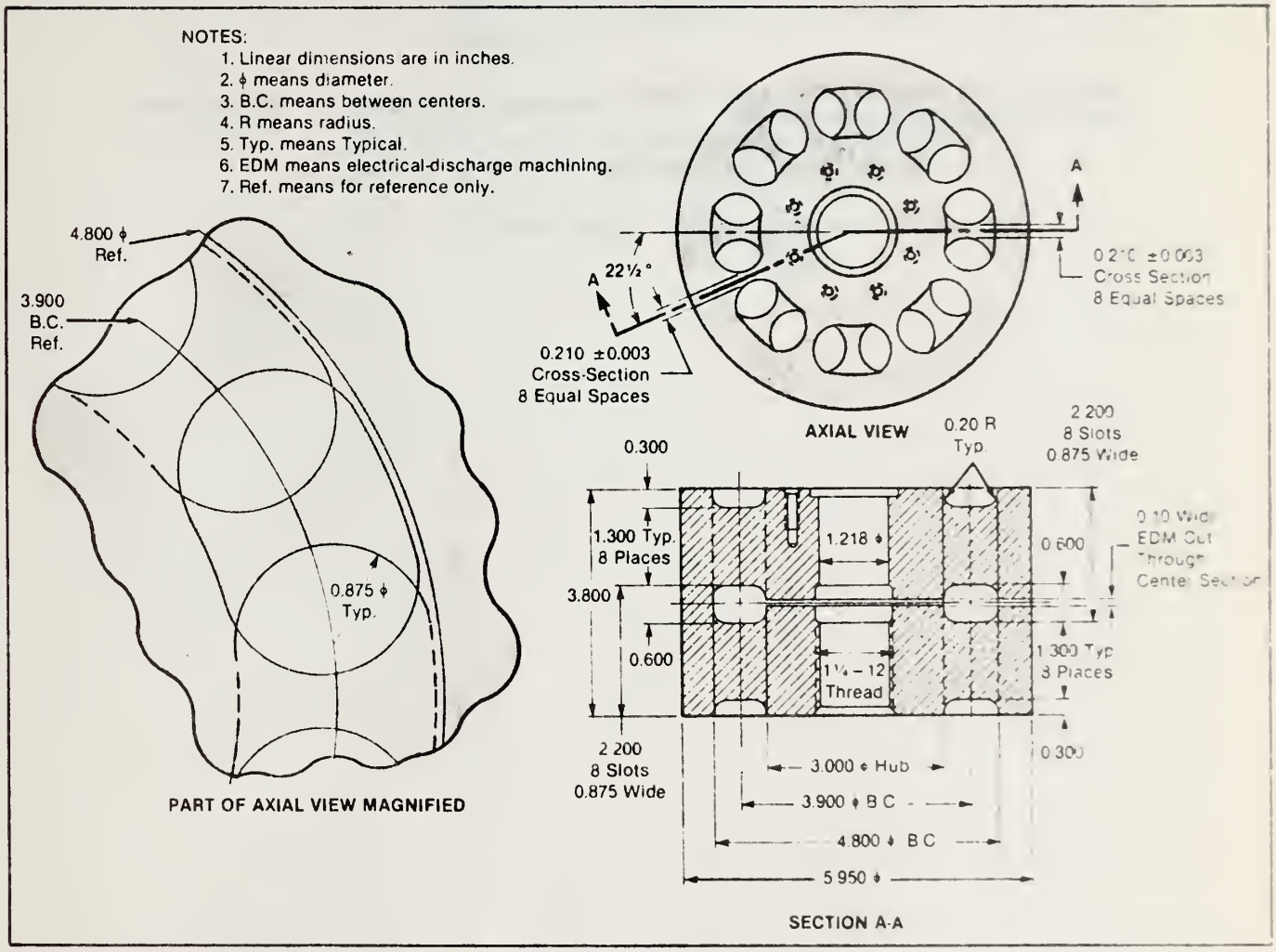

The **Symmetrical Force-Transducer Body** is machined in this configuration from a piece of bar stock.

A force-transducer body is designed for the measurement of loads on specimens tested in hydrogen gas at temperatures up to 2,000 °F (1,090 °C). The body has a symmetrical radial-shear-beam configuration and is machined in one piece from bar stock.

Shear-beam load cells are in general use. Some commercially available units are of the rectangular S-bend beam design, which is asymmetrical about the axis of load application. This asymmetry is considered undesirable. Another type of commercial unit is circularly symmetrical but is manufactured in several pieces, with spokes radiating from a central hub to an outer hub through a bolt circle. The sensing structure is bolted through the bolt circle to a second circular adapter plate that incorporates a central thread. A central loading thread is thus available at opposite ends of the load-cell assembly.

The symmetrical commercial units have several disadvantages. They are unreliable in the severe testing environment because of the large number of highly stressed joints between the parts. Assembly requires the painstaking concentric alignment of the two parts that contain the central thread. Mating parts can slip relatively to each other under load. The relative motion of parts can

cause fretting fatigue of the joint surfaces under cyclic reversed loading. The slippage of bolted joints can cause hysteresis in the measurements. Even if properly designed, bolted joints exhibit asymmetry because they have different spring stiffnesses in tension and compression.

The new symmetrical load-cell body (see figure) is rugged. It has all of the stiffness, strength, accuracy, and low overall height of a conventional two-piece radial shear beam. However, because it is made in only one piece — as opposed to two major pieces and at least eight fasteners in the conventional design — it is both more reliable and less expensive. The concentricity between the opposite central threads is machined in, eliminating the need of alignment in assembly. The new configuration has no inherent asymmetry between tension and compression. Finally, the new unit is easier to seal against the environment because there are no bolted joints, each of which would otherwise have to be sealed individually.

This work was done by Richard A. Meyer of MTS Systems Corp. for **Marshall Space Flight Center.**

MFS-28140 /TN

FOR ADDITIONAL INFORMATION: *Contact: Director, Technology Transfer Division, P.O. Box 8757, BWI Airport, MD. 21240; (301) 621-0100 Ext. 241*

REFER TO THE NUMBER LISTED AT THE END OF THE ARTICLE

Environmental Science & Technology

564 Modified Generator Puts Out More Power with Less Noise

565 An Evaluation of Densification Technologies for Solid Waste

566 Integrated Global Background Monitoring Network—Preliminary Results

Software

567 An Interactive Computer Model for Calculating V-I Curves in ESPs Version 1.0

Other items of interest

561 Urban Hydrology Software for Small Watersheds

611 A Virtual Impactor for Personal and Area Air Sampling

U.S. Army Belvoir R&D Center
Technology Application

Army Troup Support Command, Fort Belvoir, VA 22060

Modified Generator Puts Out More Power with Less Noise

The standard generator that powers the Army's Regency Communications Network has been modified by the Troop Support Command's Belvoir RDE Center to comply with local noise ordnances in populated areas.

In addition to a significant reduction in the noise level, electrical engineers at the Center have increased the generator's output from 15 to 20 kilowatts and "hardened" it to resist nuclear attack.

"The requirement came from the project manager for the system because they needed a set that would comply with local noise ordinances" according to Dr. Larry I. Amstutz of the Power Generation Division of the Center's Logistics Support Directorate. "We decided to do the work in-house because the time schedule was too short to send it out on contract".

Work on the project involved modifying a standard 15kW generator to convert it to 20kW. "That was easy, Ronald B. White, project engineer explained, "What was hard was to silence it within a reasonable weight and cost, and still fit it on the same trailer."

The modified set consists of the same basic parts as the original unit so that it can be easily supported in the field. "We put a silencer on the inlet air filter, installed a better muffler, isolated the vibration between the housing and the generator's working parts, and installed noise baffles in the generator's cooling inlet and exhaust," White said. "And we did all that while increasing the weight by less than 300 pounds. That's something we're really proud of."

Thanks to the modifications, the generator now registers less than 65 dBA at seven meters in any direction, about as loud as a normal conversation. Before the modifications, the set registered 80 to 85 dBA and was so loud its operator was required to wear hearing protection.

FOR ADDITIONAL INFORMATION:

Public Affairs Office
US Army Troop Support Command's
Belvoir Research & Development Center
Fort Belvoir, VA 22060-5606
Tel: (703) 664-5813 or 5598
Refer to: Modified Generator 10-86

energygram®

An Evaluation of Densification Technologies for Solid Waste

DOE/TIC/EG-86/117
OFFICE OF SCIENTIFIC AND TECHNICAL INFORMATION

This technical note was based on research conducted by Idaho National Engineering Laboratory for the U.S. Department of Energy.

INEL
Idaho National Engineering Laboratory

The state of the art of densification technology as applied to producing densified refuse derived fuel (RDF) is assessed and evaluated in the report as discussed here. Aspects of the technology, such as performance, economics, pacing problems, operational practice, and available equipment, are addressed as these relate to the study.

There has been a growing interest in the past decade in the production of fuel from municipal solid waste. The fuel, called RDF, is produced by mechanically separating the noncombustible elements of solid waste and reducing the particle size. RDF, as produced, is in a low-density form. In this form, it is typically burned in large suspension-fired boilers as a supplement to pulverized coal.

RDF can be further processed to a form that is more conducive to handling, transportation, and storage. This form is called densified refuse derived fuel (d-RDF) and is much better suited for stoker-fired and other boilers. d-RDF has physical properties similar to those of coal, this makes it easier to handle and distribute than standard RDF in stoker-fired systems. Problems exist with the d-RDF technology, however, and those problems are evaluated in this research report.

Individual sections of the report are devoted to each aspect of the technology:

(1) Description of chemical, physical, handling, storage, and combustion properties of d-RDF.

(2) Evaluation of pellet mills in d-RDF production applications.

(3) Assessment of cuber densification techniques.

(4) Assessment of other densification techniques.

(5) Overall assessment of state of the d-RDF production industry.

Information contained in the report cited here is of potential interest to waste disposal firms, municipalities, and other groups concerned with multi-use recycling of solid wastes.

FOR ADDITIONAL INFORMATION

DOE report(s):
An Evaluation of Densification Technologies
Report number: EGG-EA-6775/NAB
Order number: DE86002326/NAB
Price: $5.95 (microfiche only)

Order from:
National Technical Information Service
5285 Port Royal Road
Springfield, VA 22161

For additional information, contact
J. M. Welch
EG&G Idaho, Inc.
P.O. Box 1625
Idaho Falls, ID 83415
Telephone No. (208) 526-8318

or

E. M. Steverson
EG&G Idaho, Inc.
P.O. Box 1625
Idaho Falls, ID 83415
Telephone No. (208) 526-0558

energygram

Integrated Global Background Monitoring Network—Preliminary Results

DOE/TIC/EG-86/157
OFFICE OF SCIENTIFIC AND TECHNICAL INFORMATION

This technical note was based on research conducted by Idaho National Engineering Laboratory for the U.S. Department of Energy.

Idaho National Engineering Laboratory

Preliminary results from two of three initial sites established as part of an integrated global background monitoring network indicate basic agreement with initial hypotheses, that the Olympic and Torres del Paine National Parks are not polluted. Long-range plans call for the establishment of a worldwide system of monitoring sites to determine the status of pollution worldwide.

The objectives of the establishment of the three sites in the pilot network are:

1. Establish reference levels for acidic and toxic compounds and other pollutants that have potential for global contamination.

2. Serve as early warning sites for detecting long-term transport of acidic and toxic pollutants and potential changes of ecosystem processes.

3. Establish baseline levels for selected ecosystem parameters against which data from more impacted areas can be compared.

During the process of establishment of such baseline parameters, samples of soil, water, air, two species of vegetation (moss and lichen), and forest litter were collected and analyzed. The samples were compared against reference samples and against similar samples from the other initial sites.

The report as cited here contains useful information for monitoring pollution of all remote areas and assessment of the magnitude of pollution by the Environmental Protection Agency, forestry, and other environmental organizations both in the United States and worldwide.

FOR ADDITIONAL INFORMATION

DOE report(s):
Integrated Global Background Monitoring Network—Preliminary Results from Torres del Paine and Olympic National Parks.
Report number: EGG-M-26785/NAB
Order number: DE87000531/NAB
Price: $9.95

Order from:
National Technical Information Service
5285 Port Royal Road
Springfield, VA 22161

For additional information, contact:
J. M. Welch
EG&G Idaho, Inc.
P.O. Box 1625
Idaho Falls, ID 83415
Telephone No.: (208) 526-8318

or

G. B. Wiersma
EG&G Idaho, Inc.
P.O. Box 1625
Idaho Falls, ID 83415

United States
Environmental Protection
Agency

Air and Energy Engineering
Research Laboratory
Research Triangle Park NC 27711

Research and Development

EPA

Project Summary

An Interactive Computer Model for Calculating V-I Curves in ESPs Version 1.0

The manual describes two microcomputer programs written to estimate the performance of electrostatic precipitators (ESPs): the first, to estimate the electrical conditions for round discharge electrodes in the ESP; and the second, a modification of the EPA/SRI ESP model, to estimate the particle collection efficiency of the ESP operating with the electrical conditions predicted by the first program. Both programs, written in the BASIC computer language, are designed for the IBM-PC and compatible computers and the Tandy 2000 computer. The programs require Advanced BASIC and a color graphics adapter.

The V-I program allows prediction of electrical conditions for both positive and negative corona and for arbitrary discharge electrode diameters and wire-to-wire spacing. This means that most commercial discharge electrode geometries can be simulated by proper selection of wire diameters and spacing.

Both the V-I and performance models are completely documented in the report, including a discussion of the theory on which the models are based. Most of the report is devoted to instructions, with examples, for using both models. Guidance for adapting the programs to other computers is also presented.

The models are quite useful and allow rapid assessment of expected ESP performance under a wide variety of conditions.

Introduction

Electrostatic precipitators (ESPs) are used to collect particulate pollutants from a wide range of sources. Considerable effort has been spent developing computer models for predicting the performance of ESPs. The most successful of these models is the EPA/SRI ESP model. The predictions of the EPA/SRI ESP model have been verified for several sources - especially for coal fired power plants. Before the EPA/SRI ESP model can be used, the electrical operating conditions in the ESP must be estimated by the user because the model cannot calculate electrical conditions.

Because electrical conditions in the ESP are so important, the V-I predictor model described in this report was written. In the initial development of the model, it became apparent that rapid mathematical computation would be necessary. Thus, it was decided to use analytic approximations as much as possible and to avoid use of numerical solutions of partical differential equations. This led to the development of several new approximations for the electrical conditions in an ESP. These approximations have been checked against experimental data and the detailed numerical solutions. In all cases, the answers provided by the approximations were in excellent agreement.

Model Version 1.0 enables the prediction of the electrical conditions for round-wire discharge electrodes. The wires in a given section can have varying diameters and be at various spacings. The effects of an immobile, constant space charge can be included, and this component of space charge can decrease by a certain fraction for each wire, thereby simulating the effects of real particulate space charge. This

System Requirements

The programs, developed on a Tandy 2000 microcomputer, make full use of all its graphic capabilities. Because of the large number of IBM-PCs in use, the program was written to include the capability to run on those machines without modification. However, some sacrifices in graphics are noticed when the models are run in the IBM mode.

Tables 1 and 2 list the minimum hardware and software requirements for running the program and suggest options that will enhance the use of the programs.

The models could be rewritten to run on other computers. However, the modifications required to adapt the data entry portions of the program to computers that do not use Microsoft BASIC would be extensive.

Table 1. *Tandy 2000 Hardware Requirements*

System	*Minimum*	*Beneficial*
RAM	*256*	·256
Disks	1 floppy, double sided	2 floppies or 1 floppy/1 hard
Graphics	High resolution	
Color	Optional	Standard or Tandy CGP-220 for graphics[a]
Software	GW-BASIC	
DOS	2.11 or higher	

[a]If high resolution color is not available, the Tandy 2000 can be run as an IBM configured computer.

Table 2. *IBM PC PC-XT PC-AT Requirements*

System	*Minimum*	*Beneficial*
RAM	*128K*	·256K
Disks	1 floppy, double sided	2 floppies or 1 floppy/1 hard
Graphics	Optional	High resolution, B&W
Color	Optional	Color monitor
Printer	Optional	Standard
Software	BASICA (Advanced BASIC)	
DOS	2.0 or higher	

P. A. Lawless is with Research Triangle Institute, Research Triangle Park, NC 27709; the EPA author, ***Leslie E. Sparks*** *(also the EPA Project Officer, see below), is with the Air and Energy Engineering Research Laboratory, Research Triangle Park, NC 27711.*

The complete report consists of two parts, entitled "An Interactive Computer Model for Calculating V-I Curves in ESPs, Version 1.0,"
Paper copy (Order No. PB 87-100 046/AS; Cost: $24.95)
Computer diskettes (2) (Order No. PB 87-126 025, Cost: $90.00)
The above items will be available only from: (costs subject to change)
National Technical Information Service
5285 Port Royal Road
Springfield, VA 22161
Telephone: 703-487-4650
The EPA Project Officer can be contacted at:
Air and Energy Engineering Research Laboratory
U.S. Environmental Protection Agency
Research Triangle Park, NC 27711

Manufacturing, Machinery, & Tools

568 Developing a Reliability-Centered Maintenance Plan— Effective preventive maintenance can be implemented with minimum expenditure of resources.

569 Manufacturing Fiber-Optic Bundles With Low-Loss Glass— It is feasible to make long bundles for highly sensitive imagescopes and similar optical instruments.

570 Draft Standard for Robots Issued

571 Turning Workstation Being Developed for Mare Island Naval Shipyard

572 Multifunction Vacuum Chamber for IC Metallization— One system performs several operations without transferring wafers between vacuum chambers. (Licensing Opportunity)

573 Laser Vacuum Furnace for Zone Refining— A laser beam is scanned to produce a moving melt zone. (Licensing Opportunity)

574 Producing Refractory Microballoons— Metals, ceramics, and glasses are just some of the possible raw materials. (Licensing Opportunity)

575 Redundant Pyrotechnic/Manual Release Mechanism— When all else fails, manual intervention is possible. (Licensing Opportunity)

Other items of interest

538 Reinforced Masks for Ion Plating of Solar Cells— Long fingers would be held more rigidly. (Licensing Opportunity)

578 Steels for High-Temperature Gears— Potential replacements for a standard steel are evaluated.

MANUFACTURING TECHNOLOGY NOTE

U.S. ARMY MATERIEL COMMAND

Deputy Chief of Staff for Manufacturing Technology, Alexandria, VA

Project Number: NONE

Filing Code: 70C031

Developing a Reliability-Centered Maintenance Plan

Effective preventive maintenance can be implemented with minimum expenditure of resources.

A report presents procedures for performing reliability-centered maintenance (RCM). The report, prepared by the U.S. Army Material Command, is a guide for those who write and develop detailed maintenance plans for systems and equipment using the RCM philosophy.

RCM is a disciplined logic or methodology used to identify preventive maintenance tasks in order to realize the inherent reliability of equipment with a minimum expenditure of resources. With the aid of RCM logic and the RCM technique known as failure mode, effects, and criticality analysis (FMECA), a scheduled maintenance plan can readily be developed. The plan will include maintenance tasks and maintenance intervals, and will provide information for overhaul, age exploration, economic analysis, and redesign.

FMECA identifies potential design weaknesses through systematic, documented consideration of the likely ways in which a component or equipment can fail, the causes for each failure mode, and the effects of each failure. Age exploration is a systematic evaluation of an item based on analysis of information collected while the item is in service (see figure). It assesses the resistance of the item to a deterioration process associated with increasing age.

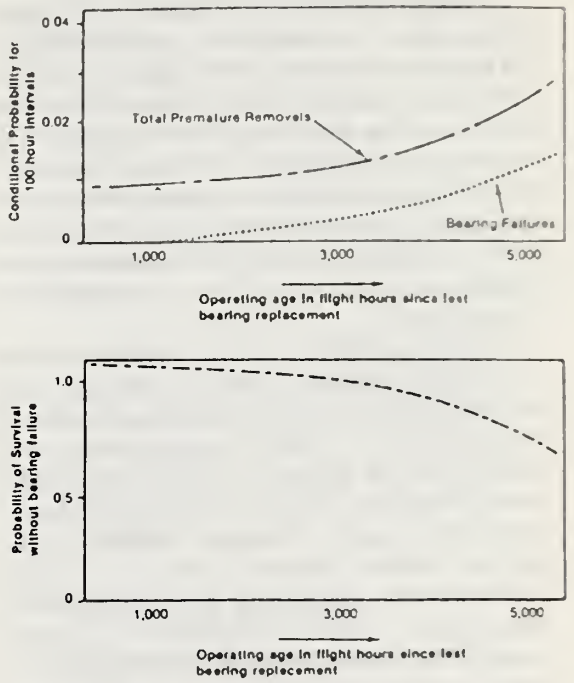

Age Exploration Yields a conditional probability curve derived from operating experience (top). Here, an engine-driven generator serves as an example. There is little change in the failure rate until 2,000 hours, thereafter, the conditional probability of the failure increases as this failure mode becomes more dominant. The survival curve (bottom) derived from the conditional probability curve shows the probability that the generator will not suffer a bearing failure.

FOR ADDITIONAL INFORMATION

You can learn more details about this technology by ordering the NTIS report(s):

Developing a Reliability-Centered Maintenance
Order number: AD-A170938/NAA
Price code: A05

Order from:

National Technical Information Service
5285 Port Royal Road
Springfield, VA 22161

This document was prepared under the sponsorship of the U.S. Government. Neither the United States Government nor any person acting on behalf of the United States Government assumes any liability resulting from the use of the information contained in this document, or warrants that such use will be free from privately owned rights.

MANUFACTURING TECHNOLOGY NOTE

U.S. ARMY MATERIEL COMMAND

Deputy Chief of Staff for Manufacturing Technology, Alexandria, VA

Project Number: NONE

Filing Code: 46C086

Manufacturing Fiber-Optic Bundles With Low-Loss Glass

It is feasible to make long bundles for highly sensitive imagescopes and similar optical instruments.

A program has shown the feasibility of making long bundles of low-attenuation fused silica fibers. The program for the U.S. Army Ballistic Research Laboratory produced 1-meter lengths of bundles having a 4- by 4-millimeter cross section. The bundles have a resolution of more than 50 line pairs per millimeter, transmission of greater than 40 percent, and numerical apertures ranging from 0.26 at 1,050 nanometers to 0.29 at 400 nanometers. An imagescope was fabricated from a bundle as part of the program.

The basic building block for a bundle is an array six by six fibers square in a matrix of low-index cladding material. A layer of multifiber arrays is laid on a traversing drum 1 meter in circumference and hand packed so that each is in intimate contact with its neighbors. Epoxy is brushed on the arrays to hold them together. The epoxy is partially cured, and the multifiber ribbon thus formed is removed from the drum. A number of ribbons are stacked and pressed to form a solid block of fully cured epoxy holding the ribbons together in a bundle. The bundle can then be mounted in the imagescope hardware and polished.

The attenuation in multifiber arrays was found to range from about 0.26 dB/m for step-index fibers to about 0.55 dB/m for graded-index material (see figure). These values, although significantly lower than those for silica glass arrays, are still higher than the attenuation in single fused silica fibers. The reasons for the increase over single fibers are the nonoptimum core-to-cladding index ratio in the multifiber and the greater difficulty in controlling multifiber geometry during drawing. A closed-loop measurement system like that used in monofiber manufacturing would ensure precise geometry control.

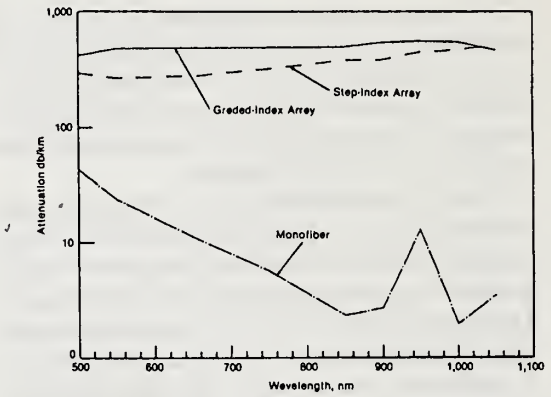

Arrays of **Step-Index Fibers** have slightly lower attenuation than graded-index arrays. Improvements in the manufacturing equipment and adjustments in the core and cladding indexes of refraction should allow multifibers to approach the very low attenuation of single fibers.

FOR ADDITIONAL INFORMATION:

You can learn more details about this technology by ordering the NTIS report(s):

A Coherent Fused Silica Fiber-Optic Array.
Order number: AD-A171083/NAA
Price code: A02

Order from:

National Technical Information Service
5285 Port Royal Road
Springfield, VA 22161

This document was prepared under the sponsorship of the U.S. Government. Neither the United States Government nor any person acting on behalf of the United States Government assumes any liability resulting from the use of the information contained in this document, or warrants that such use will be free from privately owned rights.

Navy Manufacturing Technology

AMRF Automated Manufacturing Research Facility

National Bureau of Standards, Gaithersburg, MD 20899

Draft Standard for Robots Issued

A draft standard, issued in January, 1987, defines conformance classes and names for robots and robotic systems used in communications networks which employ the Open Systems Interconnection (OSI) application layer standard EIA RS 511. Upon approval, the new standard, to be known as RIA 15.06-1986, will become a formal part of the Manufacturing Automation Protocol (MAP).

RS 511, Manufacturing Message Service for Bidirectional Transfer of Digitally Encoded Information — Service and Protocol, contains many features not required for robots and robotic systems. Some would be impractical to implement in robotic systems. The RIA companion standard, developed with input from NBS, defines a family of subsets of RS 511 for this application area.

Four conformance classes for robots are provided for in the draft standard. A base class is considered the minimum information service and protocol. Conformance classes provide the flexibility necessary for a robot to be connected as a slave to a network or to act as a controller of other equipment such as vision systems or grippers or to operate in a network of peer robots and other equipment.

The standard recognizes that safe operation of robots must be assured at all times and defines safety requirements for industrial robots and robot systems. All robot actions defined by this companion communication standard are permissible under the safety standard.

The RIA committee will continue efforts which lead to the formal adoption of this robot specific application layer of MAP. Additional responsibilities of the committee include the review and critique of companion standards which affect RIA 15.06 — 1986.

Since initiation of this effort, committees on numerical control, programmable logic controllers, process control, and vision systems have established similar efforts to define subsets of RS 511 for their applications.

For Additional Information:

To discuss this effort further, contact:

Dr. James Albus
AMRF Project Manager
Building 220—Room B-124
National Bureau of Standards
Gaithersburg, MD 20899
(301) 975-3418

Navy Manufacturing Technology

AMRF Automated Manufacturing Research Facility

National Bureau of Standards, Gaithersburg, MD 20899

Turning Workstation Being Developed for Mare Island Naval Shipyard

NBS, in cooperation with the Mare Island Naval Shipyard, is developing a turning workstation for use in production of submarine parts used by the shipyard. The workstation will initially be assembled, programmed, and tested in the AMRF. Upon completion, the workstation, which is designed to accommodate one robot and two turning centers, will be transferred to the shipyard in California.

The first parts machined at Mare Island will be a family of vibration isolators used on nuclear submarines. The workstation, with only one turning center initially, will machine the metal parts that form a rubber insert sound insulation coupling (RISIC).

The RISIC is a critical component of the sound silence program for nuclear submarines. These parts, which have a limited life because the rubber seals deteriorate and must be replaced at least every five years, are among the Navy's "difficult to procure" parts. The metal parts have a longer life than the rubber components, but are frequently damaged during replacement of the rubber seals or display corrosion damage and must be replaced.

The fittings are currently manufactured from gunmetal bar stock by the Mare Island Naval Shipyard and other shipyards that repair and refurbish nuclear submarines. Applying automation techniques developed at the AMRF is expected to reduce the total production time of the parts to approximately two hours.

The workstation will be delivered to Mare Island in the fall of 1988. It is an example of the way in which technology developed at the AMRF can be transferred to other government facilities or private industry, reducing costs and production times.

NBS is looking for other ways to transfer the technology developed at the AMRF. If you would like to propose such a project, contact Dr. Philip Nanzetta, AMRF Project Manager.

For Additional Information:

To discuss this effort further, contact:

Dr. Phillip Nanzetta
AMRF Project Manager
National Bureau of Standards
Gaithersburg, MD 20899
(301) 975-3421

NASA Tech Brief
National Aeronautics and Space Administration
Marshall Space Flight Center, Alabama

Licensing Opportunity

Multifunction Vacuum Chamber for IC Metallization

One system performs several operations without transferring wafers between vacuum chambers.

A vacuum system chamber for processing multilayer metallization on integrated circuits (IC's) performs four operations ordinarily done in separated equipment. The chamber etches holes, removes photoresist, cleans by sputter etching, and deposits the final layer of metal.

The combined-function chamber costs less than the separate equipment performing the same functions. The chamber avoids exposing the integrated circuits to room air and, consequently, to oxidation and dust, between steps. It also eliminates the time spent in transferring the circuits from one apparatus to the next.

Unlike the conventional process, the multifunction process does not use liquid acids and reducing agents for hole etching and photoresist removal. The cost of disposing of these hazardous materials is therefore avoided.

The chamber (see Figure 1) contains turntables that continuously turn silicon integrated circuit wafers to ensure uniform processing of several wafers at a time. It also contains radio-frequency and magnetron sputtering guns. External tanks furnish gases to the chamber.

Wafers are introduced into the chamber after transistors or other circuit elements have been formed in them and after layers of oxide, metal, more oxide, and photoresist have been built up. Holes yet to be formed are delineated by the photoresist pattern. In the first vacuum processing step, a mixture of helium, oxygen, and a chlorofluorocarbon gas is admitted to the chamber, forming a plasma under the radio-frequency sputtering gun. A permanent magnet directs the plasma to the wafer surface, where it etches away the oxide

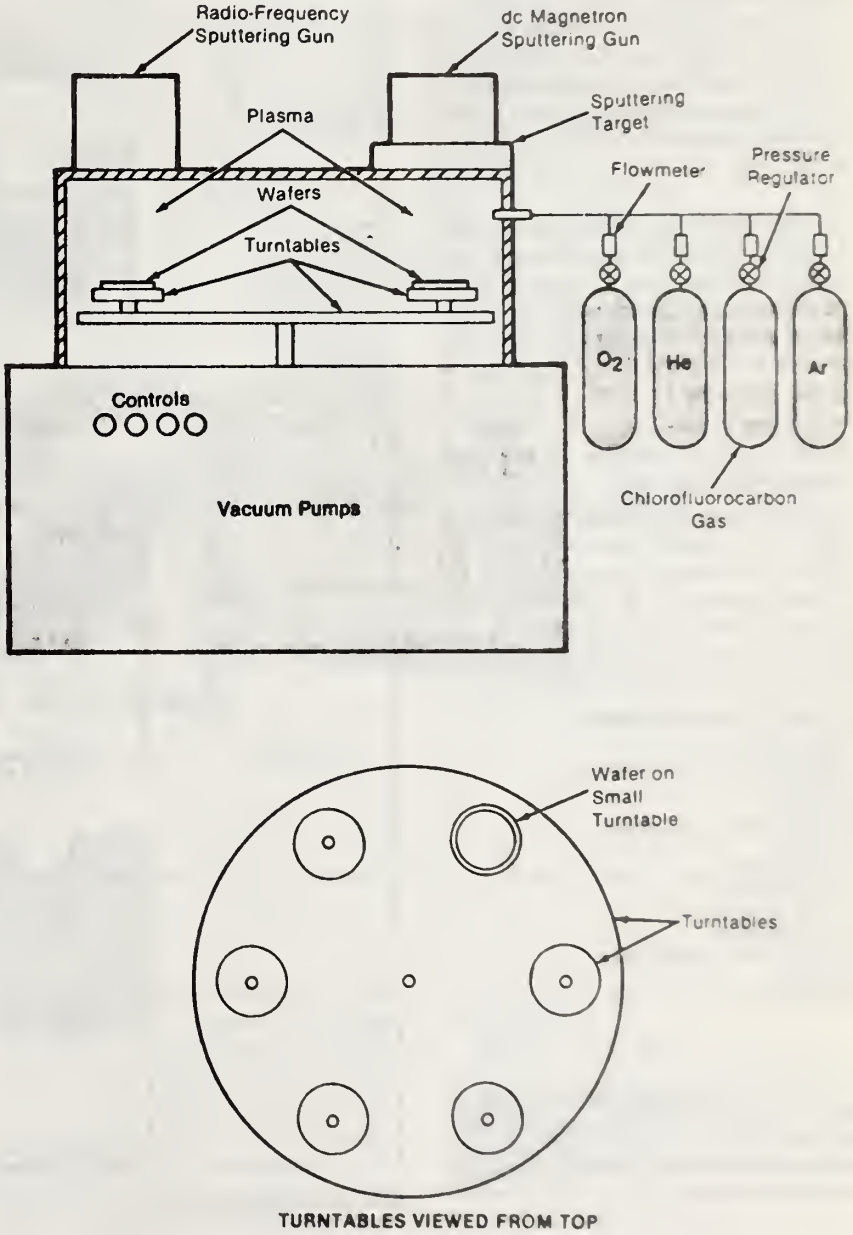

Figure 1. **External Tanks Supply Gases** to the vacuum chamber for forming plasmas. Permanent magnets direct the plasmas to the wafers as they pass under the sputtering guns. The wafers are continuously rotated about their own centers and about the center of the upper turntable for uniform coverage.

in the holes, exposing the metal layer at the bottoms of the holes (see Figure 2). When etching is done, the gas mixture is pumped out.

In the second step, oxygen is admitted and forms an oxygen plasma under the radio-frequency sputtering gun. This plasma etches away the photoresist layer. It also forms aluminum oxide at the bottoms of the newly etched holes. The oxide layer prevents the formation of good contacts and must be removed.

After the oxygen has been pumped out, argon is admitted. The argon plasma under the radio-frequency sputtering gun cleans the entire wafer surface, removing the aluminum oxide from the bottoms of the holes. The argon is then pumped out.

In the fourth step, the magnetron sputtering gun deposits a layer of metal from a target onto the wafers. This layer is the upper conductor and joins the lower conductor through the holes. The wafers can now be removed from the chamber for further processing.

This work was done by Donald E. Routh and Gian Sharma of **Marshall Space Flight Center.**

This invention has been patented by NASA (U.S. Patent No. 4,437,961). Inquiries concerning nonexclusive or exclusive license for its commercial development should be addressed to the Patent Counsel, Marshall Space Flight Center Refer to MFS-25670. /TN

George C. Marshall Space Flight Center
Technology Utilization Officer:
Ismail Akbay
Code AT01
Marshall Space Flight Center,
AL 35812
(205) 544-2223
Patent Counsel:
Leon D. Wofford, Jr.
Mail Code CC01
Marshall Space Flight Center,
AL 35812
(205) 544-0014

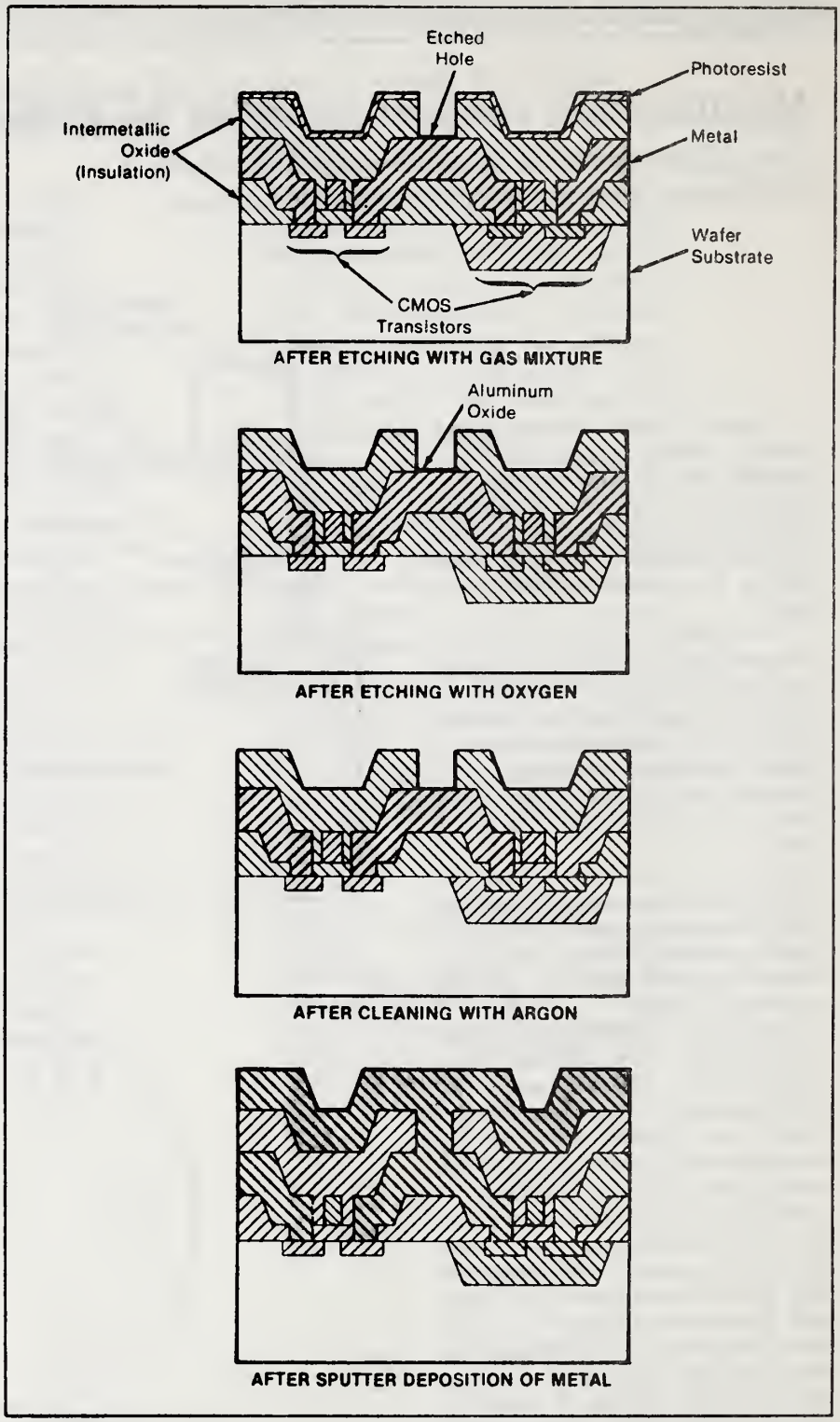

Figure 2. The **Layer Structure** of a silicon wafer changes at each processing step. The wafer structure shown here contains complementary metal-oxide/semiconductor (CMOS) transistors.

NASA Tech Brief
National Aeronautics and Space Administration
Marshall Space Flight Center, Alabama
Licensing Opportunity

Laser Vacuum Furnace for Zone Refining

A laser beam is scanned to produce a moving melt zone.

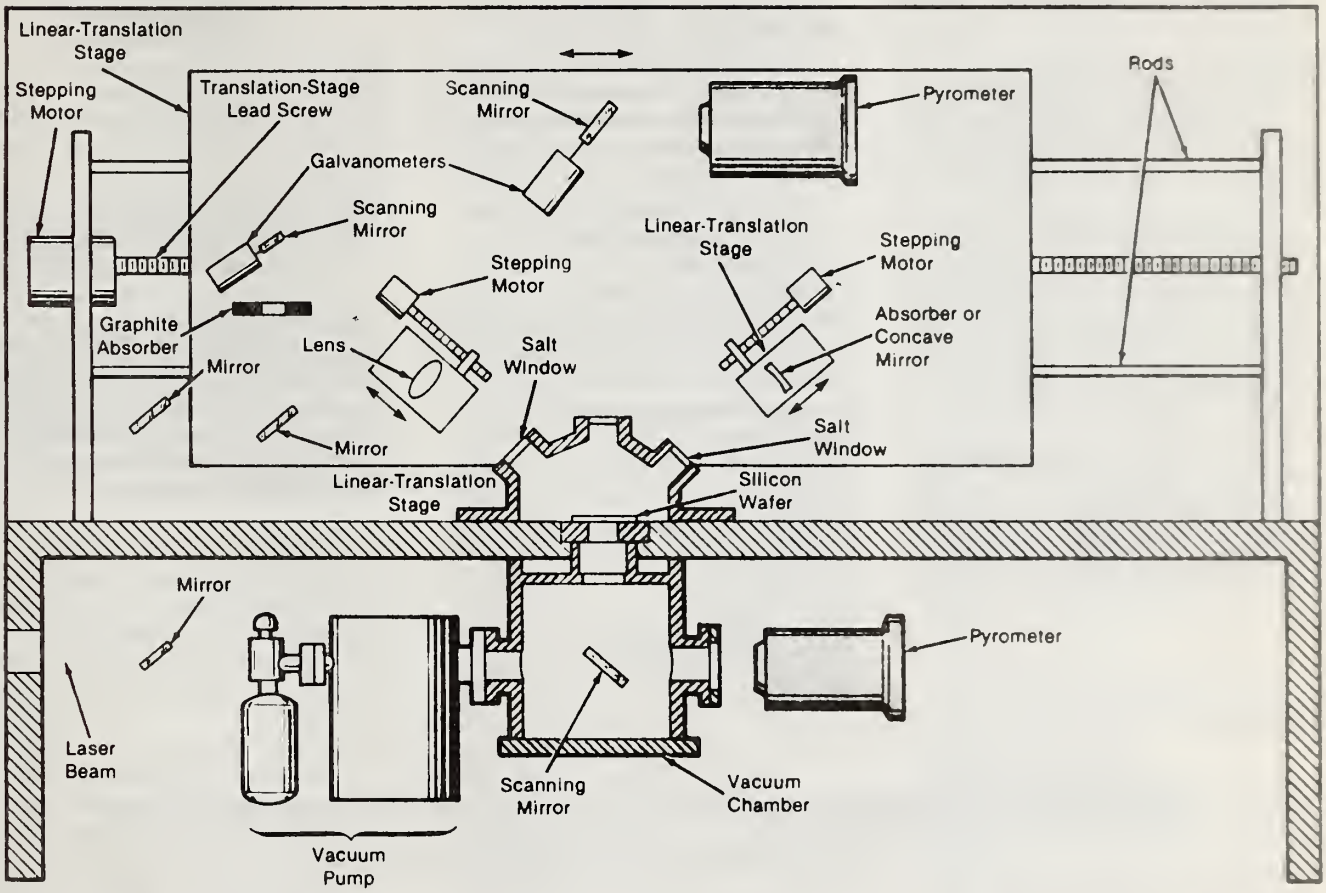

Figure 1. The **Laser Vacuum Furnace** includes a vacuum system with windows to admit the laser beam and a system of scanning optics to move the beam over the surface of the water to be heat treated.

An experimental laser vacuum furnace scans a crystalline wafer with a high-power CO_2-laser beam to generate a precise melt zone with precise control of the temperature gradients around the zone. Intended for the zone refining of silicon or other semiconductors in low gravity (where convection would be suppressed), the apparatus can also be used in normal gravity.

The wafer is mounted in a vacuum system near a set of salt windows that permit the passage of infrared and visible light (see Figure 1). A system of mirrors mounted on a large translation stage directs the laser beam toward the wafer. A graphite absorber has a hole in the middle to allow the beam to pass but stops the beam if it becomes laterally misaligned. A lens mounted on a small linear translation stage focuses the beam to a spot on the wafer. By the motion of its transaction stage, the lens is focused or defocused slightly to obtain the desired spot size. The minimum spot diameter is about 0.5 mm.

The large translation stage moves slowly to the right or the left while the laser beam is scanned rapidly back and forth across the wafer (into and out of the page) by a scanning mirror on a galvanometer. When driven by a triangular wave at any convenient frequency up to about 60 Hz, the laser spot moves in the zigzag pattern shown in Figure 2. The horizontal spacing between lines is exaggerated

here. To an observer, the illuminated region looks like a perpendicular line that coincides with the melt zone as it moves along the wafer.

A second small translation stage on the large stage holds an absorber to trap the portion of the laser beam reflected from the sample. Alternatively, the stage could hold a concave mirror to reflect this energy back onto the wafer to increase the heating efficiency. In this case, the stage is driven in synchronism with the beam-scanning galvanometer but at such a phase that the incident and back-reflected spots move in opposite directions across the wafer within the melt zone.

The temperature in the melt zone is monitored by either or both of two pyrometers that view the wafer perpendicularly to its surface. A scanning mirror moves in synchronism with the large translation stage to keep the melt zone within the view of the operating pyrometer.

A control computer (not shown) coordinates the operation of all the equipment. It monitors the laser output power, controls the laser power supply, generates the driving waveforms for the scanning galvanometers, and commands the stepping motors. The computer can be programmed to provide scanning speeds, scanning patterns, and laser powers over a wide range, thereby providing a range of melt-zone movements and temperature distributions.

This work was done by Donald B. Griner, Frederick W. Zurburg, and Wayne M. Penn of Penn-Penn Research Corp. for **Marshall Space Flight Center.**

In accordance with Public Law 96-517, the contractor has elected to retain title to this invention. Inquiries concerning rights for its commercial use should be addressed to:

Penn-Penn Research Corporation
2652 South Main Street
P.O. Box 3357
Kennesaw, GA 30144

Refer to MFS-26043, volume and number of this NASA Tech Briefs issue, and the page number. MFS-26043 /TN

George C. Marshall Space Flight Center
Technology Utilization Officer:
Ismail Akbay
Code AT01
Marshall Space Flight Center,
AL 35812
(205) 544-2223
Patent Counsel:
Leon D. Wofford, Jr.
Mail Code CC01
Marshall Space Flight Center,
AL 35812
(205) 544-0014

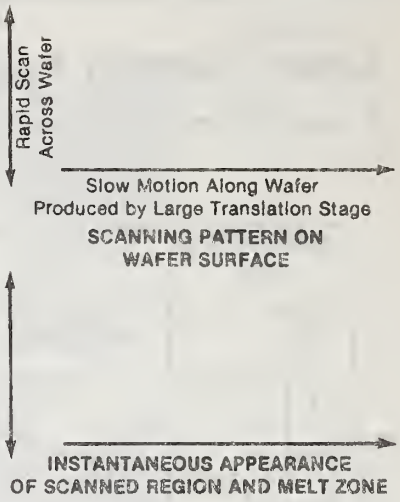
Rapid Scan Across Wafer
Slow Motion Along Wafer
Produced by Large Translation Stage
SCANNING PATTERN ON WAFER SURFACE
INSTANTANEOUS APPEARANCE OF SCANNED REGION AND MELT ZONE

Figure 2. The **Laser Beam Scans** rapidly across the wafer while the wafer moves to the right or left. Since the crosswise scan is much faster than the lengthwise scan, to a human observer the scanned zone looks like a vertical line coincident with the melt zone at any given moment.

FOR ADDITIONAL INFORMATION: *Contact: Director, Technology Transfer Division, P.O. Box 8757, BWI Airport, MD. 21240; (301) 621-0100 Ext. 241*
REFER TO THE NUMBER LISTED AT THE END OF THE ARTICLE

NASA Tech Brief

National Aeronautics and Space Administration

Licensing Opportunity

NASA's Jet Propulsion Laboratory, Pasadena, California

Producing Refractory Microballoons

Metals, ceramics, and glasses are just some of the possible raw materials.

An apparatus produces tiny spherical shells, or microballoons, from refractory metals, ceramics, and glasses. The microballoons are generated at rates of 400 per second or higher with uniform shape and size. The size is selected from a wide range of diameters, ranging from 800 μm to less than 150 μm.

As in previous processes, microballoons are formed in two stages. Liquid-shell generation and free-fall solidification. Gas is ejected from an inner orifice into molten shell material in an outer orifice, thus forming a bubble that hardens as it falls through a vertical chamber. The new process, however, has several improvements over previous processes:

- The inner orifice is now recessed (see figure) instead of being coplanar with the outer orifice; as a result, the outer orifice can be fabricated with a smaller diameter than if it had to contain the inner orifice; therefore, smaller balloons can be generated;
- The Bernoulli acceleration in the flowing molten material in the nozzle as it converges toward the orifice tends to center the gas bubble in the emerging microballoon; thus, precise concentricity of the inner and outer orifices is no longer necessary;
- The recess distance of the inner orifice reduces the possibility of blockage of the outer orifice by impurity particles entrained in the melt; a ceramic filter further reduces the chances of undissolved particles from reaching the outer orifice, and
- The nozzle and crucible are made of the same material to eliminate differences in thermal expansion; this reduces the incidence of gross misalignment, overstress, cracking, and leakage.

In many cases, the crucible and nozzles could be made of machinable graphite, which is compatible with a variety of molten substances including refractory ones. With conventional machining, the inner orifice diameter can be made as small as 50 μm, enabling the formation of microballoons less than 150 μm in diameter. Even orifices as small as 1 μm can be made with such techniques as chemical vapor deposition, laser machining, and slip casting. Materials other than graphite can be selected for special applications.

The inner nozzle is an integral part of the filling-gas tube, which supplies gas for bubbles at a constant flow rate. The flow of the melt is regulated by the pressure of a gas blanket above the melt in the crucible. The crucible and nozzle assembly is enclosed in a bell jar above a vertical drop tube.

The temperature decreases from the top to the bottom of the drop tube. This allows the normal oscillations of the liquid shell — which promote centering of the gas core in the shell — to dampen before the shell solidifies. Otherwise, the shell could contain frozen oscillation ripples on its surface. At the same time, the temperature profile is chosen to prevent solidification from occurring too late in the fall when aerodynamic forces would have distorted and decentered the microballoon.

The drop tube is 45 ft (13.7 m) long. For a melt at a typical temperature of 2,000 °C, the gas in the upper part of the chamber might be kept at or near 1,500 °C. The microballoons then enter a cryogenic zone kept at about − 195 °C for rapid quenching. Finally, the microballoons collect in a room-temperature zone at the bottom of the chamber.

The product has many applications. The microballoons can be used for example in fluidized-bed heat exchangers as containers for hazardous materials, catalysts in chemical and pharmaceutical processes, solid fuel for rockets, fuel containers for fusion power experiments, shock-wave dampers, and starting materials for high-strength, low-density sintered alloys and ceramics.

This work was done by Mark C. Lee, Christopher Schilling, George O. Lanier, Jr., and Taylor Wang of Caltech for **NASA's Jet Propulsion Laboratory.**

This invention is owned by NASA, and a patent application has been filed. Inquiries concerning nonexclusive or exclusive license for its commercial development should be addressed to the Patent Counsel, NASA Resident Office-JPL.

Refer to NPO-16489, volume and number of this NASA Tech Brief when you write.

Jet Propulsion Laboratory
Technology Utilization Manager
Norman L. Chaffin
Mail Stop 201-110
4800 Oak Grove Drive
Pasadena, CA 91109
(818) 354-2240

Key Components of equipment for the new microballoon fabrication process are the nozzle, crucible assembly, and drop tube. The recessed, conical inner orifice aids in producing uniform, symmetrical microballoons. The all-graphite crucible assembly is resistant to misalinement and cracks. The drop tube ensures timely solidification of the microballoons.

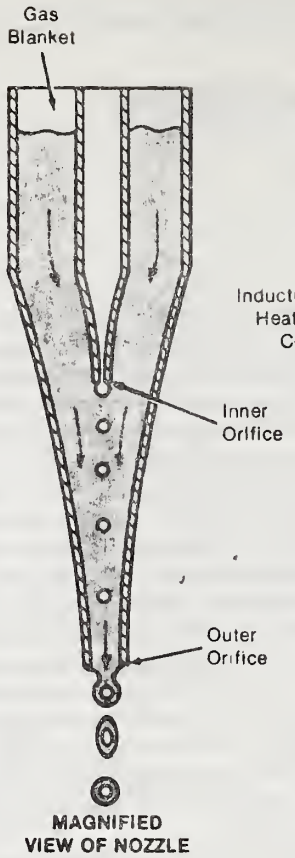

MAGNIFIED VIEW OF NOZZLE

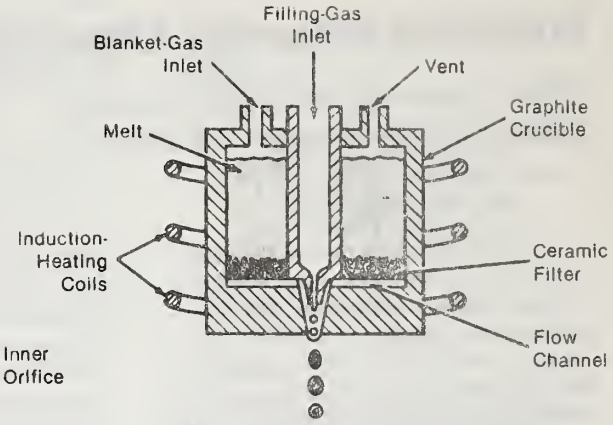

MICROBALLOON GENERATOR

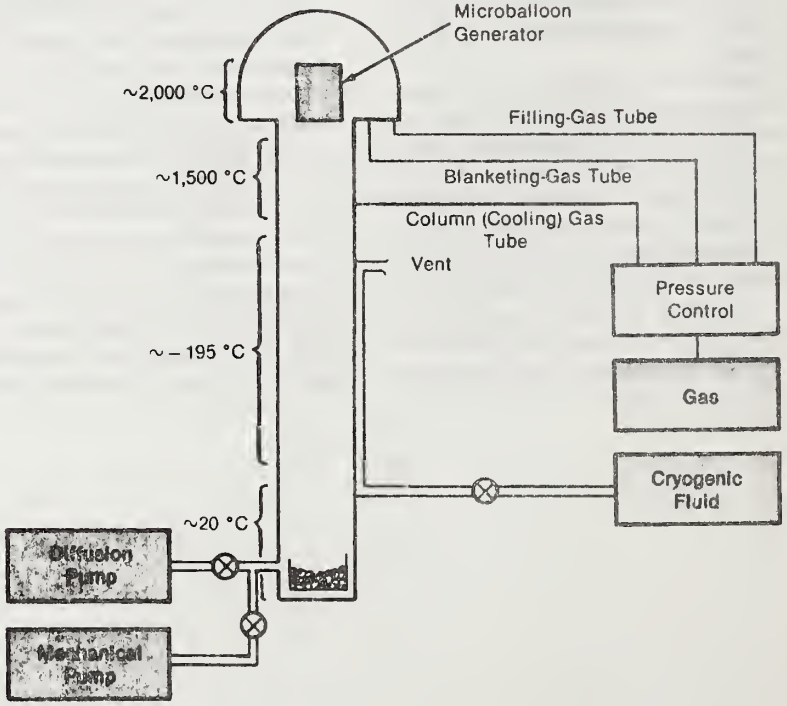

FOR ADDITIONAL INFORMATION: *Contact: Director, Technology Transfer Division, P.O. Box 8757, BWI Airport, MD. 21240; (301) 621-0100 Ext. 241*

REFER TO THE NUMBER LISTED AT THE END OF THE ARTICLE

NASA Tech Brief
National Aeronautics and Space Administration
Marshall Space Flight Center, Alabama

Licensing Opportunity

Redundant Pyrotechnic/Manual Release Mechanism

When all else fails, manual intervention is possible.

A release mechanism is designed to be operable by remote control even if many of its components fail. In the unlikely event that it does become inoperable, it can still be actuated manually.

The mechanism was developed for releasing the Space Station and its tether line from the Space Shuttle in orbit. There are two such mechanisms, each having two releasable links: one on the Space Station side and one on the Space Shuttle side (see figure). The actuation of either link on either mechanism will separate the two systems. Such a mechanism may be useful on Earth for the emergency release of modular structures or vehicle sections.

First, a pair of dual-initiator pyrotechnic pin pullers on the station side is fired by an electric signal from the station so that the open-faced link disengages from its cam roller. If one of the initiators or pullers in a pair should fail, the link will still disengage. If both sets of initiators and both pin pullers fail, the pair of pin pullers on the vehicle side would be fired by a signal from the vehicle. Again, if one of the initiators or pin pullers should fail, the link would still open.

Since there are eight pyrotechnic initiators altogether, the probability that no release will occur is very small indeed. But if it should, or if a power failure should prevent firing signals from being

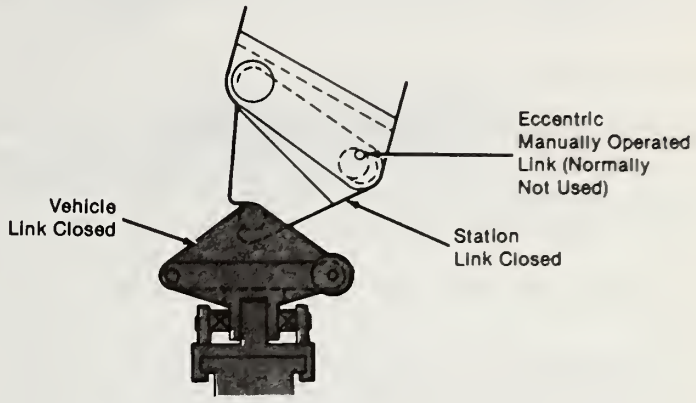

MECHANISM LOCKED

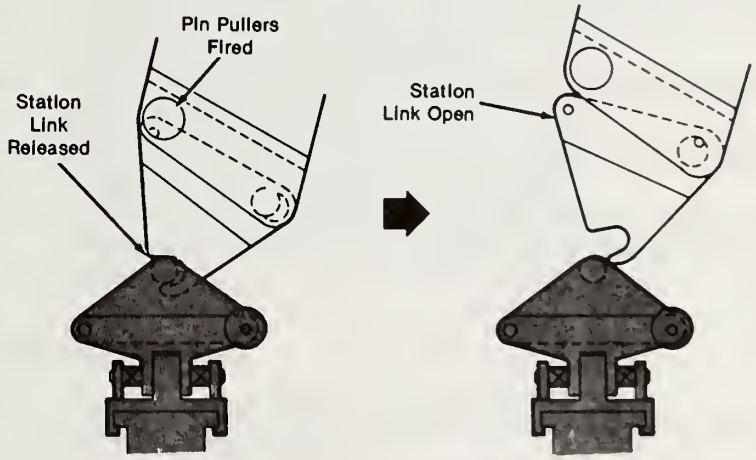

RELEASE BY FIRING OF PIN PULLERS ON STATION LINK

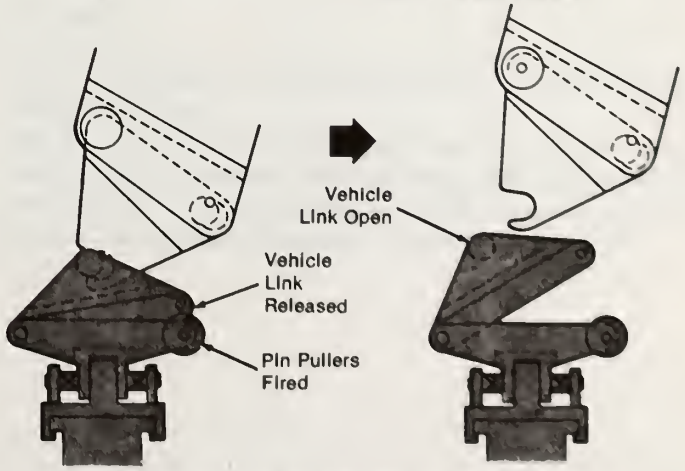

RELEASE BY FIRING OF PIN PULLERS ON VEHICLE LINK

Two Modes of Separation—on the station side of the mechanism (top) and on the vehicle side (bottom) ensure highly fail-safe operation. If only one of the eight pyrotechnic initiators in the pin pullers fires, the links of the mechanism will separate.

sent, a crew member, working outside would turn the cam roller on the station link by 180° and thereby open the link.

This work was done by Gilbert M. Kyrias of Martin Marietta Corp. for **Marshall Space Flight Center.**

MFS-28096 /TN

George C. Marshall Space Flight Center
Technology Utilization Officer:
Ismail Akbay
Code AT01
Marshall Space Flight Center,
AL 35812
(205) 544-2223
Patent Counsel:
Leon D. Wofford, Jr.
Mail Code CC01
Marshall Space Flight Center,
AL 35812
(205) 544-0014

FOR ADDITIONAL INFORMATION: *Contact: Director, Technology Transfer Division, P.O. Box 8757, BWI Airport, MD. 21240; (301) 621-0100 Ext. 241*
REFER TO THE NUMBER LISTED AT THE END OF THE ARTICLE

Materials

576 Compatibility of Greases With Seal Elastomers— Minimum swelling or shrinkage is not the sole criteria for choosing materials.

577 Yielding and Deformation of PWA 1480 Superalloy— Three distinct temperature regimes are found.

578 Steels for High-Temperature Gears— Potential replacements for a standard steel are evaluated.

580 Carburized Steels for High-Temperature Service— A 2.3-percent-nickel low-carbon steel is found to be both hard and tough; aircraft gears and bearings are likely applications.

581 Variability in Metal-Matrix Composites— Source of variability are analyzed, and metal matrices are compared with polymer matrices.

582 Deuterides of Rare-Earth/Transition-Metal Alloys— Neutron diffraction studies shed light on both crystal and magnetic structures.

583 Consolidation Methods for Rapidly Solidified Type 304 Stainless Steel

584 New Structural Materials Technologies— Opportunities for the Use of Advanced Ceramics and Composites

585 Behavior of Pressurized Incoloy 800H Tubes in Environments Pertaining to Coal Gasification

586 Fire-Resistant Belt Panel for Airplane Windows— The layered structure incorporates materials that generate little smoke. (Licensing Opportunity)

587 Two-Step Vapor/Liquid/Solid Purification— One process approaches the theoretical limit of multiple zone refining and distillation. (Licensing Opportunity)

588 Fire-Resistant Aircraft Ceilings— New materials retard flames but keep panel strong and light. (Licensing Opportunity)

589 Strong Adhesive Tape for Cold Environments— This strong tape remains sticky over a wide temperature range.

590 Fuel Manifold Resists Embrittlement by Hydrogen— A completely-cast hydrogen-compatible alloy is preferable to protective plating.

591 Neutron-Scattering Measurements of Tungsten Alloy— Neutron diffraction yields information about microstructure that x-ray diffraction cannot. (Licensing Opportunity)

Testing & Instrumentation

579 Thermal Analysis of Epoxy Mixtures— Differential scanning analysis is used to study the curing of resins.

Other items of interest

537 Effects of Radiation on Capacitor Dielectrics— Data have been gathered on key design parameters.

569 Manufacturing Fiber-Optic Bundles With Low-Loss Glass— It is feasible to make long bundles for highly sensitive imagescopes and similar optical instruments.

574 Producing Refractory Microballoons— Metals, ceramics, and glasses are just some of the possible raw materials. (Licensing Opportunity)

MANUFACTURING TECHNOLOGY NOTE

U.S. ARMY MATERIEL COMMAND

Deputy Chief of Staff for Manufacturing Technology, Alexandria, VA

Project Number: NONE

Filing Code 60H015

Compatibility of Greases With Seal Elastomers

Minimum swelling or shrinkage is not the sole criteria for choosing materials.

A study has determined swelling or shrinkage and changes in physical properties of several commercial seal elastomers. The elastomers had previously been exposed to multipurpose greases. The preliminary results of the study, which was done by the U.S. Army Belvoir Research, Development, and Engineering Center, indicate that compatibility between seal and grease cannot be assumed merely on the basis of favorable minimum swelling or shrinkage.

Eleven seal materials encompassing four types of elastomers (nitrile, silicone, acrylic, and fluorinated polymers) were evaluated. They were exposed to three greases, selected to represent different fluid and thickener types: (1) a low-viscosity naphthenic mineral oil and a calcium thickener, (2) a combination of PAO-SHC fluid and mineral oils with a lithium 12 hydroxystearate thickener, and (3) a PAO-SHC fluid thickened with polyurea.

The data generated in the study clearly emphasize the complexity of compatibility between elastomers and wheel-bearing greases. Static immersion testing can be used to screen out obvious poor seal compounds. However, selection of optimum seal candidates involves compromise; i.e., what degree of modulus buildup and swelling or shrinkage can be tolerated without sacrificing service life.

Limits based on the high performance of Viton fluoroelastomer compound WB-10 (see table) would preclude acceptance of seals fabricated from nitrile, acrylic, or silicone rubber. Ideally, acceptance criteria should be supplemented by dynamic performance tests and limits. Additional physical data such as tensile, elongation, and modulus properties are suggested. The data would be gathered before and after exposure to grease and compression.

TENSILE RETENTION, %	TENSILE RETENTION, %	ELONGATION RETENTION, %	MODULUS RETENTION, %	MODULUS RETENTION, %	VOLUME CHANGE, %
87.0	83.9	88.9	100.0	96.7	3.6
99.1	89.0	91.8	107.8	96.4	10.3
55.1	48.0	74.9	79.6	69.3	21.1
96.4	97.6	107.3	98.7	97.8	6.2
103.7	93.4	81.8	135.7	122.2	17.8
94.2	90.6	96.5	133.0	127.5	6.1
112.3	108.7	109.3	104.3	101.3	4.9
90.6	90.8	78.9	110.5	110.7	10.3
90.1	87.3	84.4	104.2	101.2	4.8
93.9	93.5	100.7	98.9	98.5	0.6
91.4	89.4	91.2	107.3	105.1	3.4

Eleven Different Elastomers were exposed to three different greases. Data for one of the greases a low-viscosity naphthenic mineral oil with a calcium thickener are presented here. Tensile and modulus retentions are given both as a percentage of the initial value and as a percentage based on the swollen cross-sectional area (indicated by an asterisk).

Project officer Paul E. Gatza
(703) 664-5488 or AV 354-5488

FOR ADDITIONAL INFORMATION

You can learn more details about this technology by ordering the following publication:
Compatibility of Wheel Bearing Seal Elastomers
with MIL-G-10924 Greases
Order number AD A[illegible]
Price code A02
Order from
National Technical Information Service
5285 Port Royal Road
Springfield, VA 22161

This document was prepared under the sponsorship of the U.S. Government. Neither the United States Government nor any person acting on behalf of the United States Government assumes any liability resulting from the use of the information contained in this document, or warrants that such use will be free from privately owned rights.

MANUFACTURING TECHNOLOGY NOTE

U.S. ARMY MATERIEL COMMAND

Deputy Chief of Staff for Manufacturing Technology, Alexandria, VA

Project Number: NONE

Filing Code: 71J043

Yielding and Deformation of PWA 1480 Superalloy

Three distinct temperature regimes are found.

Interrupted tensile tests have been conducted to fixed strain levels on <001> oriented single crystals of the nickel-base superalloy PWA 1480. Testing was done in the temperature range from 20 to 1,093 °C at strain rates of 0.5 and 50 percent per minute.

No currently available precipitation hardening model could adequately describe the behavior observed in the low-temperature regime because the penetration into the precipitate was not rate-limiting at all temperatures. In the high-temperature regime, the functional form of the Brown-Ham bypass model fit the data fairly well. The study, which was done for the U.S. Army Aviation Research and Development Activity (AVSCOM), demonstrated that the initial deformation mechanism was frequently different from that which would be inferred from examination of failed specimens.

The yield strength was constant from 20 to 760 °C, above which the strength dropped rapidly and became a strong function of strain rate. The high-temperature data could be represented well by an Arrhenius-type equation, leading to three distinct temperature regimes (see figure). At high temperatures, the true activation energy for yielding was calculated to be 500 kJ/mol. At low temperatures, the activation energy was zero. Intermediate temperatures exhibited transitional behavior. The deformation substructures could also be grouped in the same three regimes, indicating a fundamental relationship between the deformation mechanisms and the activation energies.

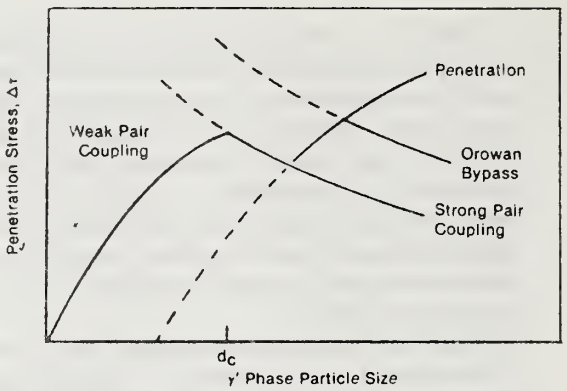

The **Relationship Between Penetration Stress and Particle Size** of the γ′ phase is divided into three regimes. At small particles sizes, the Brown-Ham model is valid. Above a critical particle size d_c, strong pair coupling becomes dominant. At very large particle sizes, Orowan bypass becomes competitive with shearing.

FOR ADDITIONAL INFORMATION

You can learn more details about this technology by ordering the NTIS report(s).

Yielding and Deformation Behavior of the Single Crystal Nickel Base Superalloy PWA 1480
Order number AD-A171035/NAA
Price code A05
Order from
National Technical Information Service
5285 Port Royal Road
Springfield, VA 22161

This document was prepared under the sponsorship of the U.S. Government. Neither the United States Government nor any person acting on behalf of the United States Government assumes any liability resulting from the use of the information contained in this document, or warrants that such use will be free from privately owned rights.

MANUFACTURING TECHNOLOGY NOTE

U.S. ARMY MATERIEL COMMAND

Deputy Chief of Staff for Manufacturing Technology, Alexandria, VA

Project Number: NONE

Filing Code 71J042

Steels for High-Temperature Gears

Potential replacements for a standard steel are evaluated.

A report describes the heat-treatment responses of the most prominent candidate steels for high-temperature aircraft gears: Vasco X-2M, CARTECH X-53 (PYROWEAR 53), and CBS600. The report, which was prepared by the U.S. Army Mechanics and Materials Research Command, also discusses three additional alloys — M50NiL, CBS100M, and AMAX B — in less detail.

The report presents the effect of tempering temperature on R_C hardness value (see figure). From the data, it is estimated that Vasco X-2M, CARTECH X-53, and CBS600 can operate continuously at 315, 275, and 230 °C, respectively.

Vasco X-2M is the only high-temperature gear steel currently flying in the main drive trains of helicopters in the United States. Because of the extensive engineering data available on this alloy, its long history of manufacturing development, and the significant improvements in its properties over the years, it seems the obvious choice for critical aircraft applications. However, both CBS600 and CARTECH X-53 have higher fracture toughness.

CBS600 is a carburizing steel used in roller bearings at temperatures up to 230 °C. Except in special applications, however, it is not expected to find wide application in helicopter drive trains because its high-temperature capability is only marginal and because secondary-hardening tool steels are approaching its high fracture toughness.

Despite improvements in Vasco X-2M, CARTECH X-53 still has significantly higher fracture toughness. It appears that X-53 could become a competitor to Vasco X-2M as the next aircraft-quality high-temperature gear steel, but it is not clear whether the possible benefits are worth the added costs of the necessary engineering and manufacturing studies.

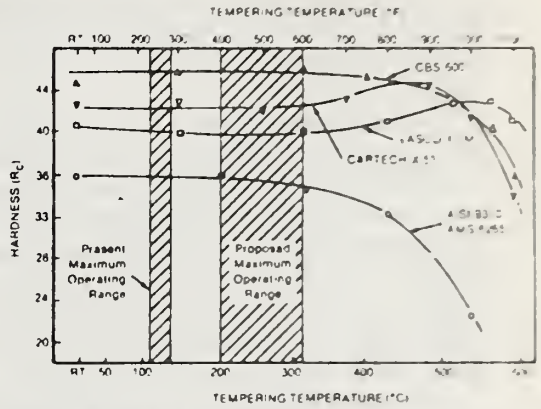

Hardness Versus Tempering Temperature curves for the prime candidate steels are contrasted with a curve for AISI 9310, a representative high-strength alloy steel. Also shown are the maximum operating temperature ranges for present and future helicopter transmissions.

FOR ADDITIONAL INFORMATION

You can learn more details about this technology by ordering the NTIS report
Directions of R&D and Current Status of Understanding of Advanced Gear Steels
Order number AD-P005061/0/XAA
Price code A02
Order from
National Technical Information Service
5285 Port Royal Road
Springfield, VA 22161

This document was prepared under the sponsorship of the U.S. Government. Neither the United States Government nor any person acting on behalf of the United States Government assumes any liability resulting from the use of the information contained in this document, or warrants that such use will be free from privately owned rights.

MANUFACTURING TECHNOLOGY NOTE

U.S. ARMY MATERIEL COMMAND

Deputy Chief of Staff for Manufacturing Technology, Alexandria, VA

Project Number: 1L1612105AH84 Filing Code: 60H014

Thermal Analysis of Epoxy Mixtures

Differential scanning analysis is used to study the curing of resins.

The curing behavior of epoxy resins has been studied by differential scanning calorimetry. The study was done by the U.S. Army Materials Technology Laboratory.

The differential scanning analysis was carried out in open aluminum pans with a thermal analyzer. The role of dicyandiamide (dicy) as a high-temperature hardening agent was explored. The cure of epoxy resins by dicy is dramatically accelerated by a class of trisubstituted urea derivatives such as Monuron (or equivalent). The accelerator (urea) undergoes a cyclocondensation reaction with the epoxy ring to form a 2-oxyzolidone derivative.

A computer program calculated the constants for various epoxy blends. The program considered the cure temperature used in practice and, at that temperature, determined dynamic reaction rates. The rates reflect the rapidity with which a sample approaches maximum heat flow. The dynamic reaction rates and the infrared analysis of the isothermally cured epoxy blends were mutually consistent.

For a mixture of 95.9 percent epoxides and 4.1 percent urea by weight, an analysis with a heating rate of 0.5 °C/min produced a heat of reaction of 73.5 cal/g. A higher heating rate (2 °C/min) decreased the caloric value to 20.6 cal/g (see figure). An epoxy/dicy/Monuron system cured at 130 °C yielded a heat of reaction of 100.9 cal/g. The dynamic reaction of the same system measured at 2 °C/min gave a caloric value of 102.4 cal/g. The caloric agreement between the two heating modes makes it possible to calculate the isothermal yields of samples that do not realize total cure.

Project officer Robert E. Sacher
(617) 923-3147 or AV 955-3147.

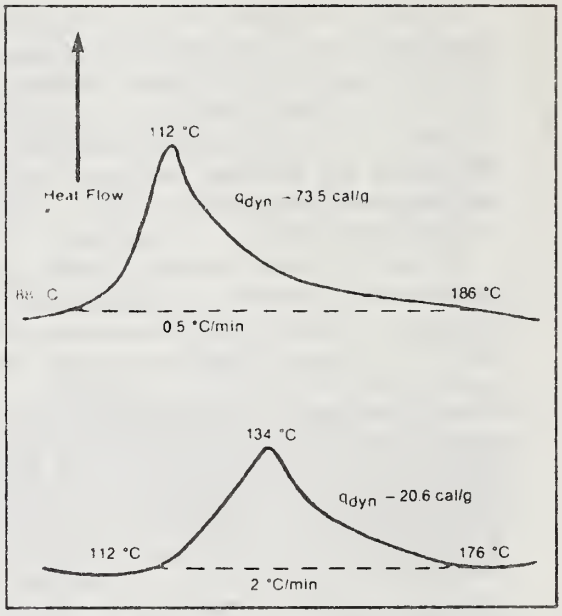

Different **Heating Rates** yield different heats of reaction (q_{dyn}). A low heating rate (top) produces a stronger exothermic reaction than a high heating rate (bottom).

FOR ADDITIONAL INFORMATION:

You can learn more details about this technology by ordering the NTIS report(s):
Thermal Analysis of Various Epoxy Mixtures
Order number AD-A167609/NAA
Price code A02

Order from
National Technical Information Service
5285 Port Royal Road
Springfield VA 22161

This document was prepared under the sponsorship of the U.S. Government. Neither the United States Government nor any person acting on behalf of the United States Government assumes any liability resulting from the use of the information contained in this document, or warrants that such use will be free from privately owned rights.

MANUFACTURING TECHNOLOGY NOTE

U.S. ARMY MATERIEL COMMAND

Deputy Chief of Staff for Manufacturing Technology, Alexandria, VA

Project Number: NONE

Filing Code 710341

Carburized Steels for High-Temperature Service

A 2.3-percent-nickel low-carbon steel is found to be both hard and tough; aircraft gears and bearings are likely applications.

Five steels similar to CBS1000 and low-carbon M50 compositions were evaluated for carburizing characteristics, temper resistance, hot hardness, and carburized fracture toughness. In the evaluation for the U.S. Army Materials and Mechanics Research Center, silicon, molybdenum, and nickel levels were varied in an effort to identify a composition that would maintain a surface hardness of 58 HRC minimum at 315 °C without deterioration of fracture-toughness properties.

Such steels are likely to find application in airborne equipment, where a prime concern is to avoid a brittle fracture in gearing or bearings; such a fracture could lead to catastrophic engine or propulsion-system failure. Projected requirements for advanced aircraft and helicopters suggest that currently used through-hardened materials will no longer be adequate for these applications because of their low fracture toughness. Hence there is an interest in carburized materiels, which have somewhat similar surface characteristics to the through-hardened materials but have inherently higher core toughness because of the lower core-carbon levels.

Silicon and nickel were both found to retard carburization but to have little influence on hardness retention or fracture toughness. A composition with 2.3 percent nickel was found to have optimum carburizing, hardness, and fracture-toughness properties.

This modified steel, called steel D, showed an improvement over CBS1000 in case fracture toughness, but the core fracture toughness was lower than that of CBS1000. The modified steel was tested in rolling-contact fatigue and found to be similar in performance to through-hardened M50 (see figure).

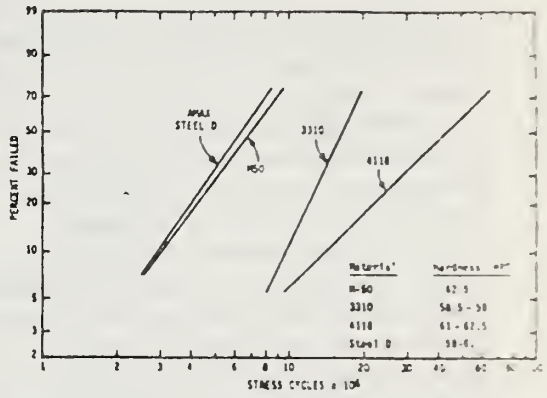

Rolling-Contact-Fatigue-Tests of steel D produce results similar to those for M50 steel. The fatigue resistance is somewhat less, however, than that of SAE 3310 and 4118 steels.

FOR ADDITIONAL INFORMATION

You can learn more details about this technology by ordering the NTIS report:
Carburizing Steel for High Temperature Service
Order number AD A168327/NAA
Price code A03

Order from
National Technical Information Service
5285 Port Royal Road
Springfield, VA 22161

This document was prepared under the sponsorship of the U.S. Government. Neither the United States Government nor any person acting on behalf of the United States Government assumes any liability resulting from the use of the information contained in this document, or warrants that such use will be free from privately owned rights.

MANUFACTURING TECHNOLOGY NOTE

U.S. ARMY MATERIEL COMMAND

Deputy Chief of Staff for Manufacturing Technology, Alexandria, VA

Project Number: 8H363304D215 Filing Code: 71F105

Variability in Metal-Matrix Composites

Source of variability are analyzed, and metal matrices are compared with polymer matrices.

A study has examined two sources of variability in fiber-reinforced metal-matrix composites: the metal-matrix structure and metal-matrix coating process. The study by the U.S. Army Materials Technology Laboratory defined the roles of the two sources, identified and modeled the dominant parameters, and measured the behavior of a graphite-fiber, aluminum-matrix composite.

The statistical strength of several graphite spools was measured by testing single-filament specimens at the beginning and end of the spools; the statistical parameters associated with the strength variability among the spools and within a spool were thereby characterized. Graphite/aluminum wire produced by a continuous liquid-infiltration process was tested in tension. The metal-matrix statistical strengths from different spools were compared with the statistical strengths of the parent fibers.

The results of the study suggest that, given proper interpretation, single-filament fiber strength is a sensitive parameter for quality assurance of metal-matrix composites. In addition, the study compared the dominating parameters for a typical polymer matrix with those for an aluminum matrix (see table). The study concludes that, given the same fiber material, aluminum should be more effective than polymer as a matrix binder material for high-performance composites.

Matrix Material	Matrix Strength / Fiber Strength	Matrix Shear Modulus / Fiber Ext. Modulus	Matrix Strain / Fiber Strain
Polymer	1/100	1/1000	2
Aluminum	1/50	1/5	4

Key Parameters for Matrices were compared for polymer and aluminum. The matrix effectiveness is porfional to the ratio of matrix strength to fiber strength, to the ratio of the shear modulus to the fiber modulus, and to the ratio of the matrix ultimate strain to the fiber ultimate strain. The greater the numerical value of each of these ratios, the stronger the composite will be.

FOR ADDITIONAL INFORMATION:

You can learn more details about this technology by ordering the NTIS report(s)
Statistical Strength Comparison of Metal Matrix and Polymeric Matrix Composites
Order number AD-A168847/NAA
Price code A03

Order from
National Technical Information Service
5285 Port Royal Road
Springfield, VA 22161

This document was prepared under the sponsorship of the U.S. Government. Neither the United States Government nor any person acting on behalf of the United States Government assumes any liability resulting from the use of the information contained in this document, or warrants that such use will be free from privately owned rights.

MANUFACTURING TECHNOLOGY NOTE

U.S. ARMY MATERIEL COMMAND

Deputy Chief of Staff for Manufacturing Technology, Alexandria, VA

Project Number: NONE

Filing Code: 71N016

Deuterides of Rare-Earth/Transition-Metal Alloys

Neutron diffraction studies shed light on both crystal and magnetic structures.

Neutron diffraction experiments were performed on rare-earth/transition-metal alloys and alloy deuterides. The object of the study for the U.S. Army Research Office was to determine the crystal and magnetic structures of the materials.

At 77 K, Ho_6Mn_{23} was found to have a face-centered-cubic crystal structure and a noncollinear magnetic structure (see figure), with the Ho moments tilted at an angle of 33.4° to the Mn moments. Unusually low Ho moments were measured in the alloy and its deuteride, $Ho_6Mn_{23}D_{22}$.

Three $Y_6(Fe_{1-x}Al_x)_{23}$ compounds ($x = 0.05$, 0.10, 0.15) at 523 and 77 K revealed substantial preferential atomic ordering of Fe and Al atoms on the four transition crystallographic sites. The Fe atoms exhibited different magnetic moments on the four sites.

The ternary alloys $Y_6(Fe_xMn_{1-x})_{23}$ exhibited interesting magnetic behavior over a range of solid solutions of iron and manganese. As x increases, the ordering temperature increases dramatically.

The effect on magnetic properties of substitution of Fe by Al in $R_2(Fe_{1-x}Al_x)_{14}B$ compounds, where R = Y or other rare earths, was investigated. The experimental data indicate that intermetallic compounds based on $Nd_2(Fe_{1-x-y}Al_xCo_y)_{14}B$ have both high Curie temperatures and high coercive fields. It therefore appears possible to improve the thermal properties and reduce the total losses of Nd/Fe/B magnets by substitution of Fe with Al and Co atoms.

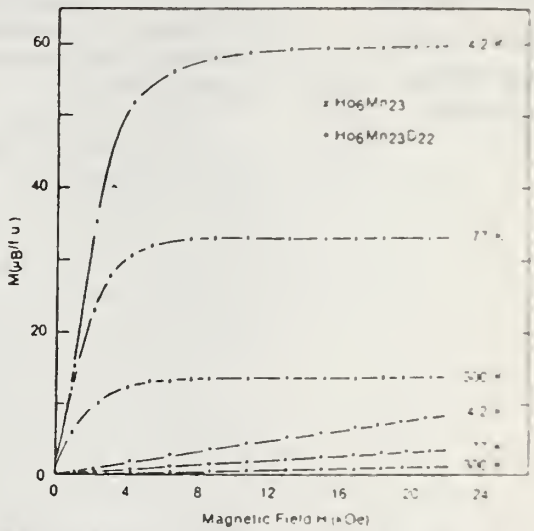

Magnetization Curves are plotted for the alloy Ho_6Mn_{23} and its deuteride. The magnetization decreases with increasing temperature, possibly indicating an increasing magnetic disorder in the rare-earth sublattice; such disorder would lead to a lower average magnetic moment per atom.

FOR ADDITIONAL INFORMATION

You can learn more details about this technology by ordering the NTIS report:

Neutron Diffraction Studies of Some Rare Earth Transition Metal Deuterides
Order number AD-A168995/9/AA
Price code A05

Order from
National Technical Information Service
5285 Port Royal Road
Springfield VA 22161

This document was prepared under the sponsorship of the U.S. Government. Neither the United States Government nor any person acting on behalf of the United States Government assumes any liability resulting from the use of the information contained in this document, or warrants that such use will be free from privately owned rights.

energygram®

Consolidation Methods for Rapidly Solidified Type 304 Stainless Steel

DOE/TIC/EG-86/143
OFFICE OF SCIENTIFIC AND TECHNICAL INFORMATION

This technical note was based on research conducted by Idaho National Engineering Laboratory for the U.S. Department of Energy.

INEL
Idaho National Engineering Laboratory

A report has been prepared which provides product microstructure evaluation data for compaction (by three different methods) of centrifugally atomized and vacuum gas atomized rapidly solidified metal powders.

Rapidly solidified Type 304 stainless steel powders can be consolidated to full density by explosive compaction, hot isostatic pressing, hot pressing, and hot extrusion. The report cited herein discusses the merits of the various consolidation processes in terms of producing fully dense, metallurgically bonded, monolithic forms suitable for engineering applications.

Several conclusions are cited:

- Powders processed by centrifugally atomized (CA) and vacuum gas atomized (VGA) methods were generally spherical.
- The VGA powder tends to have a finer particle size, and many of the particles have small satellites.
- The smoother CA powder has a higher pour density, although both powders can be settled to greater than 65% of the theoretical density. The larger, more spherical CA powder appears to be more suited to explosive consolidation.
- The finer average particle size of the VGA powder may be an advantage for hot isostatic pressing.
- The VGA powder has a somewhat thicker oxide layer, which is apparent in the microstructure after consolidation by hot isostatic pressing where there is little mechanical dispersion.
- In general, there is no evidence of an influence of the oxide layer on the consolidation of the CA powder.
- Evidence of the original microstructure from the powder can still be seen after hot pressing, hot isostatic pressing, and shock consolidation.
- Hot extrusion results in a dynamically recrystallized microstructure.
- Only explosive consolidation results in retention of metastable ferrite in the powders.

The work cited here summarizes the ongoing investigations, and the information is of use for developing industrial processes to handle the materials.

FOR ADDITIONAL INFORMATION

Reference(s):
R. N. Wright, J. E. Flinn, and G. E. Korth, Consolidation Methods for Rapidly Solidified Type 304 Stainless Steel, *Metal Powder Report EGG-J-00886, April 1986.*

For additional information, contact:
Jane M. Welch
EG&G Idaho, Inc.
P.O. Box 1625
Idaho Falls, ID 83415
Telephone No.: (208) 526-8318

New Structural Materials Technologies

Opportunities for the Use of Advanced Ceramics and Composites

The past 25 years have witnessed remarkable developments in structural materials technologies; new nonmetallic materials, such as ceramics and polymer matrix composites, are replacing metals in a wide variety of applications, ranging from cutting tools to tennis rackets. The new materials represent both an opportunity and a challenge for U.S. manufacturing industries. In an era of concern about the long-term economic viability of the manufacturing sector, they open a promising avenue to renewed international competitiveness, new industries, and employment opportunities.

By the year 2000, large markets for ceramic and composite products will be found in military, aerospace, automotive, medical, and construction applications. However, these opportunities cannot be taken for granted. The United States does not enjoy a comfortable lead (indeed it often lags) in new structural materials technologies; key advances continue to come from abroad. Moreover, through well-coordinated government-industry efforts, several countries have succeeded in bringing ceramic and composite products to the market years in advance of comparable U.S. products. Japan in particular has initiated aggressive programs to commercialize its evolving materials technologies. In order to realize the promise represented by the new materials, a consensus is developing in the materials community that U.S. policymakers in government, universities, and industries will have to come together to define feasible goals and materials applications, coordinate research and development efforts toward these goals, and, especially, focus on reducing the barriers to commercial introduction of advanced ceramic and composite products.

A technical memorandum assesses the opportunities for the use of structural ceramics and polymer matrix composites in the next 25 years, outlines the research and development priorities implied by those opportunities, and concludes with a discussion of some key prerequisites for

The Family of Structural Materials

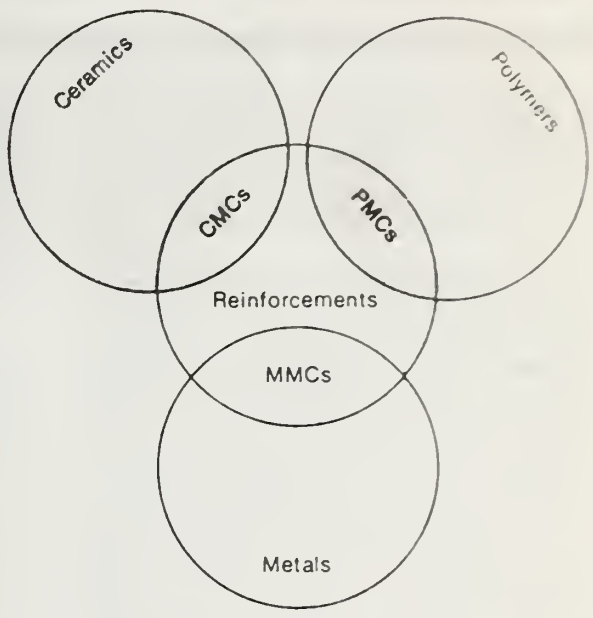

The family of structural materials includes ceramics, polymers, and metals. Reinforcements added to these materials produce ceramic matrix composites (CMCs), polymer matrix composites (PMCs), and metal matrix composites (MMCs). Materials in the shaded regions are discussed in this report.

Some Future Applications of Structural Ceramics

Application	Performance advantages	Examples
Wear parts seals bearings valves nozzles	High hardness, low friction	Silicon carbide alumina
Cutting tools	High strength, hot hardness	Silicon nitride
Heat engines diesel components gas turbines	Thermal insulation, high temperature strength, fuel economy	Zirconia, silicon carbide, silicon nitride
Medical implants hips teeth joints	Biocompatibility, surface bond to tissue, corrosion resistance	Hydroxylapatite, bioglass alumina zirconia
Construction highways bridges buildings	Improved durability, lower overall cost	Advanced cements and concretes

SOURCE: Office of Technology Assessment

their realization. A parallel treatment of metal matrix composites, as well as a discussion of public policy options for accelerating the development and commercialization of advanced structural materials, is deferred until the final report.[1]

[1]Projected publication date September 1987.

For Additional Information:

The report presenting the overview of these new opportunities is available from the National Technical Information Service (NTIS), Springfield, VA 22161: (703) 487-4650. Refer to order number, PB87-118253/NAC, price code A05.

energygram

Behavior of Pressurized Incoloy 800H Tubes in Environments Pertaining to Coal Gasification

DOE/TIC/EG-86/112
OFFICE OF SCIENTIFIC AND TECHNICAL INFORMATION

This technical note was based on research conducted by Idaho National Engineering Laboratory for the U.S. Department of Energy.

INEL
Idaho National Engineering Laboratory

Interdependencies between applied stress and environmental parameters have been investigated for Incoloy 800H pressurized tubes in environments having oxygen and sulfur potentials under temperature conditions similar to those of coal gasification processes. The results have been reported and discussed.

Components in coal gasification plants are subjected to severe conditions, which include high temperatures, low oxygen activities, and significant sulfur potentials. Many of these components will contain tubular metallic products subjected to stresses from pressurization, thermal cycling, structural loading, etc. Enhanced understanding of behavior under the combined influences of stress and environment will contribute to materials selection and performance predictions.

Incoloy 800H was used to examine the combined influences of environment and stress in sulfur-bearing environments simulating those of coal gasification. Tubular specimens were pressurized during exposures at 870°C in environments with controlled oxygen and sulfur potentials. Lifetimes, ductilities, and failure modes were determined. The influence of preoxidation on lifetime was investigated. Mechanisms contributing to failure, i.e., surface cracking and the development of phases both on and within the alloy were investigated relative to sulfur potentials, time, and strain.

The investigation reports, among other conclusions, that the stresses from pressurization or induced surface cracking did not promote the development of external sulfides in environments associated with the oxide forming regime. Internal damage in the form of sulfur and oxygen penetration and precipitation along grain boundaries was promoted by stresses sufficiently high to cause deformation. These penetrations were related to incurred strain rather than stress/time history. Greater penetrations were also observed with increasing sulfur content. These substantial penetrations resulted in reduced lifetimes and ductilities at higher stress levels in sulfur-bearing gases relative to those in air and an environment with a reduced partial pressure of oxygen.

These results are valuable material property information for suppliers, design engineers, and users.

FOR ADDITIONAL INFORMATION

DOE report(s):
Behavior of Pressurized Incoloy 800H Tubes in Environments Pertaining to Coal Gasification.
Report number: EGG-MS-6852/NAB
Order number: DE85016533/NAB
Price: $11.95

Order from:
National Technical Information Service
5285 Port Royal Road
Springfield, VA 22161

For additional information, contact
J. M. Welch
EG&G Idaho, Inc.
P.O. Box 1625
Idaho Falls, ID 83415
Telephone No.: (208) 526-8318

or

J. E. Flinn
EG&G Idaho, Inc.
P.O. Box 1625
Idaho Falls, ID 83415
Telephone No.: (208) 526-8127

NASA Tech Brief
National Aeronautics and Space Administration
Lyndon B. Johnson Space Center, Houston, Texas

Licensing Opportunity

Fire-Resistant Belt Panel for Airplane Windows

The layered structure incorporates materials that generate little smoke.

A window-belt panel for airplanes is fire resistant and generates little smoke when exposed to flames. The panel incorporates a fire-shield layer that adds minimal weight but delays or prevents a fire from burning through.

The structural core of the panel (see figure) is a Nomex (or equivalent) polyamide paper honeycomb. The fire shield, made of fluororubber sheet, is incorporated in a multiple-ply facing bonded to the core. The outer layers of the multiple-ply facing and the back face of the panel consist of biwoven carbon-cloth impregnated with phenolic resin.

A conventional belt panel consists of a Nomex (or equivalent) polyamide honeycomb core with a phenolic-resin-impregnated glass-cloth facing and a back-surface ply of epoxy-resin-impregnated glass-cloth reinforcement. The impregnated carbon cloth in the new panel weighs less than the glass cloth and gives off less smoke. The fire-shield layer in the new panel causes only a slight net increase in weight, yet significantly enhances passenger protection by delaying burn-through.

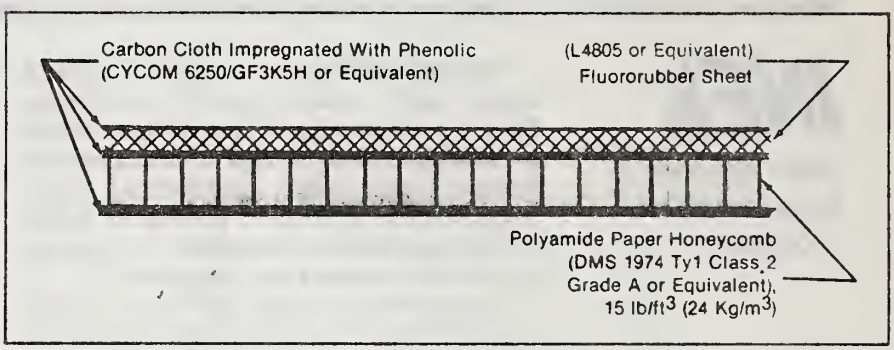

The **Multiple-Ply Structure** of the window-belt panel provides strength and fire resistance at low weight. Such standard parts as windows, shade assemblies, and air grills can be attached to the panel.

This work was done by Edward L. Trabold and Meade F. Murphy of McDonnell Douglas Corp. for **Johnson Space Center**. *No further documentation is available.*

Inquiries concerning rights for the commercial use of this invention should be addressed to the Patent Counsel, Johnson Space Center
Refer to MSC-21064 /TN

Lyndon B. Johnson Space Center
Technology Utilization Officer:
Dean C. Glenn
Mail Code AL32
Houston, TX 77058
(713) 483-3809
Patent Counsel:
Marvin F. Matthews
Mail Code AL3
Houston, TX 77058
(713) 483-4871

FOR ADDITIONAL INFORMATION: *Contact: Director, Technology Transfer Division, P.O. Box 8757, BWI Airport, MD. 21240; (301) 621-0100 Ext. 241*
REFER TO THE NUMBER LISTED AT THE END OF THE ARTICLE

NASA Tech Brief
National Aeronautics and Space Administration
Marshall Space Flight Center, Alabama

Licensing Opportunity

Two-Step Vapor/Liquid/Solid Purification

One process approaches the theoretical limit of multiple zone refining and distillation.

A vertical distillation system combines in a single operation the advantages of multiple zone refining with those of distillation. Developed specifically to load Bridgman-Stockbarger (vertical-solidification) growth ampoules with ultrapure tellurium and cadmium, this system, with suitable modifications, could serve as a material refiner.

In the new system (see figure), the raw charge is placed in an evaporator, from which it is distilled upward. The ampoule is connected to the evaporator by a dry, ground, vitreous-silica ball joint. The ampoule and evaporator are placed in a high-vacuum bell jar, which is pumped down to a pressure of 10^{-7} torr (10^{-5} N/m^2) or lower.

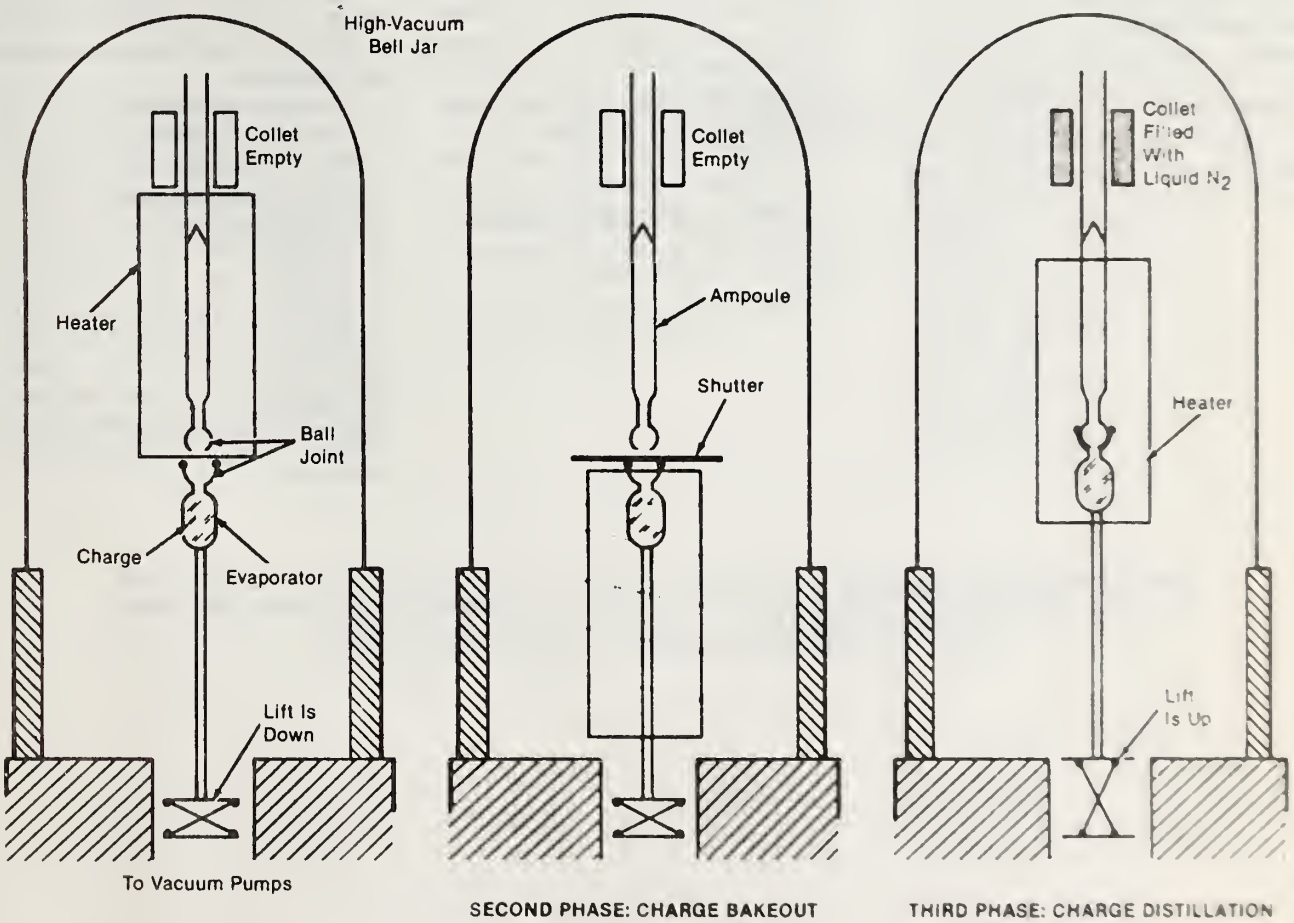

In the First Phase of the Purification Process (left), the ampoule is heated to drive off absorbed volatiles. In the second phase (middle), the evaporator is heated to drive off volatiles in the charge. In the third phase (right), the slowly descending heater causes distillation from the evaporator to the growing crystal in the ampoule.

The evaporator has a long stem supported by a lift system controlled through a ferrofluidic rotary vacuum seal. The crystal-growth ampoule is also supported by a stem — a tube of the same inside and outside diameters as those of the ampoule body, so that it is a smooth continuation of the ampoule body. The stem extracts heat from the ampoule by thermal conduction. The stem is grasped by the spring fingers of a double-walled chuck cooled by liquid nitrogen.

The evaporator and the ampoule are surrounded by a movable heater 14 in. (36 cm) long that has a double winding of platinum wire 0.020 in. (0.05 cm) in diameter, 10 turns/in. (4 turns/cm) on the bottom 2 in. (5 cm) and 5 turns/in. (2 turns/cm) on the upper 12 in. (30 cm), wound on a vitreous-silica tube 1.1 in. (2.8 cm) in inside diameter. The heater is mounted on a recirculating-ball lead screw driven by a stepping motor that gives translation rates from 1 mm/h to 18mm/s, programmed by a preset indexer.

In the first phase of the operation, the evaporator is at its lowest position (with the ball joint open), the heater is positioned to heat only the ampoule, and the cold chuck is not supplied with liquid nitrogen. In this configuration, the ampoule is prebaked to about 400 °C in the vacuum to remove any adsorbed volatiles.

In the second phase, the heater is lowered to cover only the evaporator, and a shutter is placed in the open ball joint to mask off the ampoule. The charge in the evaporator is warmed until its vapor pressure is about 10^{-3} torr (10^{-1} N/m^2), so that moisture and other volatiles are driven off.

The third phase is initiated by removing the shutter, closing the ball joint, and raising the heater so that the top of the free volume in the ampoule is just inside the top of the heater. In this configuration, the charge in the evaporator is melted and heated until the vapor pressure is several torr (several hundred N/m^2), and the distillation process is started. As the distillation proceeds, the heater is moved downward, so that the top of the ampoule cools, thereby causing a crystal of purified material to start growing.

Because the crystal grows down from the top of the ampoule into the heater until it passes the melting-point isotherm, the solid material always has a drop of melt at the bottom end that is held up by surface tension. There is a segregation of impurities as the molten raw material is distilled to this drop and a second segregation as the material in the drop is solidified. When the growing drop reaches a certain size, it falls back into the evaporator, carrying with it impurities rejected in the solidification process. In this way, the solid growth face is constantly washed by fresh molten distillate. Thus the material is effectively purified by multiple zone refining and by distillation.

This work was done by Lawrence R. Holland of the University of Alabama, Huntsville, for **Marshall Space Flight Center**.

In accordance with Public Law 96-517, the contractor has elected to retain title to this invention. Inquiries concerning rights for its commercial use should be addressed to:

University of Alabama
Huntsville, AL 35899
Refer to MFS-26004, /TN

George C. Marshall Space Flight Center
Technology Utilization Officer:
Ismail Akbay
Code AT01
Marshall Space Flight Center, AL 35812
(205) 544-2223
Patent Counsel:
Leon D. Wofford, Jr.
Mail Code CC01
Marshall Space Flight Center, AL 35812
(205) 544-0014

FOR ADDITIONAL INFORMATION: *Contact: Director, Technology Transfer Division, P.O. Box 8757, BWI Airport, MD. 21240; (301) 621-0100 Ext. 241*
REFER TO THE NUMBER LISTED AT THE END OF THE ARTICLE

NASA Tech Brief
National Aeronautics and Space Administration
Lyndon B. Johnson Space Center, Houston, Texas

Licensing Opportunity

Fire-Resistant Aircraft Ceilings

New materials retard flames but keep panel strong and light.

A ceiling panel for airplane cabins is more fire resistant than conventional panels. The new panel incorporates a core of polyimide foam as a fire shield. The core significantly delays burn-through by flames and thus offers passengers greater protection.

Biwoven carbon cloth impregnated with precured phenolic resin is glued to both faces of the polyimide core for reinforcement (see figure). In a conventional panel, the core is an aramid paper honeycomb, and the reinforcing layers are phenolic-impregnated glass cloth. Although the new core material weighs more than the old, the new reinforcing layer maintains panel stiffness and weighs less than the old reinforcing material. The net weight gain associated with the greater fire resistance is therefore minimal.

This work was done by Edward A. Trabold and Meade F. Murphy of McDonnell Douglas Corp. for **Johnson Space Center**. *No further documentation is available.*

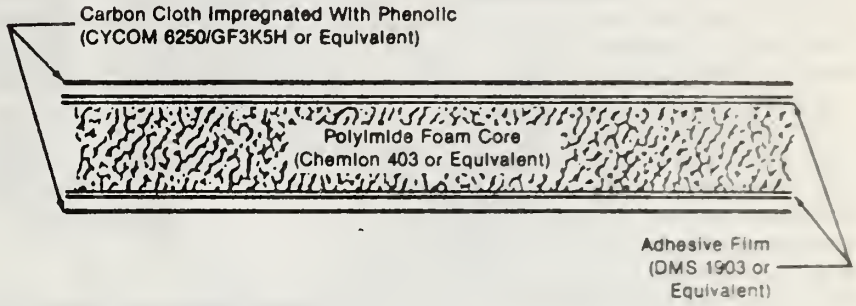

The Foam Core of the panel chars instead of burning. Decorative layers, speaker grills, and other details can be attached as on conventional panels.

Inquiries concerning rights for the commercial use of this invention should be addressed to the Patent Counsel, Johnson Space Center
Refer to MSC-21065 /TN

Lyndon B. Johnson Space Center
Technology Utilization Officer
Dean C Glenn
Mail Code AL32
Houston, TX 77058
(713) 483-3809
Patent Counsel:
Marvin F. Matthews
Mail Code AL3
Houston, TX 77058
(713) 483-4871

FOR ADDITIONAL INFORMATION: *Contact: Director, Technology Transfer Division, P.O. Box 8757, BWI Airport, MD. 21240; (301) 621-0100 Ext. 241*
REFER TO THE NUMBER LISTED AT THE END OF THE ARTICLE

NASA Tech Brief

National Aeronautics and Space Administration

Lyndon B. Johnson Space Center, Houston, Texas

Strong Adhesive Tape for Cold Environments

This strong tape remains sticky over a wide temperature range.

An improved tape devised for repairs in space may also find use on Earth in polar regions and in superconducting applications. The tape retains its adherence and strength at extreme temperatures, where conventional tapes would fail.

Experience on the Space Shuttle had shown that ordinary duct tape loses most, if not all, of its stickiness at the orbital temperatures. Kapton (or equivalent) polyimide tape, for example, maintained adequate adhesion but had to be layered for sufficient strength to resist inadvertent tearing by crewmembers. Multiple layers, however, make the tape stiffer.

The improved tape (see figure) consists of two layers of the polyimide tape with a reinforcing intermediate layer of thin, open-weave Kevlar (or equivalent) aromatic polyamid. Other mesh materials may also be suitable.

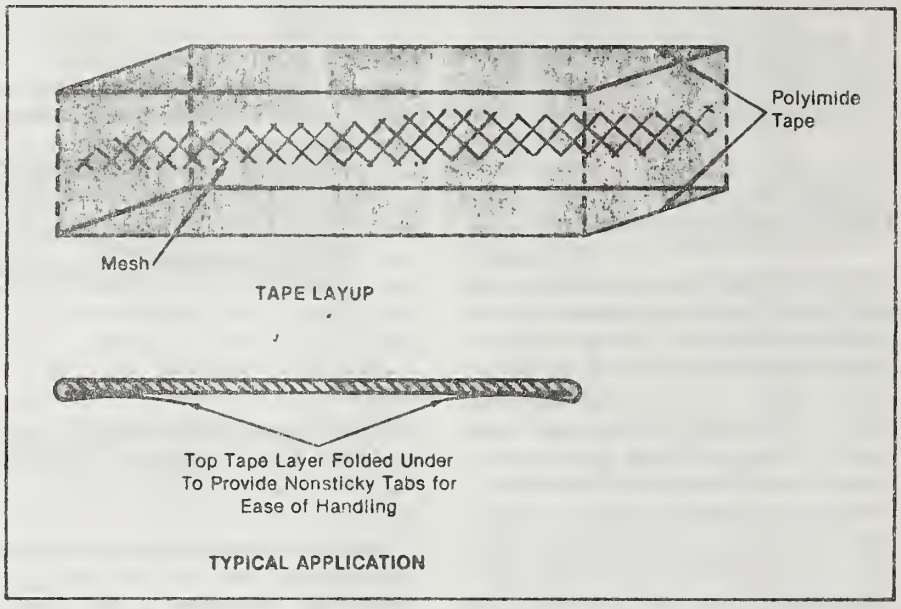
Polyimide Tape
Mesh
TAPE LAYUP
Top Tape Layer Folded Under To Provide Nonsticky Tabs for Ease of Handling
TYPICAL APPLICATION

The **Strong Tape for Low Temperatures** consists of two layers of polyimide tape with a layer of reinforcing mesh.

This work was done by Thomas G. Woods of McDonnell Douglas Corp. for **Johnson Space Center.** *No further documentation is available. MSC-20924 /TN*

FOR ADDITIONAL INFORMATION: *Contact: Director, Technology Transfer Division, P.O. Box 8757, BWI Airport, MD. 21240; (301) 621-0100 Ext. 241*

REFER TO THE NUMBER LISTED AT THE END OF THE ARTICLE

NASA Tech Brief
National Aeronautics and Space Administration
Marshall Space Flight Center, Alabama

Fuel Manifold Resists Embrittlement by Hydrogen

A completely-cast hydrogen-compatible alloy is preferable to protective plating.

Parts exposed to high-pressure hydrogen can be made immune to hydrogen embrittlement if they are fabricated from a new alloy, Incoloy 903* (or equivalent). This material is strong and compatible with hydrogen at all temperatures and has been adapted for the outlet manifold of the Space Shuttle main combustion chamber.

The manifold was formerly made of Inconel 718*, an alloy that is susceptible to hydrogen embrittlement at the engine operating temperatures. For protection, it had to be plated with copper on internal surfaces. In addition, overlays of Incoloy 903* had to be welded to it in certain areas, and a tube of the same alloy had to be brazed to it (see figure).

Substituting Incoloy 903* for the entire part eliminated the plating, welding, and brazing operations. As a result, the part can be made in less time and with fewer manufacturing flaws.

(*"Inconel" and "Incoloy" are registered trademarks of the INCO family of companies.)

This work was done by T. C. Adams of Rockwell International Corp. for **Marshall Space Flight Center.** *No further documentation is available.*
MFS-29089 /TN

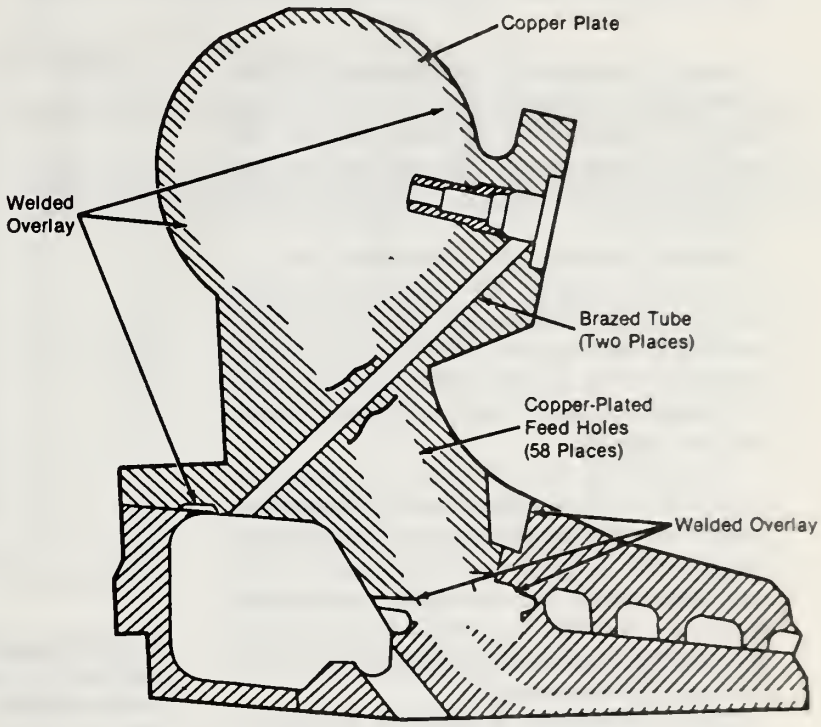

The Complexity of Plating, Welding, and Brazing becomes unnecessary if a hydrogen-compatible alloy is used for the entire casting instead of merely as a protective overlay.

FOR ADDITIONAL INFORMATION: *Contact: Director, Technology Transfer Division, P.O. Box 8757, BWI Airport, MD. 21240; (301) 621-0100 Ext. 241*
REFER TO THE NUMBER LISTED AT THE END OF THE ARTICLE

MANUFACTURING TECHNOLOGY NOTE

U.S. ARMY MATERIEL COMMAND

Deputy Chief of Staff for Manufacturing Technology, Alexandria, VA

Project Number: 1L161101A91A

Filing Code: 46C083

Neutron-Scattering Measurements of Tungsten Alloy

Neutron diffraction yields information about microstructure that x-ray diffraction cannot.

A study has used wide- and small-angle neutron scattering to investigate the variation of microscopic properties in unswaged, swaged, and strain-aged tungsten alloy. The material was composed of 90 percent tungsten, 7 percent nickel, and 3 percent iron.

Neutron scattering can reveal certain structural and material properties not readily determined by other methods. For example, it is a much more sensitive probe than x-ray diffraction of the matrix properties of the tungsten alloy because of the comparable coherent cross sections of nickel, iron, and tungsten.

The study by the U.S. Army Armament Research and Development Center showed that swaging dramatically changes the preferred orientation of both tungsten and matrix grains in the specimen, as expected. In addition, the difference in relative intensities for reflection and transmission peaks indicates that significant texture is present even before swaging.

Neutron diffraction is especially sensitive to structural changes in each phase of a sample (see figure). Crystallographically, the tungsten phase is body-centered cubic, and the matrix phase is face-centered cubic. The fact that the D-spacings are different in the reflection and transmission measurements indicates the presence of measurable residual stresses.

The tungsten phase shows no measurable strain broadening. After swaging, significant rms strains are present. After strain-aging, the magnitude of rms strain is essentially unchanged, whereas the distribution of stress changes appreciably.

Project officer C. S. Choi
(201) 724-2852 or AV 880-2852.

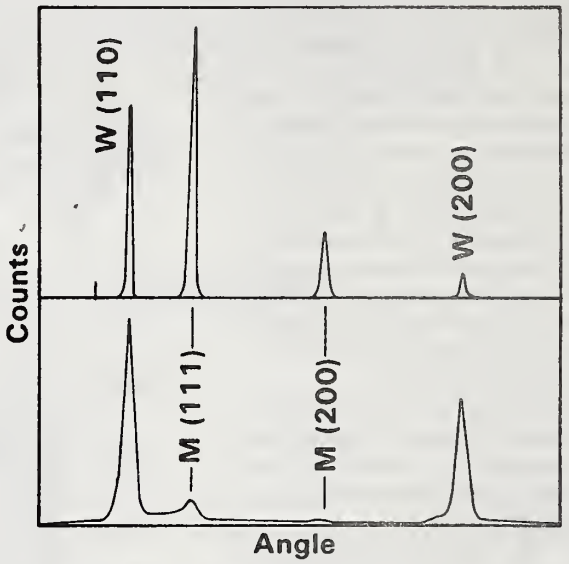

Relative Sensitivities of x-ray and neutron diffraction techniques to tungsten and matrix components of the alloy are compared. The upper curve is combined neutron data. The lower curve is the molybdenum K-alpha x-ray pattern.

FOR ADDITIONAL INFORMATION:

You can learn more details about this technology by ordering the NTIS report(s):
Neutron Diffraction Characterization of Tungsten-Nickel-Iron Alloys.
Order number: AD-A165796/NAA
Price code: A03

Order from:
National Technical Information Service
5285 Port Royal Road
Springfield, VA 22161

This document was prepared under the sponsorship of the U.S. Government. Neither the United States Government nor any person acting on behalf of the United States Government assumes any liability resulting from the use of the information contained in this document, or warrants that such use will be free from privately owned rights.

Medicine & Biology

592 Low-Molecular-Weight, Cobalt-Binding Proteins from Saccharomyces cerevisiae and Bacillus subtilis

593 Human Factors Guidelines and Methodology in the Design of a User-Computer Interface: A Case Study

594 Electron Microscopy Technique Improves Image Quality— Rapid sample freezing eliminates structural distortion.

595 Binding of Antiviral Agents to Cold Viruses

596 Information Available on Determining Radiopharmaceutical Dosages

597 Cutting Head for Ultrasonic Lithotripsy— Kidney stones are disintegrated safetly and efficiently. (Licensing Opportunity)

energygram®

Low-Molecular-Weight, Cobalt-Binding Proteins from *Saccharomyces cerevisiae* and *Bacillus subtilis*

DOE/TIC/EG-86/144
OFFICE OF SCIENTIFIC AND TECHNICAL INFORMATION

This technical note was based on research conducted by Idaho National Engineering Laboratory for the U.S. Department of Energy.

INEL
Idaho National Engineering Laboratory

Low-molecular-weight, cobalt-binding proteins have been isolated from *S. cerevisiae* and *B. subtilis*. This study represents the first isolation of any metallothionein-like proteins from *B. subtilis* and the first isolation of cobalt-binding metallothionein-like proteins from microorganisms.

Further research is needed to characterize the proteins and to measure the metal-binding capacities and specificities. In addition, if basic studies indicate possible technical and economic feasibility, extensive process engineering research will also be warranted and needed. The isolation of these proteins indicates at least the theoretical feasibility of using metal-binding biomolecules in cobalt recovery processing.

Metal-binding biomolecules may prove economical for use in industrial processing. With additional research, such biomolecules could be isolated from nature, perhaps be improved upon through genetic engineering techniques, and processes could be developed. In addition, genetic engineering and the recently developed field of protein engineering could be applied to actually change the molecules to enhance their properties.

This finding could hold potential industrial significance in metal recovery processing.

The study cited here describes preliminary research to isolate specific cobalt-binding proteins. More recent work deals with actual applications of these proteins to cobalt metal recovery and waste stream decontamination by biological agents

FOR ADDITIONAL INFORMATION

DOE report(s):
Stephen A. Leeper, James H. Wolfram, and Thomas E. Ward, Low-Molecular-Weight, Cobalt-Binding Proteins from Saccharomyces cerevisiae *and* Bacillus subtilis
Report number: EGG-M-26185/NAB
Order number: DE86013449/NA8
Price: $9.95

For additional information, contact
Jane M. Welch
EG&G Idaho, Inc.
P.O. Box 1625
Idaho Falls, ID 83415
Telephone No. (208) 526-8318

0592

energygram®

Human Factors Guidelines and Methodology in the Design of a User-Computer Interface: A Case Study

DOE/TIC/EG-86/145
OFFICE OF SCIENTIFIC AND TECHNICAL INFORMATION

This technical note was based on research conducted by Idaho National Engineering Laboratory for the U.S. Department of Energy.

INEL
Idaho National Engineering Laboratory

A report describes the process and benefits obtained by incorporating human factors guidelines and methods in system design.

In this case study, human factors personnel were requested to participate in a project team of programmers and operations specialists to design a cathode-ray-tube (CRT) display system for a complex process control application. Standard human engineering guidelines and techniques were used by the project team. In addition, previously published documents and research findings sponsored by the United States Nuclear Regulatory Commission were used.

Preliminary tasks involved a review of the draft plant procedures. Then interviews with operators were conducted to establish the initial information for the displays. These initial requirements were evaluated against existing guidelines and criteria to determine the optimal presentation formats.

Detailed steps of the approaches used, design decisions made, and tradeoffs that resulted in the final user-acceptable design are discussed.

The report develops a methodology used and guidelines to be applied when designing a CRT display system for a complex process or system. This methodology and the guidelines described would be applicable during the design of a CRT-human interface for complex manufacturing, chemical processing, process control, or other type of complex monitoring and/or control systems.

FOR ADDITIONAL INFORMATION

DOE report(s):
R. E. Richards, W. E. Gilmore, and L. N. Haney,
Human Factors Guidelines and Methodology in the Design of a User Computer Interface: A Case Study
Report number: EGG-M-16986/NAB
Order number: DE86013470/NAB
Price: $9.95

For additional information, contact:
Jane M. Welch
EG&G Idaho, Inc.
P.O. Box 1625
Idaho Falls, ID 83415
Telephone No.: (208) 526-8318

NIH
Research & Technology

U.S. Department of Health and Human Services Public Health Service National Institutes of Health

Electron Microscopy Technique Improves Image Quality

Rapid sample freezing eliminates structural distortion.

Using an upgraded technique for imaging biological specimens, researchers have obtained electron micrographs of at least comparable quality to those made from cells or tissues prepared by standard methods.

The technique combines high-voltage electron microscopy with rapid sample freezing to eliminate structural distortions caused by conventional chemical preparations, but experience with it is still limited.

"Our first step has been to obtain images of cells and tissues that reveal structures to the same extent seen by traditional methods," says Dr. Mircea Fotino, professor in the department of molecular, cellular and developmental biology at the University of Colorado in Boulder. "It is surprising that we could get such good pictures by this approach because years ago it was thought that this would not be possible." Until recently Dr Fotino was coprincipal investigator with Dr Keith Porter and director of the Laboratory for High-Voltage Electron Microscopy (HVEM) since its establishment in 1972. Conventional chemical fixatives and stains tend to alter the cell structures. These alterations may be substantial or they may be so subtle that they are not readily visible on a micrograph. Dr. Fotino says. "It is assumed that the freezing approach is less distorting and modifying to the appearance of the cell, especially when done fast, because chemical reactions are altogether eliminated," he says.

Microscopists have worked for many years on developing effective cryopreservation techniques that minimize specimen distortions. According to Dr. Fotino, the usefulness of the Colorado technique lies in employing some of these developments in conjunction with a HVEM. "It's a combination of several improvements and advantageous features," he says.

The Boulder HVEM features a top-entry, high-resolution cryostage developed several years ago by Dr. Fotino and incorporated into the microscope column. This "cold stage" allows the researchers to insert specimens that are still frozen and unexposed to the atmosphere and to view them at low temperatures. The instrument can be switched from normal operation to cryoHVEM mode in about 20 minutes. The 1 million-volt cryoHVEM can magnify specimens directly up to 250,000 times. After further photographic enlargement of the image, Dr. Fotino says one can achieve magnifications of several millions.

According to Dr. Fotino, cryopreservation is usually done in freeze dryers located outside the microscope. Before frozen specimens can actually be visualized, they must be warmed to room temperature and carried to the microscope, risking damage to the cells by reactions of temperature-sensitive chemicals. In addition, exposure to the atmosphere while transferring the specimen from the freeze dryer to the microscope may also cause cellular distortions. "You expose all those structures to whatever is in the air," Dr. Fotino says. "Humidity and various gases may induce chemical reactions. The dehydrated structures in the cell may become rehydrated and that rehydration may modify the structures."

Using their cryoHVEM technique, Dr. Fotino and his colleagues have fast frozen whole cultured cells of normal rat kidney by first immersing them in liquid propane for about 10 sec[illegible] is left consists of native structures of good contrast [illegible]onds and then preserving them in liquid nitrogen for ease of handling. Without ever exposing the fast-frozen specimens to the atmosphere, which is accomplished by keeping them immersed in liquid nitrogen, the researchers have transferred them in a small receptacle first to a vacuum lock in the microscope column and then into the precooled cryostage. Because the top-entry objective lens of the HVEM is large, its bore can accommodate a relatively massive cryostat of good cylindrical symmetry. The cryostat surrounds the specimen grid with cold surfaces on both sides, providing good thermal and mechanical stability. The instrument's high resolution of a few angstrom units is thus preserved at any arbitrary point between liquid nitrogen and room temperature.

Through refrigerating and heating units incorporated in the cryostage, the researchers are able to control and maintain low temperatures while viewing the frozen cells and, if so desired, to monitor the progress of sublimation. They may also sublime the frozen matrix entirely by adjusting the temperature in the cryostat. Sublimation is the passage from solid ice directly to vapor without going through the liquid phase. Dr. Fotino says. "When you raise the temperature to an appropriate level, the ice molecules escape from the surface of the ice progressively and are drawn off by the vacuum pump." Complete sublimation or freeze-drying may require from 16 to 48 hours at about 183 kelvin, depending on the thickness of the specimen and of the ice embedment. The frozen matrix in the densest parts of the cell takes the longest to sublime [illegible] damaged during [illegible]

modified by chemical fixation or staining.

An important advantage of the fast-freezing technique is the ability to prevent the formation of large ice crystals—an unavoidable difficulty produced by slow freezing. According to Dr. Fotino as ice crystals grow around a nucleation center consisting of ions or clusters of molecules they damage biological specimens by pushing against fine cellular components such as the membranes, chromosomes or mitochondria, giving the micrograph a "mushy" appearance. Thus the faster the freezing, the smaller the crystals and the less extensive is the specimen damage.

Before a specimen is examined by electron microscopy, the movement of all organelles such as granules, vacuoles and other internal cellular structures—which travel inside the cell at various velocities—must be arrested or fixed. Standard protocols that use chemical fixatives, generally aldehydes such as formaldehyde or glutaraldehyde, arrest the cell's activity at a relatively slow rate, taking up to several seconds to act completely, Dr. Fotino says. All the while the cell structures rearrange. "It's a sort of slow death," he says. But in the process of fast freezing, cellular activity stops in milliseconds, yielding an instantaneous, real-life arrangement of the cell.

Scientists also have to prepare cells and tissues to withstand the vacuum in electron microscopes. The vacuum is necessary because otherwise electrons would be badly scattered by air at atmospheric pressure. "An untreated cell put in a vacuum will explode," Dr. Fotino says. To render the specimen insensitive to the vacuum, standard chemical preparations involve removing intracellular fluid and embedding the specimen in an epoxy to hold the remaining solid structures of the cell in place. The specimen can then be cut into thin slices for observation by electron microscopy. But the epoxy matrix hinders the imaging contrast, Dr. Fotino says, and so the embedded structures need to be stained.

At the lower voltages used in conventional transmission electron microscopy, specimens must be sliced into very thin sections to allow beam penetration. Consequently, only two-dimensional views of cells and tissues can be obtained directly. To gain information in the third dimension, it has been necessary to look at many such sections, cut and viewed in a series. High-voltage electron microscopes, on the other hand, can penetrate much thicker specimens, allowing researchers to obtain sufficient three-dimensional information from a single specimen and avoid the mechanical disruptions of cell structures produced by serial sectioning. "That means one could visualize thicker objects embedded in thicker layers of ice," Dr. Fotino says. "And this is what will happen in future developments. We'll look at more objects embedded in ice that have not been cut or sectioned."

Recently, Dr. Fotino reported on the visualization of fast-frozen, unfixed and unstained suspensions of hydrated whole bacterial endospores and axonemes of sea urchin sperm while they were still embedded in noncrystallized ice. "There is great interest in having small objects like viruses or cilia embedded fully in layers of frozen water and studied under the microscope," Dr. Fotino says. But visualization by this approach remains difficult because the ice embedment reduces the inherently poor contrast of native structures and also because most specimens deteriorate very rapidly under beam irradiation.

Additional reading:

1. Fotino, M., Giddings, T. H. Ultrastructural visualization of unfixed and unstained whole mounts by high-voltage electron microscopy at low temperatures. *Journal of Ultrastructure Research* 91:112–126, 1985.

2. Fotino, M., Visualization of biological specimens by cryoHVEM, *Journal of Microscopy* 143:283–298, 1986.

3. Fotino, M., Giddings, T. H. Ultrastructural imaging of whole cells by cryoHVEM, *Proceedings of the 41st Annual Meeting of the Electron Microscopy Society of America*, Bailey, G. W. (Ed.), Claitor's Publishing Division, San Francisco Press, Inc., San Francisco, CA, 588–589, 1983.

4. Porter, K. R., Anderson, K. L. The structure of the cytoplasmic matrix preserved by freeze-drying and freeze-substitution. *European Journal of Cell Biology* 29:83–96, 1982.

5. Adrian, M., Dubochet, J., Lepault, J., McDowall, A. W., Cryo-electron microscopy of viruses, *Nature* 308:32–36, 1984.

6. Lepault, J., Pitt, T., Projected structure of unstained, frozen-hydrated T-layer of *Bacillus brevis*, *The EMBO Journal* 3:101–105, 1984.

7. Dubochet, J., Lepault, J., Freeman, R., Berriman, J. A., Homo, J. C., Electron microscopy of frozen water and aqueous solutions. *Journal of Microscopy* 128:219–237, 1982.

8. Fotino, M., Giddings, T. H., Voth, R. O., Wray, G. P., Low-temperature imaging for biological applications of high-voltage electron microscopy, *Proceedings of the 40th Annual EMSA Meeting*, Washington, D.C., 374–375, 1982.

The studies of the cryoHVEM for biological research were supported in part by the Biomedical Research Technology (BRT) Program of the NIH Division of Research Resources and by the National Science Foundation. The HVEM at the University of Colorado is supported by the BRT Program.

For Additional Information:

To locate information or professional contacts on this effort, contact:

Research Resources Information Center, 1601 Research Blvd., Rockville, MD 20850 (301) 984-2870

Refer to item XI, No. 2/TN

NIH
Research & Technology

U.S. Department of Health and Human Services Public Health Service National Institutes of Health

Binding of Antiviral Agents to Cold Viruses

Researchers at Purdue University in West Lafayette, Indiana, have pinpointed the site where antiviral compounds bind to viruses that cause the common cold. After binding to the viruses the compounds block viral uncoating—removal of the virus's protein covering—which is necessary for viral replication.

"This is the first description of an antiviral drug interaction with a virus in detail at the atomic level," says Dr. Michael G. Rossmann, professor of biological sciences at Purdue. These findings have allowed the researchers to suggest plausible mechanisms for the biological activity of this class of compounds and may help scientists design new antiviral drugs.

Dr. Rossmann's group used techniques they had developed in earlier studies investigating the structure of a cold virus, human rhinovirus 14. With the use of Cornell University's High Energy Synchrotron Source in Ithaca, New York, and a supercomputer at Purdue, the researchers constructed three-dimensional, atom-by-atom pictures of the virus. Since then the scientists have been able to detail the binding sites of agents proved effective against the virus in laboratory and animal studies.

The cold virus is partially composed of three large proteins that intertwine to form the main exterior structure of the virus. A fourth viral protein forms an interface between the viral exterior and the RNA inside.

The antiviral compounds enter through pores and then alter the three-dimensional structure formed by several amino acids comprising one of the viral proteins. The altered structure caused by the binding of the compounds prevents the outer shell of the virus from breaking open to release RNA. The virus therefore, is unable to synthesize more viral proteins and the infection is arrested.

The compounds studied by Dr Rossmann's team were developed by the Sterling-Winthrop Research Institute in Rensselaer New York. Two of these agents known as WIN 51711 and WIN 52084, were selected because they effectively reduce the numbers of a wide variety of picornaviruses in cell culture. In addition to cold viruses, this group includes enteroviruses which can cause serious syndromes such as poliomyelitis, aseptic meningitis, and hepatitis

The scientists knew that the compounds blocked the viral uncoating process, but they did not know the details of the interaction. The recent results showing

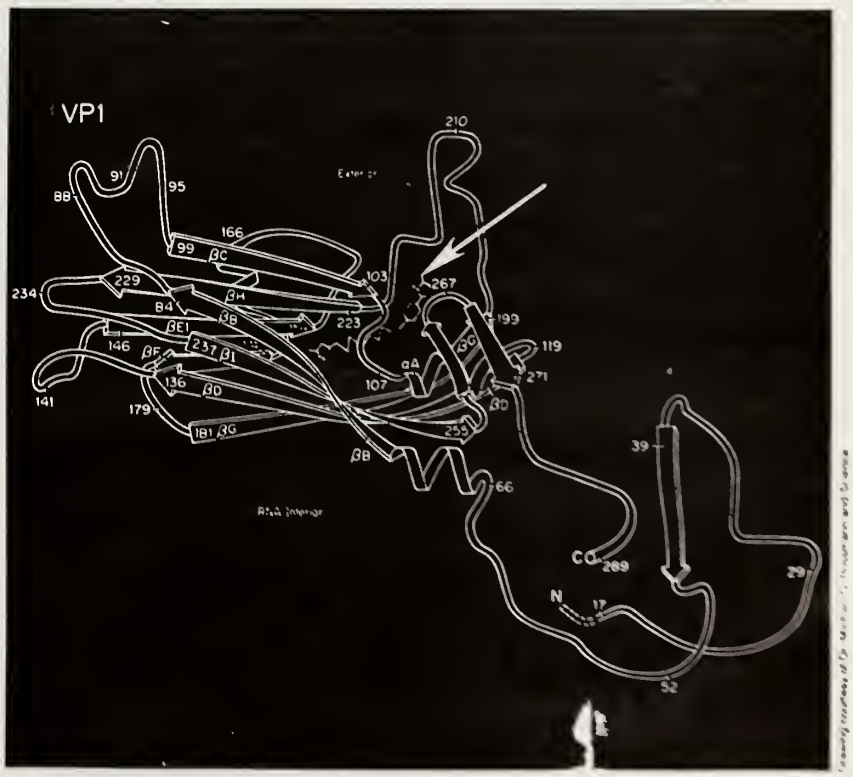

Viral protein 1 (VP1) is one of three large proteins that form the exterior structure of a cold virus. Binding of an antiviral compound (dark arrow) alters the three-dimensional structure of the protein, preventing viral replication.

how the compounds interact at the molecular level represent an important step toward better understanding of the agents' mechanisms of action, according to Dr. Rossmann.

The new knowledge may help scientists develop drugs that are more effective than current antiviral agents. For example, Dr. Rossmann and his colleagues have found that the antiviral activity of WIN 51711 and WIN 52084 can be improved by introducing suitable additional hydrophobic groups on the phenyl group of the compounds. "Specific drugs may be designed to be effective against other cold viruses or, more importantly, against other viruses causing more serious diseases," Dr. Rossmann says.

Although the research has provided fundamental knowledge about the action of the antiviral compounds, this does not mean a cure for the common cold has been achieved. The compounds have only been shown to inhibit viral replication in tissue culture and in animal models of human disease. The high efficacy of WIN 51711 in these models and the high degree of safety seen during toxicity testing, however, make the agent a potential candidate for clinical trials in humans.

—James R. Jauchem, Ph.D.

Additional reading:

1. Smith, T. J., Kremer, M. J., Luo, M., Vriend, G., Arnold, E., Kamer, G., Rossmann, M. G., McKinlay, M. A., Diana, G. D., and Otto, M. J., The site of attachment in human rhinovirus 14 for antiviral agents that inhibit uncoating. *Science* 233:1286–1293, 1986
2. McKinlay, M. A., and Steinberg, B. A., Oral efficacy of WIN 51711 in mice infected with human poliovirus. *Antimicrobial Agents and Chemotherapy* 29:30–32, 1986.
3. Rossmann, M. G., Arnold, E., Erickson, J. W., Frankenberger, E. A., Griffith, J. P., Hecht, H. J., Johnson, J. E., Kamer, G., Luo, M., Mosser, A. G., Rueckert, R. R., Sherry, B., and Vriend, G., Structure of a human cold virus and functional relationship to other picornaviruses. *Nature* 317:145–153, 1985
4. Diana, G. D., McKinlay, M. A., Otto, M. J., Akullian, V., and Oglesby, C., [[(4,5-Dihydro-2-oxazolyl)phenoxy]alkyl] isoxazoles. Inhibitors of picornavirus uncoating. *Journal of Medicinal Chemistry* 28:1906–1910, 1985.
5. McKinlay, M. A., WIN 51711 a new systemically active broad-spectrum antipicornavirus agent. *Journal of Antimicrobial Chemotherapy* 16:284–286, 1985.
6. Otto, M. J., Fox, M. P., Fancher, M. J., Kuhrt, M. F., Diana, G. D., and McKinlay, M. A., In vitro activity of WIN 51711, a new broad-spectrum antipicornavirus drug. *Antimicrobial Agents and Chemotherapy* 27:883–886, 1985.

For Additional Information:

To locate information or professional contacts on this effort, contact:

Research Resources Information Center, 1601 Research Blvd., Rockville, MD 20850 (301) 984-2870

Refer to item XI, No. 1/TN

The research described in this article was supported by the National Institute of Allergy and Infectious Diseases, the National Cancer Institute, the National Science Foundation, and the Sterling-Winthrop Research Institute. Data were gathered at the Cornell University Macromolecular Diffraction Biotechnology Resource, which is supported by the Biomedical Research Technology Program of the NIH Division of Research Resources.

NIH
Research & Technology

Federal
Technology
Resource

U.S. Department of Health and Human Services Public Health Service National Institutes of Health

Information Available on Determining Radiopharmaceutical Dosages

Researchers at government agencies and nuclear medicine centers, as well as private physicians having problems involving internal radiation dose calculations, can access the Radiopharmaceutical Internal Dose Information Center in Oak Ridge, Tennessee, for possible solutions.

The primary aim of the center which is funded by the Department of Energy and the Food and Drug Administration, is to improve radiation dose estimates through development of mathematical models and assessment of the best available biological data concerning radiopharmaceuticals. To reach that goal, information about the internal distribution of radioactive compounds is collected, interpreted and correlated.

Many variables can affect internal radiation dose, including mode of decay, metabolic pathways, chemical and physical form of the drug administered, the route of administration, and the absorption of energy in target organs. The age, sex, health, height, weight, and percentage of body fat of the patients may also affect the radiation dose.

Although the many variables do not allow an exact radiation dose to be calculated, the center staff critically evaluates the data and models available to make an educated estimate of the dose that will be received.

The center is contacted when specialized knowledge of radiation dose calculation techniques is required, such as when information about nonroutine dosimetry techniques is not available in the literature. The staff is frequently consulted when an accidental intake of radioactive material occurs.

Although the staff will evaluate data about any radioactive materials, their speciality is calculating internal radiation doses for radiopharmaceuticals used in nuclear medicine. They assist the FDA Center for Drugs and Biologics by providing the radiation dose estimates needed for evaluating investigational new drugs and new drug applications for radioactive drugs and biologics. They also provide information to researchers who are developing new radiopharmaceuticals and they answer requests for dose estimates. For example, the scientists calculated the doses for xenon 133 used to measure cerebral, hepatic, and portal blood flow, and for intraperitoneal injections of phosphorus-32 used to irradiate and kill peritoneal tumor cells.

It is particularly important to be able to calculate the radiation dose in pregnant women who were administered radiopharmaceuticals. Congenital problems may occur in the fetus as a result of radiation activity in the mother or from radiation that crosses the placenta into the fetus. One radionuclide that is potentially harmful to the fetus is iodine-131, which is used to treat patients with hyperthyroidism or thyroid cancer. The radiation from the iodine kills the thyroid cells. If the drug is administered to the pregnant woman before the fetal thyroid begins to function, at about 13 to 16 weeks, the risk to the fetus is low. If the drug is administered after this time, fetal thyroid cells may be destroyed.

As an aid in responding to requests, a computer data bank containing more than 29,000 bibliographic references concerning characteristics of radiopharmaceuticals is maintained. The data bank includes information about distribution patterns, uptake, retention, and data on variations in physiologic behavior according to age, sex, disease, and condition of the patient. Also included is information pertaining to such topics as calculation techniques and mathematical models. The system is updated each month with information from journal articles and papers, including foreign publications.

In addition to calculating radiation doses, the staff participates in various research projects. For example, resource personnel are revising the radiation dose model for the urinary bladder. The staff also teaches courses on nuclear medicine and internal dose techniques. In addition, they have developed and distributed a computer program for calculating radiation doses.

The staff organizes and conducts international symposia on radiopharmaceutical dose calculation approximately every 5 years. The most recent symposium, which was held in November 1985, focused on the special problems of radiation dose estimation for radioactive, labeled antibodies, short-lived radiopharmaceuticals, and positron emitters. Copies of the symposium proceedings as well as individual reprints are available.

For more information concerning the use of the Radiopharmaceutical Internal Dose Information Center, contact:

Mrs. Evelyn E. Watson
P.O. Box 117
Oak Ridge Associated Universities
Oak Ridge, Tennessee 37831-0117
Telephone: (615) 576-3448

NASA Tech Brief
National Aeronautics and Space Administration
Goddard Space Flight Center, Greenbelt, Maryland

Licensing Opportunity

Cutting Head for Ultrasonic Lithotripsy

Kidney stones are disintegrated safely and efficiently.

Kidney stones lodged in the urinary tract are disintegrated with increased safety and efficiency by a cutting head attached to the end of a vibrated wire probe. The cutting head aligns the probe with the stone and enables the probe to vibrate long enough (typically less than one minute) to disintegrate the stone. The design of this cutting head reduces the risk of metal-fatigue-induced breakage of the probe tip that could leave metal fragments in the urinary tract.

In a recent alternative to the surgical removal of kidney stones lodged in the upper two thirds of the ureter, an ultrasonically vibrated wire probe disintegrates a stone into small fragments that the patient can then pass spontaneously. In this procedure, a catheter is placed cystoscopically at the site of the stone. A long wire probe is then passed through a lumen of the catheter until it touches the stone. The wire probe is attached to the ultrasonic transducer that sets the wire probe into stone-fragmenting lateral and longitudinal vibrations.

This apparatus is limited in effectiveness by the slippage of the thin wire probe off the kidney stone and its lodgment between the stone and urinary tract. Attempts to prevent this slippage by providing a wider tip with a cutting surface have resulted in the dangerous breakage of the wire probe at the tip after only 10 to 20 seconds of operation.

The new cutting-head design prevents premature breakage and assures the seating of the stone on the head (see figure). Constructed of stainless steel, the head has a cutting tip and an elongated collar that relieves the stress on the wire. The wire is inserted in a central circular hole in the rear of the head. At locations shortly behind its cutting teeth, the head is swaged onto the wire. Swaging is used to avoid detempering problems associated with soldering and to minimize stress raisers.

The cutting teeth are machined into the end of the cutting tip and are provided with flat ends to prevent them from scraping the urethra. The teeth form a cup-shaped receptacle that seats a kidney stone. Even if the stone is highly irregular in shape and even if the tip and the stone are aligned imperfectly, the stone will fragment when contacted by any portion of the cutting tip.

Because part of the collar stays within the catheter while the cutting tip is extended against the stone, the mechanical bending loads imposed on the probe wire by the vibration of the head are diminished. When vibrating at the typical operating frequency of 20 kHz, the assembly lasts more than four minutes before the wire breaks off the head, this provides ample time to disintegrate the kidney stone.

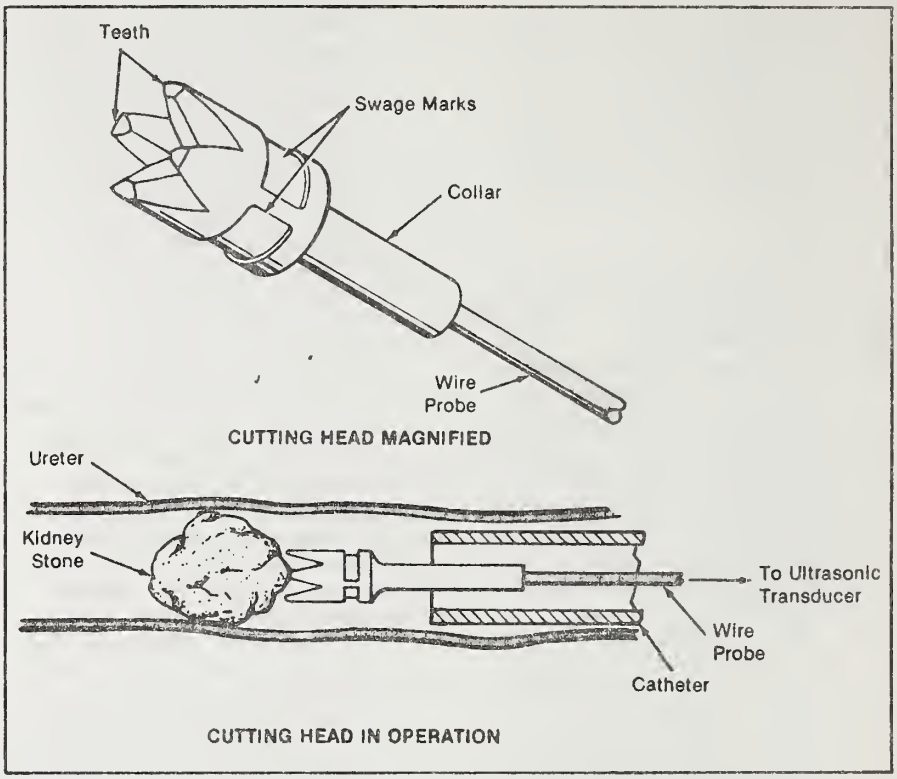

The Teeth of the Cutting Head both seat and fragment the kidney stone, while the extension of the collar into the catheter lessens mechanical strain in the probe wire, increasing probe life and lessening the danger of in situ probe breakage.

This work was done by Earl D. Angulo of **Goddard Space Flight Center** *and Roger Goodfriend of F.A.C.S.*

This invention is owned by NASA, and a patent application has been filed. Inquiries concerning nonexclusive or exclusive license for its commercial development should be addressed to the Patent Counsel, Goddard Space Flight Center. Refer to GSC-12944/TN

Goddard Space Flight Center
Technology Utilization Officer:
Donald S. Friedman
Mail Code 702-1
Greenbelt, MD 20771
(301) 286-6242
Patent Counsel:
John O. Tresansky
Mail Code 204
Greenbelt, MD 20771
(301) 286-7351

FOR ADDITIONAL INFORMATION: *Contact: Director, Technology Transfer Division, P.O. Box 8757, BWI Airport, MD. 21240; (301) 621-0100 Ext. 241*
REFER TO THE NUMBER LISTED AT THE END OF THE ARTICLE

Natural Resources Technology & Engineering

598 Climate Assessment Information Service

599 Multichannel Seismic Reflection Data— Navarin Basin-Northern Bering Sea-Alaska

Software

600 Software Package is an Integrated Finite Difference Program for Computing Two-Phase Nonisothermal Flow in Porous Media

Testing & Instrumentation

601 Meteorological Sensor Package

Other items of interest

532 Interface States in MOS Capacitors— States build up in two stages.

613 Three-Frequency Water-Vapor Radiometer— Measurements increase the accuracies of delay predictions.

NOAA Technology Brief

National Oceanic and Atmospheric Administration

National Weather Service
National Meteorological Center/Climate Analysis Center

Climate Assessment Information Service

The Climate Analysis Center (CAC) has developed a user information service that provides requesters with a wide variety of current climate products. The primary resource for this information is the Climate Assessment Data Base (CADB), which is formed from global, meteorological observations received in real time.

Table 1 shows time frames, areal coverage, and the meteorological parameters included in the primary CADB files. Data quality control measures are employed to minimize the effects of observational and transmission errors. Tables 2a and 2b show the real-time products available from the data base on the CAC microcomputer dial-up system, as well as the schedule for updating the products. The system has been operating since January 1983 on a 24-hour-a-day, seven-days-per-week, basis.

Other products are routinely issued in printed form: Weekly Weather and Crop Bulletin, Weekly Climate Bulletin, and Monthly Climate Bulletin.

For additional information, write to NOAA, Climate Analysis Center, W/NMC53, Room 808, World Weather Building, Washington, D.C. 20233. Phone (301) 763-8071.

Table 1. Climate Assessment Data Base (CADB) summary station files, coverage in time and area, and parameters.

Summary Station File Type	Basic Parameters					Other Selected Parameters
	Coverage	Max T	Min T	Rainfall	Means	
1-Day Synoptic/Airways	U.S.	X	X	24 hr		Weather Type, Max/Min RH, Wind/Chill, Heat Index
1-Day Synoptic/Airways	Global	X	X	24 hr		Weather Type
Weekly Synoptic/Airways	Global	X	X	Weekly	X	Average T, Extreme Max/Min T
Monthly Synoptic/Airways	Global	X	X	Monthly	X	Average Max/Min T, Days with Precipitation, Extreme Max/Min T
1000-Day-Daily Synoptic/Airways beginning Jan. 1, 1987	Global	X	X	24 hr	X	Weather Type Sea Level Pressure Vapor Pressure
40-Day-Daily "Coop Data"	U.S.			24 hr		
CLIMAT Special	Global			Monthly	X	Average T, Average Pressure, Precipitation Quintiles

Key: T = temperature; RH = relative humidity; and Rainfall = total for indicated periods.

TABLE 2a. Real-time products available via CAC's request/reply system.

Product Keyword	Product Description
CLIMRANK	Monthly and seasonal climate rankings by areas.
DDAYEXP	Explanation of degree-day products.
FORECAST	Five-day, six-to-ten-day, seven-day maximum and minimum, and monthly and seasonal outlooks for temperature and precipitation. Weekly heating and cooling degree-day forecasts.
GLOBAL	Weekly and monthly summaries of temperature and precipitation data for more than 6000 locations throughout the world.
GRODGREE	Cumulative weekly growing degree-days for corn.
MAPS	Maps of the weekly temperature precipitation and their departures from normal; maps of the six-to-ten-day forecast by category.
MFOREIGN	Monthly temperature and precipitation data for about 175 foreign cities.
MCTYCDDY	Monthly cooling degree-days for 200 U.S. cities.
MCTYHDDY	Monthly heating degree-days for 200 U.S. cities.
MCTYPRCP	Monthly precipitation data for more than 200 U.S. cities.
MCTYTEMP	Monthly temperature data for more than 200 U.S. cities.
MSACDDY	Monthly population-weighted state average cooling degree-days.
MSAHDDY	Monthly population-weighted state average heating degree-days.
PASTDATA	Data for the preceding three weeks and three months selectively.
PPDANOTE	Explanation of projected Palmer Drought Index.
PPDCENTR	Projected Palmer Index central U.S.
PPDEAST	Projected Palmer Index eastern U.S.
PPDSOUTH	Projected Palmer Index southern U.S.
PPDWEST	Projected Palmer Index western U.S.
SELECT	Allows the user to access data by state. Temperature and precipitation data for several hundred supplementary stations are accessible with this option. Data subjected to less rigorous quality control than primary stations.
WCTYDDAY	Weekly degree-days for more than 200 U.S. cities.
WCTYPRCP	Weekly precipitation data for more than 200 U.S. cities.
WCTYTEMP	Weekly temperature data for more than 200 U.S. cities.
WFOREIGN	Weekly temperature and precipitation data for about 175 foreign cities.
WPDANOTE	Explanation of weekly Palmer Drought Index.
WPDCENTR	Weekly Palmer Drought Index for the central U.S.
WPDEAST	Weekly Palmer Drought Index for the eastern U.S.
WPDSOUTH	Weekly Palmer Drought Index for the southern U.S.
WPDWEST	Weekly Palmer Drought Index for the western U.S.
WSACDDY	Weekly population-weighted state average cooling degree-days.
WSAHDDY	Weekly population-weighted state average heating degree-days.
WXCLSMYI	Weekly summary of internationally significant climate events.
WXCLSMYM	Monthly summary of U.S. significant climate events.
WXCLSMYU	Weekly summary of U.S. significant climate events.
WXCPSMYH	International weather and crop highlights.
WXCPSMYI	International weather and crop summary.

TABLE 2b. Schedule for updating CAC microcomputer accessible products listed in Table 2a.

Product Keyword*	Updated Schedule
CLIMRANK	Updated early each month.
FORECAST	Five-day forecasts are updated Monday through Friday mornings. Seven-day maximum and minimum temperature forecasts are updated daily Monday thru Friday mornings. Six-to-ten forecasts are updated Monday, Wednesday, and Friday. Monthly outlooks are updated about the first and 15th of the month. Seasonal outlooks are updated monthly about the first of the month.
GLOBAL	Weekly data are updated Monday morning. Monthly data are updated by the morning of the 3rd.
GRODGREE	Weekly data are updated by Monday morning.
MAPS	Updated when the tables are available.
MCTYXXXX	Updated monthly by the morning of the 3rd.
MFOREIGN	Updated monthly by the morning of the 3rd.
MSAXXXX	Updated monthly by the morning of the 3rd.
PASTDATA	Updated weekly and monthly.
PPDXXXX	Updated monthly between the 3rd and the 10th.
WCTYXXXX	Updated weekly by Monday morning.
WFOREIGN	Updated weekly by Monday morning.
WPDXXXXX	Updated weekly by Tuesday morning.
WSAXXXX	Updated weekly by Monday morning.
WXCLSMYI	Updated weekly by Tuesday afternoon.
WXCLSMYM	Updated monthly by the 3rd.
WXCLSMYU	Updated weekly by Tuesday afternoon.
WXCPSMYH	Updated weekly by Tuesday afternoon.
WXCPSMYI	Updated weekly by Wednesday morning.

*An "X" in a product keyword indicates that several keywords are implied—see Table 2a.

NATIONAL GEOPHYSICAL DATA CENTER

MULTICHANNEL SEISMIC REFLECTION DATA

Navarin Basin-Northern Bering Sea-Alaska

Approximately 3,200-km of 24-channel seismic-reflection profile data across the continental margin in the northeastern Bering Sea are available for purchase from the National Geophysical Data Center (NGDC). These profiles were provided to NGDC for public dissemination by the U.S. Geological Survey, U.S. Department of Interior. This data set has 12 seismic lines (20 sections).

These profile data were collected during the summer of 1977 by the R/V S.P. LEE using a sound source of five airguns with a volume of 1,326 cu. in. of air compressed to approximately 2,000 psi. The recording system consisted of a 24-channel streamer, 2,400 m long with a group interval of 100 m, and a GUS (Global Universal Science) model 4200 digital recording instrument. Shots were fired every 50 m. Navigational control for the survey was provided by a Marconi-integrated navigation system using transit satellites and Doppler sonar augmented by Loran C (Rho-Rho). A 2-msec sampling rate was used in the field. The data were later desampled to 4 msec during the demultiplexing process. Record lengths vary from 6 to 12 sec, depending on water depth and geologic structure, to give 6 to 8 sec of data below the seafloor. Processing was handled at the USGS Pacific Marine Geology Multichannel Processing Center in Menlo Park, California in the sequence: editing-demultiplexing, velocity analysis, CDP stacking, deconvolution-filtering, and plotting on an electrostatic plotter. The illustration below shows the location of the seismic lines. These seismic data are also available in SEG-Y format as stacked or demultiplexed magnetic tapes. Previous data offered by NGDC for the Navarin Basin are listed in the Previous Data Announcements for the Navarin Basin section of this announcement.

"Multichannel Seismic-Reflection Profiles Collected in 1977 in the Northern Bering Sea," Alan K. Cooper, Michael S. Marlow, and Dennis M. Mann, USGS Geological Survey Open File Report 86-207, U.S. Geological Survey, Dept. of Interior, Menlo Park, CA 94025.

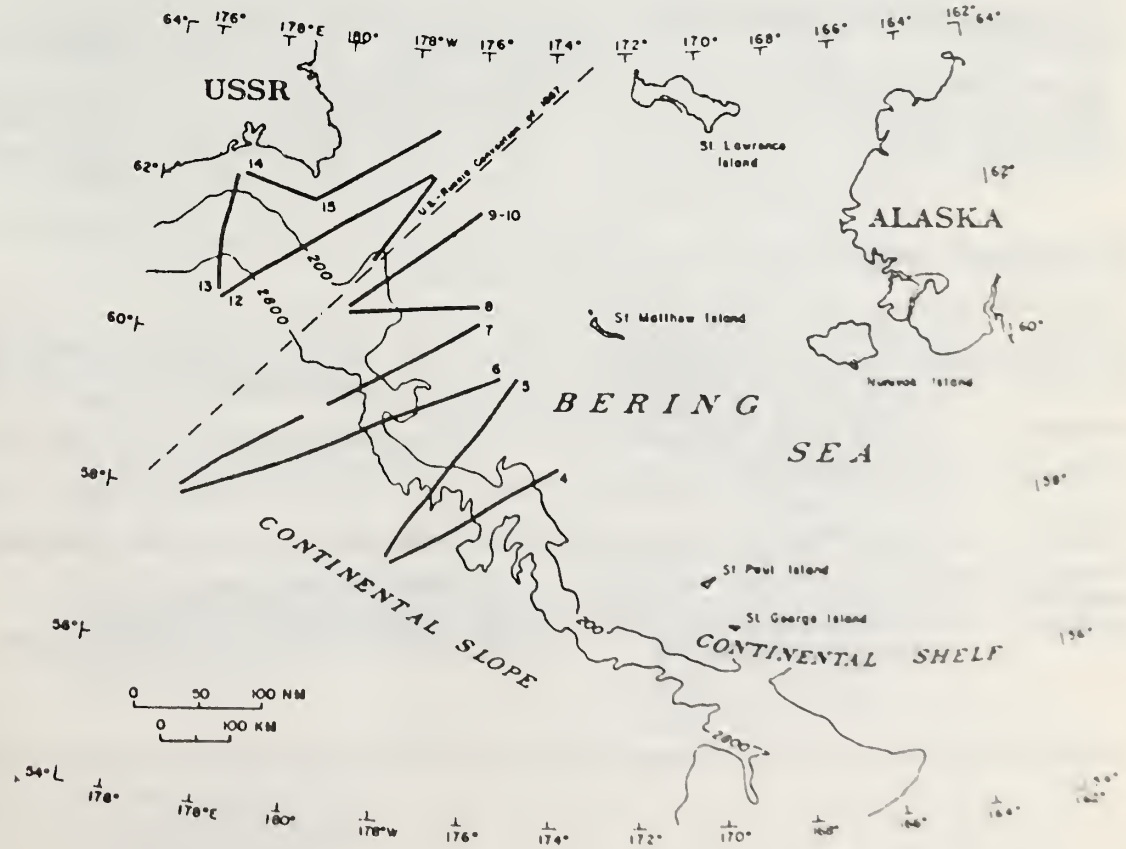

DATA AVAILABLE

Electrostatically Plotted Profiles (deconvolved and filtered after stacking):

20 Lines (sections)	Plastic Sepia	$	2,297.00
	Paper Sepia	$	2,084.00
	Paper Blackline	$	2,046.00

Navigation Data:

1 shot-point navigation map	Plastic Sepia	$	21.00
	Paper Sepia	$	12.00
	Paper Blackline	$	8.00
1 shot-point navigation tape (9-track, 1600 BPI, ASCII)		$	100.00

Digital Seismic Data:

16	Stacked Tapes	$ 2,960.00
532	Demultiplexed Tapes	$ 98,420.00

INQUIRIES ARE INVITED REGARDING THE AVAILABILITY AND PRICES OF OTHER DATA IN THE ALASKA AREA.

The prices quoted here are valid through September 30, 1987. Prices applicable after that date may be obtained by calling (303) 497-6338, FTS 320-6338.

HOW TO ORDER

DEPARTMENT OF COMMERCE REGULATIONS REQUIRE PREPAYMENT FOR ALL NON-FEDERAL ORDERS. Checks and money orders should be made payable to COMMERCE/NOAA/NGDC. Do not send cash. Please add a ten-dollar ($10) handling fee for NON-U.S.A. orders. Checks or money orders for all foreign orders must be in U.S. dollars drawn on a U.S.A. bank. Rush orders require a surcharge of fifteen dollars ($15). Orders may be charged to an American Express, MasterCard, or Visa credit card by telephone or letter. Please include card number, name of cardholder, expiration date, telephone number, and your signature with order.

Inquiries, orders, and payment should be addressed to:

National Geophysical Data Center
NOAA E/GC 3 Code 285
325 Broadway
Boulder, CO 80303

Please direct telephone inquiries and pre-orders to:

Commercial: (303) 497-6338
FTS: 320-6338
TELEX: 592811 NOAA MASC BDR

For technical details, contact:

J. Bruce Grant
NOAA E/GC 3
325 Broadway
Boulder, CO 80303

Telephone: (303) 497 6345
FTS: 320-6345

DATA PREVIOUSLY ANNOUNCED FOR THE NAVARIN BASIN AREA, ALASKA

1977 (U)	Multichannel Common Depth Point (CDP) Seismic Reflection Data - SE Bering Sea, Alaska
1980 (SE-O)	Lease Sale 70. St. George Basin, Bering Sea, Alaska; USGS Data Set AK 15947
1980 (SE-T)	Multichannel Common Depth Point (CDP) Seismic Reflection Data in the Area of Lease Sales 70 and 75, Southern Bering Sea, Alaska
82-MGG-09	Lease Sale 92. Bering Sea, Alaska - High-Resolution Seismic Reflection Data for North Aleutian Shelf
83-MGG-02	Seismic Reflection Data. Multichannel Seismic Reflection Data - North Bering Sea - Gulf of Anadyr
84-MGG-02	Seismic Reflection Data. Navarin Basin, No. Bering Sea, Alaska - High Resolution Seismic Reflection Profiles
84-MGG-04	Bathymetric Data. Navarin Basin - North Bering Sea, Alaska
84-MGG-05	Magnetic & Gravity Data. Navarin Basin - North Bering Sea, Alaska
84-MGG-09	Seismic Reflection Data. Multichannel Seismic-Reflection Profiles - Norton Sound and Eastern Bering Sea, AK

energygram

Computer Software

DOE/TIC/EG-86/031
OFFICE OF SCIENTIFIC AND TECHNICAL INFORMATION

Software Package is an Integrated Finite Difference Program for Computing Two-Phase Nonisothermal Flow in Porous Media

This technical note was based on a software package developed by Lawrence Berkeley Laboratory for the U.S. Department of Energy and available at the National Energy Software Center.

Lawrence Berkeley Laboratory

The SHAFT79 program is designed to simulate production and injection in geothermal reservoirs. It can be easily modified to be, applicable to other two-phase problems.

SHAFT79 solves coupled mass and energy balance equations based on the following major assumptions: the physical system is a system of porous rock saturated with a one-component fluid in liquid and vapor form; all rock properties, except porosity, i.e., density, specific heat, thermal conductivity, and absolute permeability, are independent of temperature, pressure, or vapor saturation; and liquid, vapor, and rock matrix are at the same temperature and pressure at all times.

A fluid table is used to provide the equilibrium thermodynamic properties of the fluid filling the void space—temperature, pressure, vapor saturation, heat conductivity, liquid and vapor viscosities, densities, specific internal energies—as functions of fluid density and fluid specific internal energy.

SHAFT79 has been developed only for systems of water and rock. The fluid table covers most of the equation of state of water substance in the temperature range of 5 to 400 degrees C and the pressure range of 0.5 to 220 bars.

The fluid table is generated by executing two auxiliary programs included in the package: WATER computes and tabulates the steam table equations as given by the International Formulation Committee. PROPER numerically inverts these tables into functions of viscosities and densities and appends parameters other than temperature, pressure, and vapor saturation.

The program is designed to run on the CDC7600 and uses the FORTRAN IV programming language and the SCOPE 2.1 operating system. It requires 725,000 (octal) words of storage. Typical problems require about 10 to 25 CP seconds on the CDC7600. (References 1-3 are included with the software package.)

REFERENCES

DOE report(s):

(1) SHAFT79 User's Manual.
Report number: LBL-10861/NAB
Price: $11.95

(2) SHAFT78, A Two-Phase Multidimensional Computer Program for Geothermal Reservoir Simulation.
Report number: LBL-8264/NAB
Price: $16.95

Other reference(s):

(3) SHAFT79 Tape Description and Implementation Information.
Report number: NESC Note 81-35
Order number: NESC No. 893 7600

References 1-2 are available separately from NTIS. See order information below.

ORDER INFORMATION

This software package (DE83048893/NAB) can be purchased for $1710 (North American Price). To obtain ordering information for software or references, contact National Technical Information Service, Computer Products Center, (703) 487-4763.

DOE offices, contractors, and nonprofit educational organizations can purchase this software package (NESC No. 893) directly or by subscription from

National Energy Software Center
Argonne National Laboratory
9700 South Cass Avenue
Argonne, IL 60439

FOR ADDITIONAL INFORMATION

For additional information, contact:

National Energy Software Center
Argonne National Laboratory
9700 South Cass Avenue
Argonne, IL 60439
Telephone No.: (312) 972-7250 (Comm.)
972-7250 (FTS)

US Army Fact Sheet

Atmospheric Sciences Laboratory (ASL)

White Sands, NM 88002

Meteorological Sensor Package

The Meteorological Sensor Package (MSP) is an integrated meteorological sensing device designed for deployment by the Army in tactical operations areas. Each MSP system will contain meteorological sensors, operator's data control unit (DCU), serial input/output (I/O) module to transmit data to other computers, mast assembly for vehicular mount and operation, and tripod and battery pack for stand-alone operation.

The basic sensor unit has the capability of measuring wind speed/direction, temperature, relative humidity, pressure and magnetic north. The microprocessor and signal conditioning circuits located in the sensor head convert all of the sensor analog outputs to digital signals. This allows a two-wire current loop to the DCU and facilitates the addition of optional sensors.

The DCU communicates with the sensors and the serial I/O module. It receives raw data from the sensors, processes it, and sends it to the serial I/O module for transmission to other computers/users. To maximize its communications flexibility, the serial port on the DCU is programmable and can therefore use a variety of communications protocols. Since the DCU is equipped with a keyboard and display, it serves as the operator terminal for the system and can therefore be used to manually input data, programs, or instructions for system operations.

The serial I/O module is the interface between the MSP and the rest of the world. It has the capability of communicating with other devices via five data ports including two RS-232C serial ports for the possible future addition of a cloud height/visibility sensor and a position location and reporting device, two serial RS-232 ports future expansion and one port to communicate with a radio modem.

The MSP is equipped with a mast that can extend the sensor module mechanically thirteen feet above the platform to which it is attached. Its mast assembly can be attached to virtually any vehicle, including trucks and military utility vehicles. It can also be installed on permanent structures.

The sensor can also be mounted on a tripod assembly if the stand alone mode of operation is desired. Battery packs developed with the system allow unattended operation for up to ten days in the field.

FOR ADDITIONAL INFORMATION:
Mr. Ray Rigert
Army Atmospheric Sciences
Laboratory
Technology Transfer Office
ATTN: SLCAS-DP-P
White Sands, NM 88002
(505) 678-3504
Refer to AS-03/TN

Physical Sciences

602 Detecting the Edges of Obstacles From Range Data— Edges of such terrain features as boulders or craters can be identified from geometrical relationships.

603 Measuring the Low-Energy Spectrum of Cobalt-60— Ionization chamber yields data for calculating dose-enhancement factor for a given specimen geometry.

606 Electromechanical Properties of Superconducting Magnets

607 JANAF Thermochemcial Tables

608 Attenuation Measurements on Deformed Optical Fibers

Testing & Instrumentation

604 Two-Beam Gamma Densitometer

605 Soft X-Ray Laser at Princeton University

609 Hydrogen CARS Spectrometer for Combustion Diagnostics— Coherent anti-Stokes Raman scattering produces data on chemical and physical events and flow.

610 Fast-Responding Thermal Fluence Gauge— With its small mass, a gauge can measure the effects of pulses as brief as 1 millisecond.

611 A Virtual Impactor for Personal and Area Air Sampling

612 X-Ray Microprobe Achieves 10 Micron Resolution

613 Three-Frequency Water-Vapor Radiometer— Measurements increase the accuracies of delay predictions.

614 Laser-Pulse/Fiber-Optic Liquid-Leak Detector— Several potential leak sites can be monitored using a single sensing fiber. (Licensing Opportunity)

615 Improved Spectrometer for Field Use— Instrument would give answers in the field without waits for lab processing. (Licensing Opportunity)

Other items of interest

579 Thermal Analysis of Epoxy Mixtures— Differential scanning analysis is used to study the curing of resins.

582 Deuterides of Rare-Earth/Transition-Metal Alloys— Neutron diffraction studies shed light on both crystal and magnetic structures.

587 Two-Step Vapor/Liquid/Solid Purification— One process approaches the theoretical limit of multiple zone refining and distillation. (Licensing Opportunity)

MANUFACTURING TECHNOLOGY NOTE

U.S. ARMY MATERIEL COMMAND

Deputy Chief of Staff for Manufacturing Technology, Alexandria, VA

Project Number: 1A52F59W1A1A

Filing Code: 46C084

Detecting the Edges of Obstacles From Range Data

Edges of such terrain features as boulders or craters can be identified from geometrical relationships.

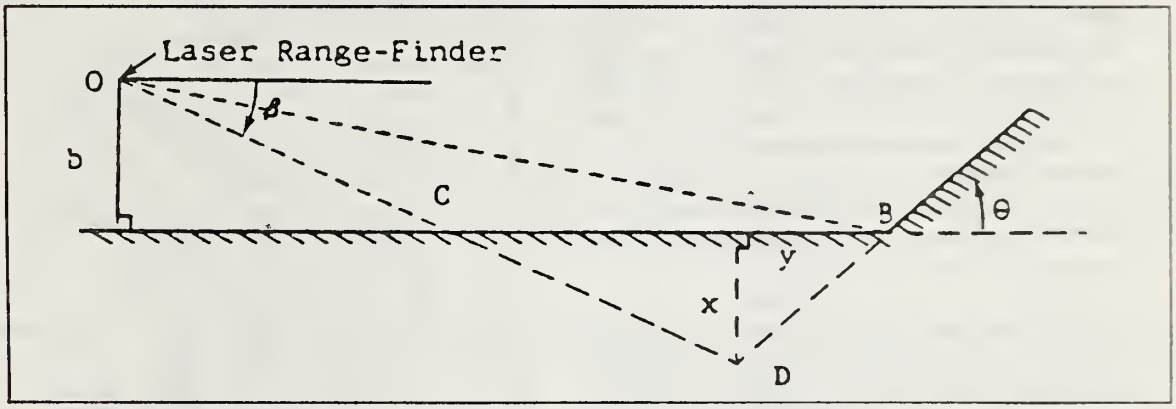

A **Laser Rangefinder** is mounted on a mast of height b. C and B are points at which the scanning laser beam bounces off the terrain and D is the estimate of the range. The slope, tan θ, of the obstacle can be computed by taking the ratio x/y

A study of remote sensing by laser rangefinders has investigated ways in which edges of objects on flat terrain can be defined by a slope or gradient change. The study by the U.S. Army Research and Development Center described the effects on minimum detectable slope change of the following:

- Noise levels,
- Probability of miss,
- Probability of false alarm,
- Spacing of measurements, and
- Random distribution of edges near range-measurement points.

The study employed a simple estimate of slope change, calculating the Laplacian from incremental range measurements taken at different elevation angles (see figure). The Laplacian is defined as the second difference of the range data. Since the range data contain noise in the form of measurement error, consideration must be given to the statistical aspects of detecting edges in order to differentiate between actual edges and noise effects.

For an assigned probability of false alarm and miss, one can determine the signal-to-noise ratio and the threshold-to-noise ratio. If one uses a special scanning scheme in which the spacing of horizontal projections is proportional to the radial distances from the laser to a horizontal plane, then the function K of angular geometry is also constant. The minimum detectable obstacle angle can be found with certain probability if K, the elevation angle β, and the terrain slope ϕ are known.

Project officer C. N. Shen
(518) 266-5414 or AV 974-5414.

FOR ADDITIONAL INFORMATION

You can learn more details about this technology by ordering the NTIS report:

Analysis of Gradient Change Thresholds in the Detection of Edges of Objects From Range Data
Order number AD A166416/XAA
Price code A02

Order from
National Technical Information Service
5285 Port Royal Road
Springfield, VA 22161

This document was prepared under the sponsorship of the U.S. Government. Neither the United States Government nor any person acting on behalf of the United States Government assumes any liability resulting from the use of the information contained in this document, or warrants that such use will be free from privately owned rights.

MANUFACTURING TECHNOLOGY NOTE

U.S. ARMY MATERIEL COMMAND

Deputy Chief of Staff for Manufacturing Technology, Alexandria, VA

Project Number: 1L162120AH25 Filing Code: 60H012

Measuring the Low-Energy Spectrum of Cobalt-60

Ionization chamber yields data for calculating dose-enhancement factor for a given specimen geometry.

The relative magnitude of the low-energy scattered component of cobalt-60 gamma radiation can be determined experimentally with a gold-and-aluminum-wall air-ionization chamber. The gold/aluminum-ionization-chamber technique, developed by Harry Diamond Laboratories, yields an immediate quantitative indication of the degree of dose enhancement that can be achieved by a given filter combination for a particular source configuration.

The results clearly identify the type of source configurations that have inherently high scatter. The results also provide empirical evidence that the spectra of most practical cobalt-60 irradiators can be hardened to a degree equal to or better than that of the best available unscattered spectrum, if the specimen is enclosed in a filter box having a 0.063-in. (0.16 cm) thickness of lead on the source side and no more than 0.030 in. (0.076 cm) of aluminum. The experimental data suggest that thinner aluminum layers are better and that no aluminum may be best.

The chamber body is made of polystyrene to minimize leakage current (see figure). No guard-ring is used because the aspect ratio of the chamber is high, and it is not necessary to know the absolute calibration of the chamber. A 60-V bias is provided by a power supply. The ionization current is measured by a digital electrometer. The resolution of the electrometer is 0.01 picoampere on its most sensitive range, and measurements of currents of tens of picoamperes is therefore feasible and accurate.

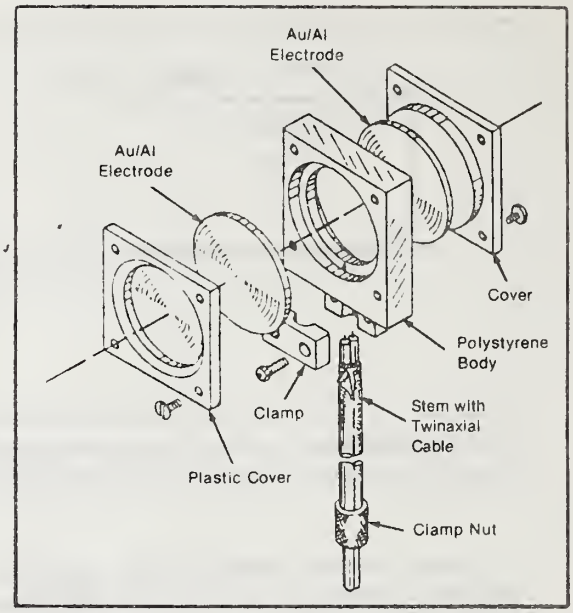

An **Exploded View of the Ionization Chamber** shows the 4-cm-diameter cavity and the 0.3-cm spacing between electrodes. Connection from the twinaxial cable is by mechanical pressure from the electrode cover plates.

FOR ADDITIONAL INFORMATION

You can learn more details about this technology by ordering the NTIS report(s):

Experimental Determination of the Low-Energy Spectral Component of Cobalt-60 Sources
Order number AD A168022/NAA
Price code A03

Order from
National Technical Information Service
5285 Port Royal Road
Springfield, VA 22161

This document was prepared under the sponsorship of the U.S. Government. Neither the United States Government nor any person acting on behalf of the United States Government assumes any liability resulting from the use of the information contained in this document, or warrants that such use will be free from privately owned rights.

energygram®

Two-Beam Gamma Densitometer

DOE/TIC/EG-86/123
OFFICE OF SCIENTIFIC AND TECHNICAL INFORMATION

This technical note was based on research conducted by Idaho National Engineering Laboratory for the U.S. Department of Energy

INEL
Idaho National Engineering Laboratory

With the use of prior knowledge or assumptions about possible distributions of a two-phase fluid flowing in a pipe, the average density and the density distribution can be determined with a two-beam radiation attenuation densitometer.

A radiation densitometer is a nonintrusive method for gaining information about the average density and density distribution of a fluid of interest.

The densitometer with an active source, and correspondingly high count rate, allows measurements to be made quickly (~1 sec) so that density fluctuations can be observed.

The general procedure for using a multibeam densitometer, after the densitometer geometry has been selected, consists of four steps:

(1) Select a density distribution model or a fluid-flow model.

(2) Calculate the densitometer readings and the average density for each of the many combinations of values of the parameters that specify the fluid distributions.

(3) Construct interpretation charts with the use of the values calculated in step 2.

(4) Interpret the experimental data.

An example of the two-beam system is presented in the figure below. A complete analysis of the system, with considerable mathematical detail, is available.

The technique does have some limitations:

- A primary difficulty lies in finding a fluid distribution model that is complicated enough to accurately represent the actual fluid distribution and still simple enough to lend itself to the mathematical analyses required.
- If the actual fluid distribution does not conform to the assumed model, absurd interpretations of the density interpretation can result.
- Designs of the two-beam system to date have been based on intuition. It would be desirable to have a procedure to optimize the densitometer geometry for a given density distribution model.

FOR ADDITIONAL INFORMATION

Reference(s):

Mass Flow Instrumentation During LOFT Nonnuclear Test Series. ISA Trans., *19(4) 43-55 (1979).*

Two-Phase Fluid Density Measurement with a Two-Beam Radiation Attenuation Densitometer. IEEE Trans Nucl Sci., *NS-23 (1) (1976)*

DOE report(s):

LOFT Three-Beam Densitometer Data Interpretation
Report number: TREE-NUREG-1111/NAB
Order number: TREE-NUREG-1111/NAB
Price: $11.95

The Development of Reconstructive Tomography for the Measurement of Density Distribution in Large Pipe Steady-State Multiphase Flows in Review Group Conference on Advanced Instrumentation Research for Reactor Safety, held at the Oak Ridge National Laboratory, July 29-31, 1980
Report number: NUREG/CP-0015/NAB
Order number: NUREG/CP-0015/NAB
Price: Contact NTIS for quote

Order DOE report(s) from
National Technical Information Service
5285 Port Royal Road
Springfield, VA 22161

For additional information, contact:
J. M. Welch
EG&G Idaho, Inc.
P.O. Box 1625
Idaho Falls, ID 83415
Telephone No. (208) 526-8316

or

B. V. Thornton
EG&G Idaho, Inc.
P.O. Box 1625
Idaho Falls, ID 83415
Telephone No. (208) 526-2038

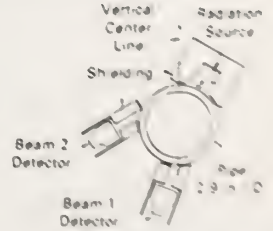

Two-beam densitometer geometry

energygram®

Soft X-Ray Laser at Princeton University

DOE/TIC/EG-86/155
OFFICE OF SCIENTIFIC AND TECHNICAL INFORMATION

This technical note summarizes a project achievement selected from the U.S. Department of Energy 1985 Basic Energy Sciences Program.

published by
Office of Scientific and Technical Information
U. S. Department of Energy
Oak Ridge, Tennessee

A technical note from your energy information center

There are many important uses for unique, high-intensity, laser-produced X-rays in medicine, physics, biology, and technology in general. In medicine, the finely focused X-ray laser would allow better localization in the use of CAT scanners and similar devices. Plasma physicists could make extensive use of soft X-ray lasers to measure temperature, impurity densities, and ion transport in fusion plasmas. In the area of solid-state physics, X-ray lasers could substantially improve structural analysis of crystalline solids. X-ray microscopes would have greater resolution than can be achieved by present-day electron-beam systems. The first step in this direction is the development of the 18.2-nm-wavelength soft X-ray laser at Princeton.

At the heart of this approach to a soft X-ray laser is the use of a fast-recombining plasma. Initially, the plasma temperature is increased until the carbon atoms become completely ionized; that is, totally stripped of electrons. The plasma then cools rapidly by intensive radiation losses and thus causes ions to recombine with free electrons. Because recombination occurs primarily at the higher energy levels (outer orbits), whereas lower levels (inner orbits) do not capture electrons, an unstable condition known as population inversion occurs. Electrons in the higher energy levels then "avalanche" to the lower levels and thus create a more stable electron configuration. In the process, each electron loses energy in the form of a soft X-ray photon. The lasing process occurs when the photons produced in this fashion stimulate the emission of additional photons from other ions and thus initiate a chain of such events. The result is an intense, coherent soft X-ray pulse of a single wavelength.

A carbon dioxide laser has been used to produce a dense carbon plasma column of 1 to 2 cm in length, which is held to a 1- to 2-mm diameter by confinement in a strong magnetic field. A 100-fold increase of the 18.2-nm soft X-ray laser line has been observed in the direction along the plasma column as a result of the desired stimulated-emission process. This result corresponds to an amplifier "gain" of about 6.5. By using a multilayer soft X-ray mirror with a reflectivity of 12%, an enhancement of 120% of the stimulated radiation was achieved. More recently, the soft X-ray laser beam divergence was measured to be as low as 5 mrad with a power of 100 kW, an energy of 1 to 3 mjoule, and a maximum amplification of stimulated emission of 500 (a gain of about 8.0). (Princeton Plasma Physics Laboratory, S. Suckewer)

FOR ADDITIONAL INFORMATION

For additional information, contact:
Plasma Physics Laboratory
Princeton University
P.O. Box 451
Princeton, NJ 08544

NBS technology update

National Bureau of Standards
U.S. Department of Commerce
Gaithersburg, MD 20899

Electromechanical Properties of Superconducting Magnets

Accurate data on superconductor performance under mechanical load is essential to the design of the magnets used in various fusion energy devices. NBS is conducting a 3-year research program sponsored by the Department of Energy to obtain this data and to quantify the electromechanical properties of promising new superconductor materials. Electromechanical Properties of Superconductors for DOE Fusion Applications (NBSIR 86-3044) reports the results of the first 18 months of the program. Included are data on the properties of experimental ($PbMo_6S_8$ and liquid-infiltrated Nb-Ta/Sn) and commercial (NB_3S_n) superconductors and stainless steel conductor-sheathing materials. A new electron-tunneling diagnostic tool for probing the energy gap of practical superconductors is described.

FOR ADDITIONAL INFORMATION: A copy of the report is available from NTIS, Springfield, VA 22161; (703) 487-4600.
NTIS order number: PB87-125753/NAC
Price code: A06

NBS technology update

National Bureau of Standards
U.S. Department of Commerce
Gaithersburg, MD 20899

JANAF Thermochemical Tables

NBS has published the third edition of the (Joint-Army-Navy-Air Force) JANAF Thermochemical Tables. The JANAF tables provide scientists in government, industry, and universities with important information on the performance of materials at high temperatures. The thermochemical data in the JANAF tables have technical application in performance calculations for chemical reactors such as rocket engines, air pollution control equipment, automotive internal combustion engines, coal gasifiers and furnaces, fuel cells, liquefaction reactors and their catalyst structures, and magnetohydrodynamic generators. The information also can be used by engineers in the design of chemical plants. The JANAF Thermochemical Tables are published as Supplement No.1 to Volume 14 of the Journal of Physical and Chemical Reference Data (1985). The journal and its supplements are published under a cooperative agreement among NBS, the American Institute of Physics, and the American Chemical Society.

FOR ADDITIONAL INFORMATION: The two-volume set is available for $130 prepaid from the American Chemical Society, 1155 Sixteenth Street, N.W., Washington, D. C. 20036. The computer-readable database, The JANAF Thermochemical Tables (1985), NBS Standard Reference Database 13, is available for $1,200 from the Office of Standard Reference Data, A323 Physics Building, National Bureau of Standards, Gaithersburg, MD 20899; (301) 975-2208.

NBS technology update

National Bureau of Standards
U.S. Department of Commerce
Gaithersburg, MD 20899

Attenuation Measurements on Deformed Optical Fibers

The optical attenuation of lightguides is one of the most important parameters to system designers. In addition to the inherent attenuation of a given fiber, designers must take into account the added losses caused by the perturbations of bending, twisting, stretching, and overlapping of uncabled fibers. NBS has investigated these losses in short lengths of a variety of multimode fibers, using optical time domain reflectometry. The results of the studies showed that bending and microbending are the sources of most of the losses, that tension causes up to 4 dB/N km of loss (depending on the type of fiber), that twisting losses are negligible, and that overlapping causes losses somewhat less than bending does.

FOR ADDITIONAL INFORMATION: These findings are presented in Attenuation Measurements on Deformed Optical Fibers (NBSIR 86-3052).

Order number: PB87-132289/NAC
Price code: A03

MANUFACTURING TECHNOLOGY NOTE

U.S. ARMY MATERIEL COMMAND

Deputy Chief of Staff for Manufacturing Technology, Alexandria, VA

Project Number: NONE

Filing Code: 60H013

Hydrogen CARS Spectrometer for Combustion Diagnostics

Coherent anti-Stokes Raman scattering produces data on chemical and physical events and flow.

A single-shot spectrometer based on hydrogen coherent anti-Stokes Raman scattering (CARS) has been developed. The CARS spectrometer yields information about the chemical and physical flow fields of a burning propellant under pressure.

Facilities were established by the U.S. Army Armament Research and Development Center for performing single-shot hydrogen CARS diagnostics on propellant ignition and flame (see figure). Preliminary experiments indicate that critical factors in the CARS techniques are the choice of background gas, flow rates through the pressure cell, yttrium/aluminum/garnet laser fluence, and spectral width of the dye laser.

CARS spectra of nitrogen product gas were obtained from burning propellant, and the spectra of hydrogen evolved in the propellant flame were observed. The use of oxygen as a background gas was shown to alter the behavior of the propellant.

Hydrogen gas was chosen as the target molecule because of its large Raman cross section, its presence in the equilibrium products of propellant combustion, and its ubiquity in the laser-induced decomposition of propellant materials. Spectroscopic analysis at frequencies corresponding to the hydrogen Q-branch is easy because the spectrum is unambiguous; the individual rotational lines narrow and separate within a convenient contour for broadband dye lasers. Moreover, other Raman-active molecules do not interfere.

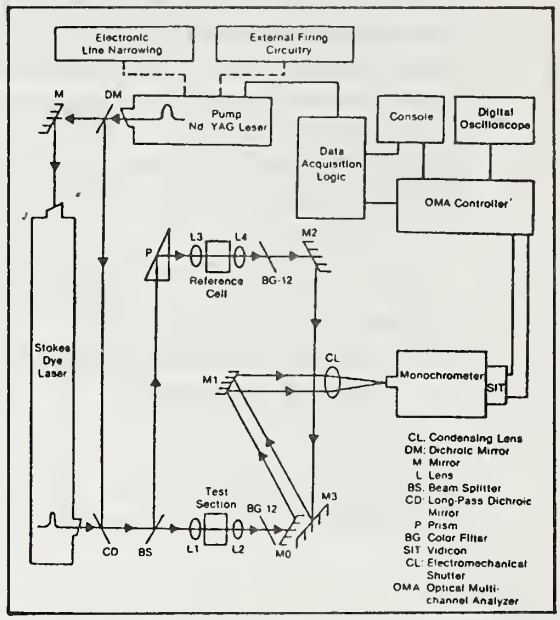

A **CARS Spectrum** is generated by the focused interaction of pump and Stokes lasers in the sample. With a colinear configuration of the two beams, the interaction volume is fairly large, the signal level is optimum, and the alignment procedure is straightforward. As they leave the sampled region, the pump and Stokes beams are blocked. The anti-Stokes beam (the CARS signal) is diverted to an optical multichannel analyzer for detection and recording.

FOR ADDITIONAL INFORMATION:

You can learn more details about this technology by ordering the NTIS report(s):

Single-Shot H(2) CARS Spectroscopy of Propellant Ignition and Combustion Under Pressure.
Order number: AD-A168054/NAA
Price code: A03

Order from:

National Technical Information Service
5285 Port Royal Road
Springfield, VA 22161

This document was prepared under the sponsorship of the U.S. Government. Neither the United States Government nor any person acting on behalf of the United States Government assumes any liability resulting from the use of the information contained in this document, or warrants that such use will be free from privately owned rights.

MANUFACTURING TECHNOLOGY NOTE

U.S. ARMY MATERIEL COMMAND

Deputy Chief of Staff for Manufacturing Technology, Alexandria, VA

Project Number: NONE

Filing Code: 60G006

Fast-Responding Thermal Fluence Gauge

With its small mass, a gauge can measure the effects of pulses as brief as 1 millisecond.

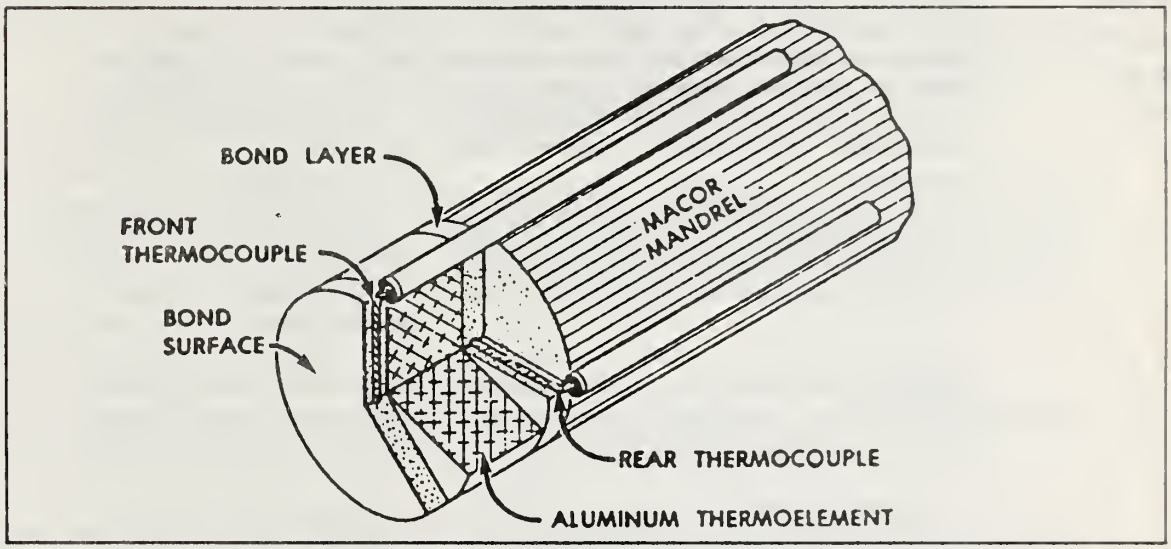

The heart of the **Thermal Conductivity Gauge** is an aluminum disk having front and rear thermocouples. The gauge replaces thin-skin total-heat gauges, which measure only the maximum temperature attained by the back surface, with no indication of the time required to reach that temperature.

A special thermal fluence gauge has been fabricated to respond to sharply rising temperatures. The gauge is used when the thermal flux is of short duration, 150 milliseconds or less, and of low total energy, 179 calories per square centimeter or less. The maximum operating temperature of the gauge is 500 °C. It can withstand severe blast and shock.

The measuring element of the gauge is a thin aluminum disk having a chromel/alumel thermocouple mounted across the center of each face with a thermoconducting epoxy adhesive (see figure). This subassembly is mounted on the end of a ceramic mandrel inserted in a ceramic sleeve so that the front surface of the disk is flush with the front of the sleeve. Wires connecting the gauge to external instrumentation are anchored to the mandrel and exit through the rear of the sleeve.

The gauge performs well, although design changes could simplify both acquisition and analysis of data. Such changes would include adoption of a two-wire shielded thermocouple and vapor-deposited thermocouple junctions. The two-wire system would reduce the number of data channels to one per gauge, thus eliminating a differencing step in the analysis. Vapor-deposited junctions would allow more accurate measurement of the gauge surface temperature.

Project officer Melinda B. Krummerich
(301) 278-6128 or AV 283-6128.

FOR ADDITIONAL INFORMATION:

You can learn more details about this technology by ordering the NTIS report(s):
A Fast Response Thermal Conductivity Gauge
Order number: AD-A168185/NAA
Price code: A03

Order from:
National Technical Information Service
5285 Port Royal Road
Springfield, VA 22161

This document was prepared under the sponsorship of the U.S. Government. Neither the United States Government nor any person acting on behalf of the United States Government assumes any liability resulting from the use of the information contained in this document, or warrants that such use will be free from privately owned rights.

energygram®

A Virtual Impactor for Personal and Area Air Sampling

DOE/TIC/EG-86/108
OFFICE OF SCIENTIFIC AND TECHNICAL INFORMATION

This technical note was based on research conducted by Idaho National Engineering Laboratory for the U.S. Department of Energy.

INEL
Idaho National Engineering Laboratory

A multistage virtual impactor has been designed and fabricated consisting of two separation stages, yielding three particle size classes. Efficiency and loss curves have been experimentally determined at ambient conditions for each stage. The small physical size and ability to operate at low flow rates make the impactor very versatile.

The virtual impactor is able to accurately measure particle size distributions by determining the mass median aerodynamic diameter and Geometric Standard Deviation. The impactor operates at close to theoretical efficiencies and sharpness of cut points. The prototype routinely collects 20 to 40 mg of aerosol mass with total internal losses of less than 9%.

A wide range of cut points is available with a single design by simply changing the flow rate through the impactor. Alternatively, the virtual impactor design could be modified to cover a variety of applications. The virtual impactor was designed and fabricated to operate at two liters per minute volume flow rate. This flow rate is particularly compatible with two applications: personal air sampling and remote environmental sampling.

The virtual impactor's design eliminates particle bounce. This characteristic is particularly desirable if the size distribution measurements are to be used to establish parameters for environmental dose pathway models.

The two-stage impactor shown was designed for small size and a 2 liter/min flow rate. Flow through each stage is controlled by an orifice. The sum of the orifice areas can be used to control the total flow through the impactor, whereas the ratios of the orifice areas are used to control the relative amounts of the major and minor flows. Filters are placed upstream of the orifices to collect the three particulate size fractions.

FOR ADDITIONAL INFORMATION

DOE report(s):
A Virtual Impactor for Personal and Area Air Sampling.
Report number EGG-M-25485/NAB
Order number: TI86004137/NA8
Price: $9.95

Order from:
National Technical Information Service
5285 Port Royal Road
Springfield VA 22161

For additional information, contact
J. M. Welch
EG&G Idaho, Inc
P.O. Box 1625
Idaho Falls, ID 83415
Telephone No. (208) 526-8318

or

J. L. Alvarez
EG&G Idaho, Inc
P.O. Box 1625
Idaho Falls, ID 83415
Telephone (208) 526-1293

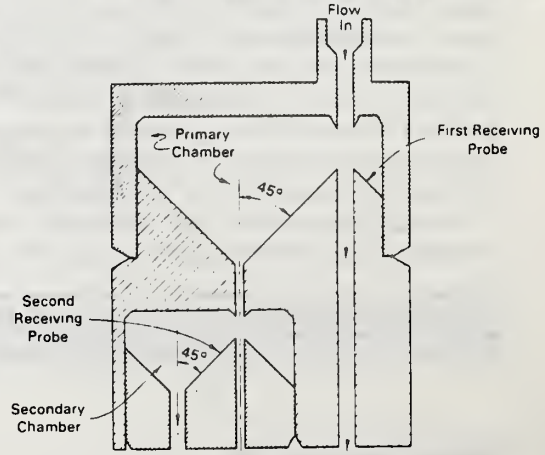

Multistage virtual impactor prototype schematic.

X-Ray Microprobe Achieves 10 Micron Resolution

A resolution of better than 10 microns, with a high enough intensity to measure trace concentrations of atomic elements, has been obtained using a new x-ray microprobe designed by scientists at the Lawrence Berkeley Laboratory.

In tests conducted at the Brookhaven National Laboratory, the new microprobe measured the concentration and spatial distribution of many elements quickly and simultaneously in a sample area of less than 100 square microns. An even higher resolution appears possible in the near future.

"In a 300 second counting time, we easily measured picogram quantities of elements from potassium to zinc," said Albert Thompson, a physicist at LBL's Center for X-ray Optics.

The beam of x-rays from the light source was focused by a pair of multilayer-coated mirrors designed and fabricated at the Center for X-ray Optics under the guidance of Underwood. When the x-rays struck a sample, elements in the sample were caused to fluoresce, yielding characteristic spectral lines which were recorded by a lithium-drifted silicon detector.

The unique mirrors that enabled the new microprobe to bring x-rays into such a crisp focus began as standard fused-silica mirrors with a 6-meter radius of curvature. To these mirrors were added deposits of tungsten and carbon in alternating layers, each a few atoms thick.

The alternating mirrors act like a crystal to select a narrow band of wavelengths from the white spectrum of the x-ray beam. The mirrors are placed on a rotating table and passed under a pair of sputtering sources. The evaporated atoms form a set of very uniform layers on the surface of the mirrors.

Unlike electron microprobes, the new x-ray probe does not require that samples be placed in a vacuum. Consequently, it permits a wider variety of samples, including living biological specimens, to be studied. The new microprobe's designers estimate their device to be about 100 times more sensitive than conventional "pinhole imaging" of x-rays for materials research, such as the study of phase transitions.

To date, the new microprobe has been used in a medical study to reveal the distribution of toxic concentrations of trace elements in biological tissue, and in a study of ceramics to locate internal cracks and flaws. An experiment using the new microprobe to reveal the geological history of rocks is scheduled to get under way soon.

FOR ADDITIONAL INFORMATION:

Mr. Robert Morris
Department of Energy
Lawrence Berkeley Laboratory
50A-4112, University of California, Berkeley, CA 94720
(415) 486-6502

NASA Tech Brief
National Aeronautics and Space Administration
NASA's Jet Propulsion Laboratory, Pasadena, California

Three-Frequency Water-Vapor Radiometer

Measurements increase the accuracies of delay predictions.

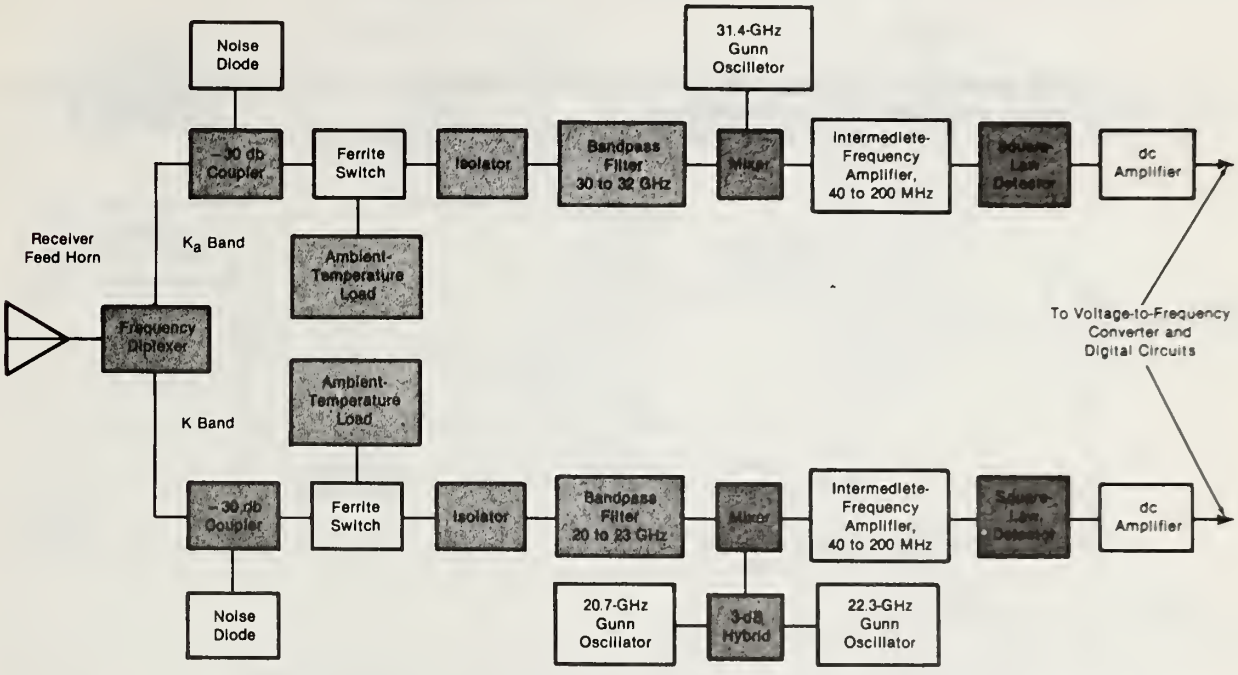

The Water-Vapor Radiometer measures thermal emissions from the sky at three microwave frequencies to determine the water-vapor content of the atmosphere and the consequent wet-path microwave delay.

A three-frequency microwave radiometer measures the quantity of water vapor in the atmosphere, as part of the effort to determine microwave-signal delays due to water vapor. The delay estimates are necessary for the accurate determination of distances in geodesy and such related applications as very-long-baseline interferometry. The water-vapor data are also directly useful in weather research.

The amount of water vapor and the microwave delay caused by the water vapor along a line of sight in the atmosphere are readily estimated from microwave observations along the same line of sight. In prior radiometer systems, the most important measured quantity was the thermal atmospheric emission at a frequency near the 22.237-GHz resonance of the H_2O molecule. In cloudy skies, a second measurement was made away from this resonance to determine the thermal contribution from liquid water. The new radiometer measures the emission at three frequencies, two (20.7 and 22.3 GHz) near the resonance and a third at 31.4 GHz. The three-frequency technique offers a modest improvement in delay estimation over the two-frequency technique.

The figure illustrates the microwave portion of the radiometer. The received sky signal is fed through a frequency diplexer, which separates the two lower frequencies from the higher one. The individual receivers are Dicke radiometers, each of which includes a ferrite switch to alternate its input between the received sky signal and an internal ambient-temperature load for temperature calibration and receiver stabilization. A constant white-noise signal from a noise diode is coupled into the sky-signal port of each ferrite switch to provide a gain-calibration reference.

The mixers are of the double-balanced, Schottky-diode type having intermediate-frequency passbands of 40 to 200 MHz. The 20.7- and 22.3-GHz signals are obtained in the lower frequency channel by passively coupling the two Gunn local oscillators into the mixer and alternately turning the oscillators on and off. The bandpass filters suppress the local-oscillator harmonics, that might otherwise cause offsets in the Dicke comparison between the sky- and ambient-temperature reference ports.

All of the radiometer components except the receiving feed horn are configured in a plane and fastened to an aluminum heat sink. The heat sink is thermally isolated from the environment except for a thermoelectric heat pump that maintains it at 35 °C. This temperature control stabilizes the radiometer gain and

noise-diode outputs within a small fraction of a percent.

A microprocessor monitors temperatures, power-supply voltages, and the output of a tilt sensor for automatic zenith-angle calibration. It controls the stepping motors that change the line of sight. It also controls the microwave switches. One cycle of the switching sequence takes about 1 s and is comprised of eight integration subcycles of about one-eighth s at each of the eight combinations of switch positions. The radiometer outputs are integrated digitally and processed into sky-brightness temperatures.

This work was done by Michael A. Janssen and Noburu I. Yamane of Caltech for **NASA's Jet Propulsion Laboratory**. *NPO-16531 /TN*

FOR ADDITIONAL INFORMATION: *Contact: Director, Technology Transfer Division, P.O. Box 8757, BWI Airport, MD. 21240; (301) 621-0100 Ext. 241*
REFER TO THE NUMBER LISTED AT THE END OF THE ARTICLE

NASA Tech Brief
National Aeronautics and Space Administration
John F. Kennedy Space Center, Florida

Licensing Opportunity

Laser-Pulse/Fiber-Optic Liquid-Leak Detector

Several potential leak sites can be monitored using a single sensing fiber.

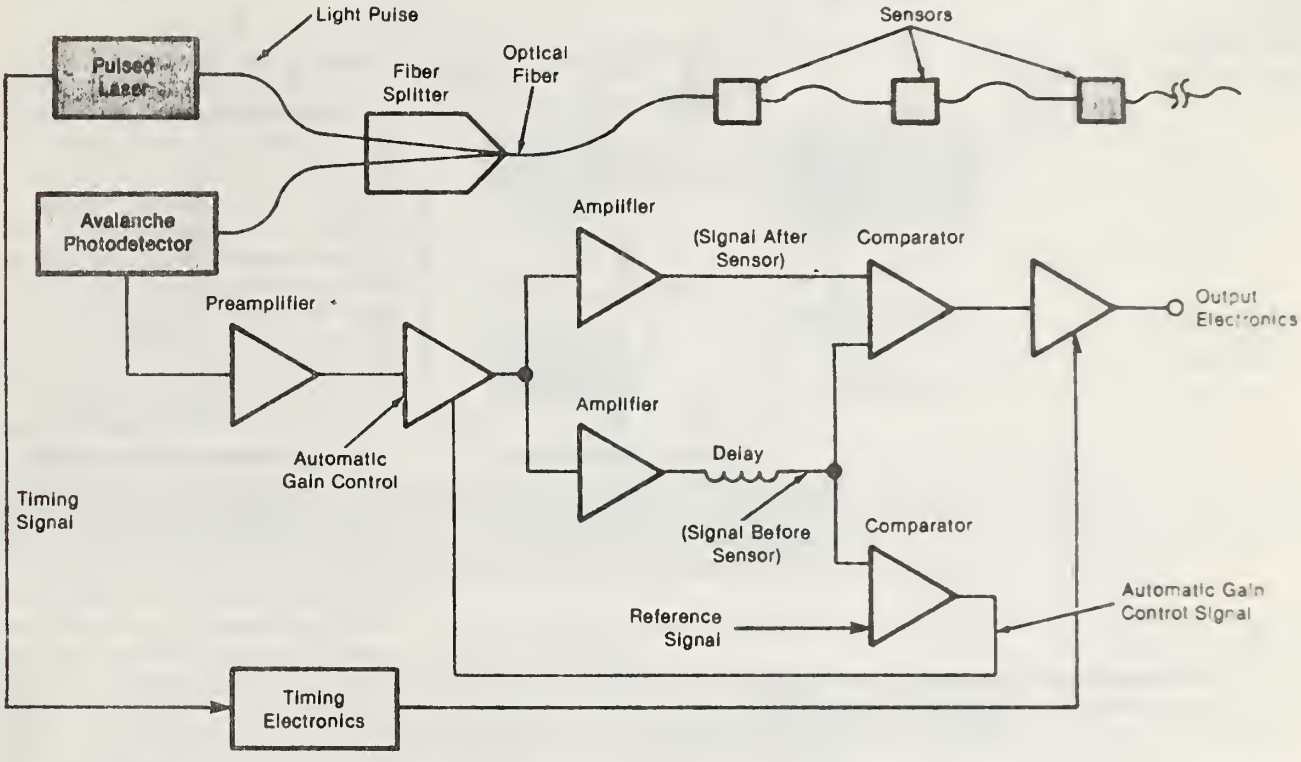

Figure 1. This **Optical Time-Domain Reflectometer** measures pulse travel times to identify the sensor or sensors from which reflected laser pulses originate. A leak is indicated by a change in the amplitude of the pulse reflected from a sensor.

Fluid systems can be monitored quickly for leaks in remote, hazardous, or inaccessible locations by a system of compact, lightweight fiber-optic leak sensors that are presently undergoing development. The sensors would be installed at such potential leak sites as joints, couplings, and fittings. A sensor is read by sending a laser pulse along the fiber, then noting the presence or relative amplitude of the return pulse. This leak-monitoring technique should be applicable to a wide range of fluid systems and would minimize human exposure to toxic or dangerous fluids.

The sensors are optical discontinuities from which light is reflected back along the sensing optical fiber or fibers to a photodetector. The intensity of the reflection is determined in part by the index of refraction of the medium surrounding a sensor, through its effect on the electromagnetic modes in the fiber core and cladding. For example, if leaking oil having an index of refraction near that of the cladding comes into contact with the cladding, a substantial amount of light is coupled out of the core and lost to the environment. In this case, the loss of reflection would indicate a leak.

The types of sensors showing the most promise include tapered constrictions, U-bends, and tilted fiber ends with and without mirrors. An individual fiber could be run to each potential leak site, which would necessitate large amounts of fiber. Alternatively, optical time-domain reflectometry can be used, as shown in Figure 1. There, the sensors are located in series along one fiber. The travel time of an affected pulse indicates the distance along the fiber to the affected sensor, thereby identifying the leak. Calculations indicate that 50 to 100 sensors can be connected along one optical fiber.

Figure 2 shows the signals reflected from a chain containing three experimental sensors in series, approximately 2 m apart. The first two returned pulses are from the connectors between the fiber and sensor chain. The next three pulses are reflections from the three sensors. The last pulse is from the end of the fiber. As can be seen, wetting one sensor increases the signal from subsequent sensors.

This work was done by Michael E. Padgett of **Kennedy Space Center** *and Opto-Electronics, Inc.*

Inquiries concerning rights for the commercial use of this invention should be addressed to the Patent Counsel, Kennedy Space Center Refer to KSC-11331 /TN

John F. Kennedy Space Center
Acting Technology Utilization Officer: Thomas M. Hammond
Mail Stop PT-TPO-A
Kennedy Space Center, FL 32899
(305) 867-3017
Patent Counsel:
James O. Harrell
Mail Code PT-PAT
Kennedy Space Center, FL 32899
(305) 867-2544

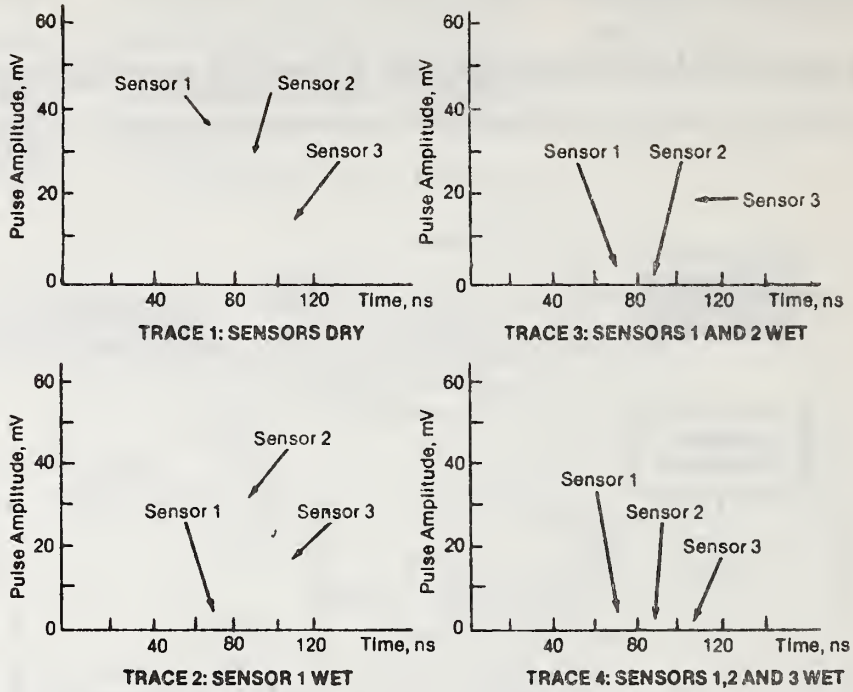

Figure 2. The **Presence of Water at Sensors** connected in series is shown by the reduction of the corresponding reflected laser pulses. The reflections from the dry sensors are indicated by peaks 3 through 5 in the first trace. The subsequent traces show the effects of successively wetting the three sensors.

FOR ADDITIONAL INFORMATION: *Contact: Director, Technology Transfer Division, P.O. Box 8757, BWI Airport, MD. 21240; (301) 621-0100 Ext. 241*
REFER TO THE NUMBER LISTED AT THE END OF THE ARTICLE

NASA Tech Brief

National Aeronautics and Space Administration

NASA's Jet Propulsion Laboratory, Pasadena, California

Licensing Opportunity

Improved Spectrometer for Field Use

Instrument would give answers in the field without waits for lab processing.

A proposed portable spectrometer for analyzing minerals in the field would generate spectral images like a camera and process the spectral data for real-time identification of materials. To identify an unknown mineral, the user would locate significant peaks in the displayed spectrum and match them to a spectrum in a portfolio of reference spectra. Alternatively, the user would call up a display of prerecorded spectra in the same wavelength region for comparison or allow the spectrometer to determine the best match automatically.

The new instrument would make it unnecessary to return the data to a laboratory or an equipment trailer for processing. In principle, it would accommodate a wide variety of minerals. The proposed spectrometer would extend the capabilities of the simpler two-wavelength instrument described in "Portable Radiometer Identifies Minerals in the Field" (NPO-15234), page 419, *NASA Tech Briefs*, Vol. 6, No. 4 (Spring/Summer 1982).

In the proposed instrument, reflected light from the terrain enters a telescope (see figure) and passes along an optical fiber to a grating spectrometer. The grating disperses the light passing through filters onto a linear array of about 1,000 individual photodetectors or a set of charge-coupled-device detectors. The array is electronically scanned so that it yields analog signals, which are processed by gain-adjusting circuits, amplifiers, and demodulators. The analog data from the signal processor are converted to digital form for use by a microprocessor. The microprocessor and a digital recorder provide signals for a liquid-crystal display.

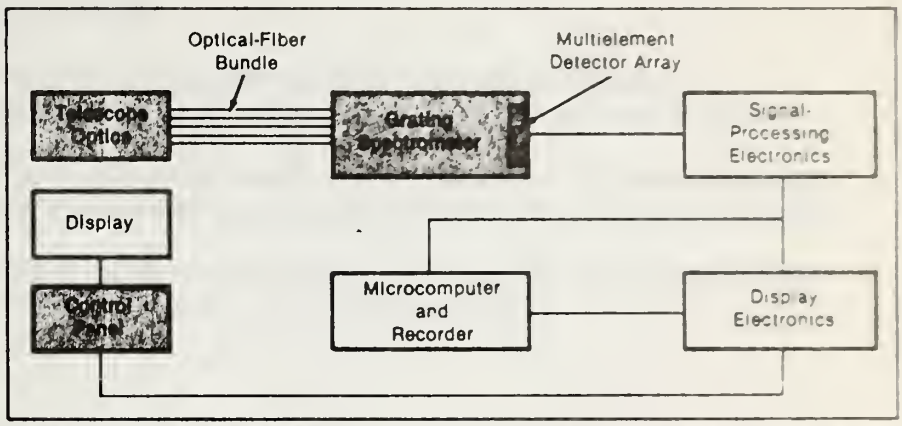

Telescope Optics Are Separated from the display and the control panel so that the instrument is easy for a user to operate. Once a sizeable library of prerecorded reference spectra is accumulated, spectrum-matching algorithm boards can be incorporated into the microprocessor to evaluate rapidly the components of a target specimen.

A control pad and spectral display are contained in a separate paddle so that the telescope can be made as light as possible. The user can select a portion of the reflectance spectrum of the surface under examination for real-time display, can expand the reflectance and wavelength display coordinates as desired, and can retain a spectrum for further processing and recording.

An initial calibration is carried out in ambient light, preferably with a target lighted by the Sun. The instrument is pointed at a standard-reflectance calibration target, and the spectrum is recorded.

The instrument is then pointed at the target terrain, and its spectrum, after ratioing with the standard, is displayed on the screen. The spectrum is recorded for future use. For analysis, prerecorded spectra are called up for comparison as a superimposed curve, or else algorithms are applied for automatic identification of the target specimen.

This work was done by Alexander F. H. Goetz of Caltech for **NASA's Jet Propulsion Laboratory**

Inquiries concerning rights for the commercial use of this invention should be addressed to the Patent Counsel, NASA Resident Office-JPL. Refer to NPO-15732 TN

Jet Propulsion Laboratory
Technology Utilization Manager
Norman L. Chaffin
Mail Stop 201-110
4800 Oak Grove Drive
Pasadena, CA 91109
(818) 354-2240

FOR ADDITIONAL INFORMATION: *Contact: Director, Technology Transfer Division, P.O. Box 8757, BWI Airport, MD. 21240; (301) 621-0100 Ext. 241*
REFER TO THE NUMBER LISTED AT THE END OF THE ARTICLE

Transportation

616 Cost and Weight of Helicopter Landing Gear— Three types of landing gear are compared.

617 Stress Analysis of a Scale-Model Helicopter Rotor Hub— Margins of safety are positive in the components checked.

618 More Durable Tracks for Heavy Vehicles— Tie bars instead of threaded fasteners make track throwing less likely.

Other items of interest

550 Water Heater/Cooler for Vehicles— At the press of a button, thermoelectric unit changes from a heating device to a cooling device.

586 Fire-Resistant Belt Panel for Airplane Windows— The layered structure incorporates materials that generate little smoke. (Licensing Opportunity)

588 Fire-Resistant Aircraft Ceilings— New materials retard flames but keep panel strong and light. (Licensing Opportunity)

MANUFACTURING TECHNOLOGY NOTE

U.S. ARMY MATERIEL COMMAND

Deputy Chief of Staff for Manufacturing Technology, Alexandria, VA

Project Number: 1L162209AH76 Filing Code: 51A051

Cost and Weight of Helicopter Landing Gear

Three types of landing gear are compared.

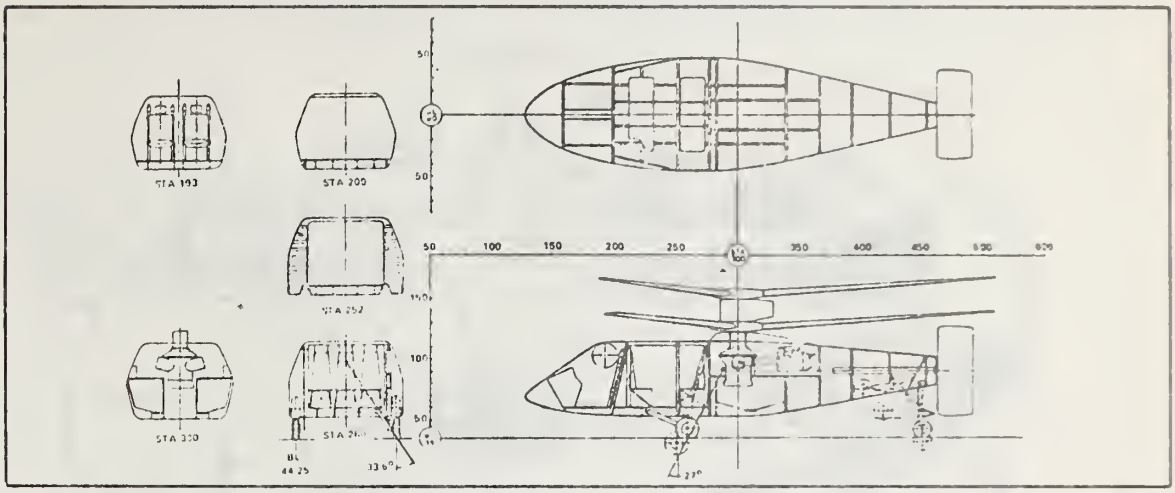

The **Helicopter Used as the Basis of the Landing Gear Study** is rated for a gross weight at take-off of 10,000 lb (4,540 kg). Twin advanced-technology engines drive the counterrotating main rotors and the auxiliary propulsor

A preliminary design study has determined weight and cost sensitivities of three types of landing gear for a 10,000-lb (4,540-kg) helicopter (see figure): noncrashworthy retractable, crashworthy retractable, and crashworthy fixed. In the study for the U.S. Army Aviation Research and Technology Activity (AVSCOM), the computer program KRASH calculated design loads at various sink rates and pitch and roll attitudes. The design loads were used to find the required landing-gear weight for the associated impact conditions. Landing-gear costs were found from the weight data.

According to the study, the maximum weight increase is 77 lb (35.0 kg) for a rectractable crashworthy landing gear and 48.5 lb (22.0 kg) for a fixed crashworthy gear, relative to the weight of a retractable noncrashworthy gear. Most of the weight increase is in the shock strut of the crashworthy gear. The aerodynamic drag of the fixed crashworthy gear represents a power loss of 26.6 percent compared to 0.7 percent for the retracted crashworthy gear.

With crashworthy gear, the roll attitude at impact can be extended from ± 10° to ± 15° at a 42 ft/s (13 m/s) sink rate. The maximum load in the shock strut occurs when the helicopter is at a nose-down pitch angle of 5° at any sink rate above 20 ft/s (6.1 m/s).

Seats designed independently of the landing gear, when combined with a crushable fuselage understructure, can protect the occupants when the helicopter crashes with the gear retracted. However, the load on high-mass components is excessive for sink rates beyond 25 ft/s (7.6 m/s).

Composite materials such as graphite/epoxy cannot be used in the main wheels because of the high temperatures generated during braking. Broken fibers in a composite shock-strut assembly can cause a pressure loss during normal landings as well as during crash landings.

FOR ADDITIONAL INFORMATION

You can learn more details about this technology by ordering the NTIS report:

Advance Technology Helicopter Landing Gear
Preliminary Design Investigation
Order number: AD-A162087/XAA
Price code: A06

Order from:

National Technical Information Service
5285 Port Royal Road
Springfield, VA 22161

This document was prepared under the sponsorship of the U.S. Government. Neither the United States Government nor any person acting on behalf of the United States Government assumes any liability resulting from the use of the information contained in this document, or warrants that such use will be free from privately owned rights.

MANUFACTURING TECHNOLOGY NOTE

U.S. ARMY MATERIEL COMMAND

Deputy Chief of Staff for Manufacturing Technology, Alexandria, VA

Project Number: NONE

Filing Code: 51A053

Stress Analysis of a Scale-Model Helicopter Rotor Hub

Margins of safety are positive in the components checked.

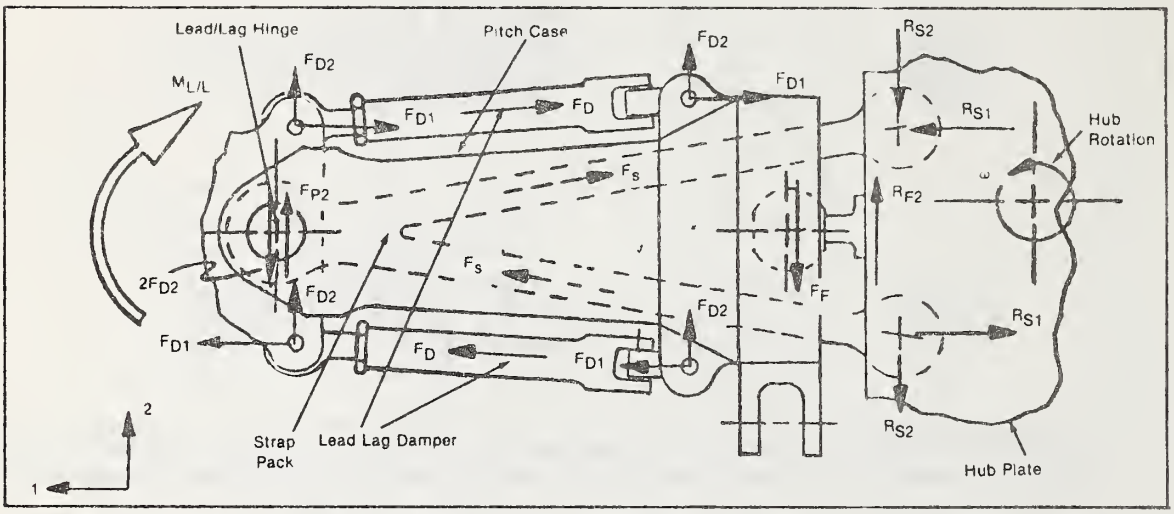

The Moment About the Lead/Lag Hinge is equal to the moment carried by the dampers. The complex load path was broken down into a series of free bodies in the analysis. The M, F, and R terms represent moment, forces, and reactions, respectively.

A stress analysis has been done on critical components of a 27-percent-scale model of a helicopter-rotor hub. The rotor system is designed for testing in a 4- by 7-meter low-speed wind tunnel. The critical components analyzed for the U.S. Army Aviation Systems Command included the pitch case, the upper hub plate, the strap pack, and the lead/lag hinge-pin assembly.

The hub retention was found to be equally critical for limit loads at the lead/lag hinge and the hub plate. The hub is critical in ultimate strength at the lead/lag hinge and in fatigue in the strap pack.

For the design loads, all margins of safety are positive, and the fatigue life is greater than 148 hours at 105 percent of rated rotor speed in revolutions per minute. This life expectancy corresponds to more than 10 million cycles. In terms of starting and stopping, the rotor life is 200,000 cycles.

The preload on the rotor joint is controlled by the bolt stretching measured at the time of installation. The bolt length is recorded and checked periodically for relaxation during the test life of the hub.

The load paths examined in the analysis were lead/lag moment (see figure), centrifugal force, flapwise moment, and torsion. The results of the analysis allow the hub and retainer to be evaluated for operating and hardware modifications.

FOR ADDITIONAL INFORMATION:

You can learn more details about this technology by ordering the NTIS report(s):

Stress Analysis of 27% Scale Model of AH-64 Main Rotor Hub
Order number: AD A164284/NAA
Price code: A04

Order from:
National Technical Information Service
5285 Port Royal Road
Springfield, VA 22161

This document was prepared under the sponsorship of the U.S. Government. Neither the United States Government nor any person acting on behalf of the United States Government assumes any liability resulting from the use of the information contained in this document, or warrants that such use will be free from privately owned rights.

NASA Tech Brief
National Aeronautics and Space Administration
NASA's Jet Propulsion Laboratory, Pasadena, California

More Durable Tracks for Heavy Vehicles

Tie bars instead of threaded fasteners make track throwing less likely.

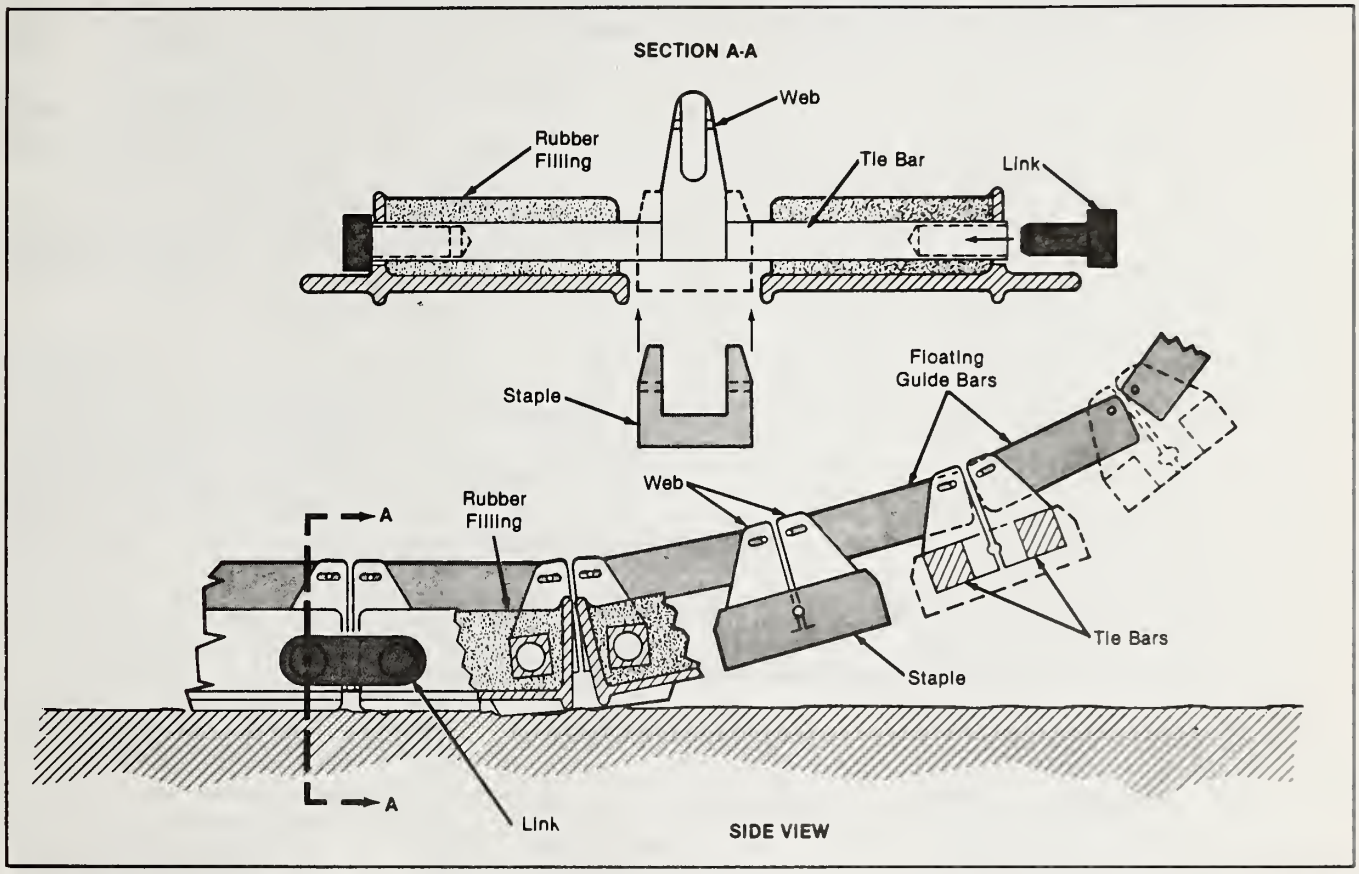

A **Continuous Chain of Floating Guide Bars** would be articulated at web junctions. Pins would replace bolted connections. The guide bars and the flanges on the vehicle (not shown) would keep out stones.

A proposed undercarriage for a tank or bulldozer would have flanged edges to prevent rocks and other road debris from getting caught in the track drive and damaging it or casting off the track. The improved track would have no threaded fasteners to be loosened by road shock and vibration.

Like conventional tracks, the proposed track includes a jointed, vertically flexible, horizontally stiff, continuous chain of sliding guide bars. Unlike conventional tracks, however, the new track includes tie bars forged integrally with webs of the guides — no bolts are used. In addition, the tie bars are forged with square cross sections so that they resist rotation when the track bends. The tie bars are cast into the rubber fillings on the treads to ensure a strong bond to the rubber.

Each pair of adjacent tie rods is held together by a staple, a massive, strong forging that is hammered into place on the webs. A pin holds each staple — again, no bolts are used.

The floating guide bar runs between web pairs in a track segment. Together the guide bars form a continuous guiding surface. The guide bars are inserted in open mortises in the web and retained by pins. The guide bars float in grooves in the top surface of the rubber fill and form a wall to keep out foreign objects. The upper edges of the bars and webs run within continuous flanges on the vehicle undercarriage so that foreign objects are excluded there. The retaining pins float in slots in the sides of the webs to accommodate the changes in the alignments of mating parts as the track bends around the end wheels and rides over bumps.

This work was done by Earl R. Collins, Jr., of Caltech for **NASA's Jet Propulsion Laboratory** *NPO-16478/TN*

FOR ADDITIONAL INFORMATION: *Contact: Director, Technology Transfer Division, P.O. Box 8757, BWI Airport, MD. 21240; (301) 621-0100 Ext. 241*
REFER TO THE NUMBER LISTED AT THE END OF THE ARTICLE

NTIS Order Form

NTIS Telephone Numbers

To Order Reports
(703) 487-4650

For Subscription Questions
(703) 487-4630

Other Information
(703) 487-4600

Editorial Questions
(703) 487-4838

Postage:
NTIS uses First Class Delivery, or equivalent service, on all shipping. For information about one day RUSH ordering, call (703) 487-4600.

NTIS PRICE CODE SCHEDULE *

This schedule gives the current values to the price codes cited in those Tech Notes having a backup report available from NTIS.

Microfiche	
A01	$6.50
Paper copy	
A02	9.95
A03	11.95
A04 through A05	13.95
A06 through A09	18.95
A10 through A13	24.95
A14 through A17	30.95
A18 through A21	36.95
A22 through A25	42.95
A99	Call for price

Customers in Canada, United States, and Mexico use this schedule. Other addresses should write for the price listing, number PR-360-4.

Prices effective January 1, 1987

Use this form ONLY to order reports designated as available from NTIS

MAIL ORDER TO: National Technical Information Service
U.S. DEPARTMENT OF COMMERCE
5265 Port Royal Road
Springfield, VA 22161
(703) 487-4650

Send me the reports I have selected on this form. I have placed order numbers in appropriate blanks and have indicated the quantity. IF ADDRESS LABEL IS NOT CORRECT, CALL OUR SUBSCRIPTIONS DEPARTMENT.

Last Name:.....

Title:.....

Company/Organization:.....

Address:.....

.....

City/State/Zip:.....

Telephone Number:.....

METHOD OF PAYMENT

☐ Check enclosed payable to NTIS for $.....

☐ Charge to my NTIS Deposit Account, No: ....-.....

☐ Purchase order number:.....

Charge to: ☐ American Express ☐ VISA ☐ MasterCard

Card Number:.....

Expation date:.....

Signature:.....
(Required to validate order)

NTIS ORDER NUMBER (Use only for backup reports stated as available from NTIS)

NTIS Order Number	*Price**	*Quantity*	*Total Price*
.....	.....	.....	.....
.....	.....	.....	.....
.....	.....	.....	.....
.....	.....	.....	.....
.....	.....	.....	.....
	Shipping and handling fee		$3.00
	Total		.....

☆ U.S GOVERNMENT PRINTING OFFICE:1987-191-378

- Agriculture & Food
- Computers
- Electrotechnology
- Energy
- Engineering
- Environmental Science & Technology
- Manufacturing, Machinery, & Tools
- Materials
- Medicine & Biology
- Natural Resources Technology & Engineering
- Physical Sciences
- Transportation

Route To:

PENN STATE UNIVERSITY LIBRARIES
A0000720098 40

RTMENT OF COMMERCE
echnical Information Service
a, 22161

JSINESS
rivate Use, $300

AN EQUAL OPPORTUNITY EMPLOYER

BULK RATE
POSTAGE & FEES PAID
NTIS
Permit No. G-292